Spring 2019

Arthropod Organic Anion Transporting Polypeptides in Tick-Borne Bacterial and Viral Infections

Vikas Kumar Taank
Old Dominion University

ARTHROPOD ORGANIC ANION TRANSPORTING POLYPEPTIDES IN TICK-BORNE BACTERIAL AND VIRAL INFECTIONS

by

Vikas Kumar Taank

B.Sc. Microbiology - August 1999, University of Delhi, India
M.Sc. Microbiology - August 2001, Chaudhary Charan Singh University, India
M.S. Cellular and Molecular Biology - August 2007, University of New Haven, USA

A Dissertation Submitted to the Faculty of
Old Dominion University in Partial Fulfillment of the
Requirements for the degree of

DOCTOR OF PHILOSOPHY

BIOMEDICAL SCIENCES

OLD DOMINION UNIVERSITY
May 2019

Approved by:

Dr. Girish Neelakanta (Director)

Dr. Hameeda Sultana (Member)

Dr. Piotr Kraj (Member)

Dr. Deborah Waller (Member)

ABSTRACT

ARTHROPOD ORGANIC ANION TRANSPORTING POLYPEPTIDES IN TICK-BORNE BACTERIAL AND VIRAL INFECTIONS

Vikas Kumar Taank
Old Dominion University, 2019
Director: Dr. Girish Neelakanta

Vector-borne diseases (VBDs) are human illness transmitted by an arthropod vector. World Health Organization (WHO) estimates that VBD has a huge impact worldwide that is responsible for affecting a billion people and causes 700,000 deaths annually. In recent years, there has been a continuous increase in the incidences of tick-borne diseases such as Lyme diseases and human anaplasmosis as reported by Center for Disease Control and Prevention. Very few reliable VBD control strategies have emerged till now. Transmission-blocking vaccines can provide effective management of VBDs but requires identification and characterization of novel vector-pathogen conserved molecules that play a significant role in pathogen survival and transmission from the vector host. This work describes two studies identifying the role of conserved tick organic anion transporting polypeptides (OATPs) in bacterial and viral infections. In the first study, the results show that *A. phagocytophilum* modulates a specific tick host organic anion transporting polypeptide (*isoatp4056*) and kynurenine aminotransferase (*kat*), a gene responsible for the production of metabolite xanthurenic acid (XA) from tryptophan catabolism pathway, for its survival in *Ixodes scapularis* ticks. Silencing of *isoatp4056* expression using RNA interference revealed that this gene has no effect on bacterial acquisition from the murine host, but affects bacterial survival in tick cells. Furthermore, silencing of gene expression for either *kat* alone or with *isoatp4056* affected both bacterial survival and expression of *isoatp4056*. Exogenous addition of XA revealed increased *isoatp4056* expression and bacterial burden in tick salivary gland and ticks cells. By using electrophoretic mobility shift assays (EMSA), the study provides evidence that both XA and *A. phagocytophilum* influences regulation of *isoatp4056* gene.

The second part of the study focuses on characterization of the role of these conserved organic anion transporting polypeptides in association with Lyme disease agent *Borrelia burgdorferi* and tick-borne Langat virus (LGTV), a viral pathogen closely related to tick-borne encephalitis virus (TBEV). Quantitative Real-Time PCR (QRT-PCR), data show that *B. burgdorferi* has no impact on the arthropod *oatps* gene expression in unfed nymphal ticks. Similarly, synchronous LGTV infection of unfed ticks (nymphs) revealed no impact on the expression of tick OATPs. However, specific OATPs were significantly downregulated upon LGTV infection in ticks cells at 24 h but not at 72 h post infection (p.i.). Furthermore, OATP inhibitor (SPZ) treatment followed by LGTV infection of tick cells showed significant reduction of LGTV loads, expression of *kat* gene, and several *oatp* genes. Bioinformatic characterization of medically important arthropod vectors including ticks, mosquitos, and lice revealed presence of several post-translational modifications sites such as glycosylation, phosphorylation and myristoylation sites. This set of studies provides a novel understanding on the manipulation of conserved OATPs, tryptophan pathway byproduct XA and *kat*, by a rickettsial pathogen for its survival in the tick vector host. In addition, these studies provide evidence on the role of tick OATPs in vector-tick-borne virus interactions. Collectively, this study provides compelling evidence on the involvement of arthropod OATPs in tick interactions with intracellular bacteria and viruses.

This manuscript is dedicated to my parents Mahender Singh Anand and Maya Devi.
To my lovely and amazing wife Sathiya Priya Gopalakrishnan, and my kids Rohin Taank and Avyan Taank.

ACKNOWLEDGMENTS

This project would not have been possible without the support of many people. I would like to express my most profound appreciation to my principal advisor and committee chair, Dr. Girish Neelakanta for providing his assistance and opportunity to perform research under his guidance. He continually conveyed a spirit of adventure in research and excitement in teaching. His wisdom of knowledge, persistence and hardworking nature has always inspired me. I appreciate all of his contributions of time, ideas and funding which made my research experience very productive. His degree of patience, tolerance and adjustment nature during this PhD dissertation are highly appreciated. I learned from him very early on how to perform excellent and meaningful science. Without his guidance and persistent help, this dissertation would not have been possible.

I humbly extend my gratitude to Dr. Hameeda Sultana, for being an important part of my research projects, for offering help and valuable scientific inputs to my research, and also teaching me various courses over the years including cell signaling and host pathogenesis and emerging infectious diseases.

Also, many thanks to my committee members, Dr. Piotr Kraj, for providing valuable input on this academic work, and for teaching functional omics in animal model. Dr. Deborah Waller who offered guidance and support throughout this project and also for allowing me to audit entomology course.

I acknowledge the contributions of Mr. Shovan Dutta and Mr. Wenshuo Zhou, graduate students in Dr. Sultana laboratory. Mr. Shovan Dutta assisted me in cloning of tick OATP genes, Western-blot, and many tick cells experiments in the first study, Mr. Wenshuo Zhou for helping me in LGTV studies with ticks and tick cells in the second study. I would like to thank Supreet Khanal, the other Ph.D. student in Dr. Neelakanta laboratory, for being a good friend and being available whenever I sought his help in scientific experiments, for helping me to organize my workspace from time to time and for being a very motivated and productive researcher in the lab. I would like to thank everyone from Drs. Sultana and Neelakanta Laboratories, especially Supreet Khanal, Ashish Vora, Shovan Dutta, Wenshuo Zhou and Jeremy Turck. Their constant support

and encouragement helped me to complete my doctoral degree program at Old Dominion University.

My sincere acknowledgements go to Old Dominion University, Dept of Biological Sciences for providing me with teaching assistantship and financial means to sustain me throughout most of the graduate program.

A debt of gratitude is also owed to my parents Sri Mahender Singh Anand and Smt. Maya Devi, my wife, Sathiya Priya Gopalakrishnan and my 4 and 2-year old sons, Rohin Taank and Avyan Taank and numerous friends who endured this lengthy process with me always offering unconditional love and support. My wife, Sathiya made too many sacrifices on my behalf, without her none of my accomplishment would have been possible. She helped me to sustain throughout the entire Ph.D. program. She showed exemplary dedication to our relationship and to my completion of the graduate school.

ABBREVIATIONS

3-HK	3-hydroxykynurenine
Ab	Antibody
ABC	ATP-binding cassette
ALKV	Alkhurma Virus
ASN	Asparagine N-glycosylation
CK2	Casein kinase II
CDC	Center for Disease Control and Prevention
DC	Dense core
EL	Extracellular loop
EM	Erythema migrans
EMSA	Electrophoretic mobility shift assay
GAF	Gametogenesis activating factor
GFP	Green fluorescent protein
HGA	Human granulocytic anaplasmosis
IAFGP	*Ixodes scapularis* antifreeze glycoprotein
KA	Kynurenic acid
KAT	Kynurenine aminotransferase
KFDV	Kyasanur Forest disease virus
LGTV	Langat virus
LIV	Louping ill virus
mGlu	Metabotropic glutamate receptors
OATP	Organic anion transporting polypeptide
OCT	Organic cation transport
OHFV	Omsk Hemorrhagic fever virus
ORF	Open reading frame
Osp	Outer surface proteins
p.i.	Post-infection
p.t.	Post-treatment

PKC	Protein kinase C
PKG	Protein kinase G
POWV	Powassan virus
PTM	Post translational modification
QRT-PCR	Quantitative real-time polymerase chain reaction
RC	Reticulate core
RSSE	Russian spring-summer encephalitis virus
RNAi	RNA interference
s.l.	sensu lato
SLC	Solute carrier
SLCO	Solute Carrier Organic Anion
SPZ	±-sulfinpyrazone
TBEV	Tick-borne encephalitis virus
TM	Transmembrane
TROSPA	Tick receptor of outer surface protein A
VBD	Vector-borne diseases
WHO	World health organization
XA	Xanthurenic acid

TABLE OF CONTENTS

Page

Page

LIST OF TABLES

LIST OF FIGURES

Figure Page

Figure Page

Figure Page

CHAPTER 1

INTRODUCTION AND BACKGROUND

1.1 VECTOR-BORNE DISEASES

Vector-borne diseases (VBDs) are human illness caused by bacteria, viruses, and parasites that are transmitted by an arthropod vector such as ticks, mosquitoes, lice, mites, fleas, and flies. It is estimated by the World Health Organization (WHO) that, every year a billion people are at risk of infection caused by vector-borne diseases (WHO, 2014). VBDs are responsible for over 700,000 deaths worldwide in 2017, which accounts for 17% of all infectious diseases in human beings (WHO, 2019). Other major VBDs include malaria, leishmaniasis, trypanosomiasis, yellow fever, dengue, Chagas disease, and Japanese encephalitis fever, in descending order of their mortality rates (WHO, 2014, 2019). There are about 19 million species of arthropods that can act as vectors of many deadly diseases in humans (Neelakanta and Sultana, 2015; Odegaard, 2008). Recently, there has been a steady increase in the incidence of tick-borne diseases such as Lyme disease and human anaplasmosis (Neelakanta and Sultana, 2015). Center for Disease Control and Prevention (CDC) – MMWR (Morbidity and Mortality Weekly Report) reported 275,589 total Lyme disease (208,834 confirmed and 66,755 probable) cases between the period of 2008 to 2015 (CDC-MMWR, 2017). Using standard national surveillance, about 30,000 cases are reported with Lyme disease annually; however, this number does not include all cases. Using alternative methods, CDC suggests that about 300,000 people may be affected annually in the United States (CDC, 2019b). For human anaplasmosis, in the year 2000, 348 cases were reported which increased to 4151 in the year 2016 (CDC, 2019a). This suggests a steep increase in human anaplasmosis incidences over recent years.

1.2 HUMAN GRANULOCYTIC ANAPLASMOSIS

The first report of human granulocytic anaplasmosis (HGA) in the United States was identified in the 1990s in a patient who died due to febrile illness two week followed

by a tick bite (Chen et al., 1994). Anaplasmosis in domestic animals is also known as tick-borne fever, which has been reported as early as 1932 in sheep (Gordon, 1932). In nature, HGA is maintained in a complex tick-ruminant-rodent life cycle. Humans in this cycle are involved as only accidental “dead-end” hosts (Blanco and Oteo, 2002). Anaplasmosis in human may cause self-limiting high fever, headaches, lack of appetite, confusion, myalgias, neutropenia, thrombocytopenia, anemia (Bakken et al., 1994; Guzman and Beidas, 2018; Rikihisa, 1991; Stuen et al., 2013) and elevation of serum hepatic aminotransferases (Lin and Rikihisa, 2003). In most humans, the infection results in minimal or no clinical manifestations. The illness usually lasts for only a few days, only 3% of infections develop life-threatening complications, and only 1% die from human anaplasmosis, especially the elderly and immunocompromised patients (Bakken and Dumler, 2015). HGA cases are on a continuous rise, and has increased by 12-fold between 2001 to 2011. No effective vaccines are available against *Anaplasma phagocytophilum* (Bakken and Dumler, 2015; Crosby et al., 2018), the causative agent of human anaplasmosis. Further research is required to understand and interrupt the survival mechanisms of this pathogen in the tick vector hosts.

1.2.1 *Anaplasma phagocytophilum*

The bacterium *A. phagocytophilum* represents a rickettsial pathogen of both veterinary and medical interest (Dumler et al., 2005). From Greek, ‘*an*’ means ‘*without*’ and *‘plasma’ means ’* anything formed’*. A. phagocytophilum* was first described in the USA (Bakken et al., 1994), and initially named human granulocytic ehrlichiosis (HGE) agent. A decade ago, Rickettsiaceae and Anaplasmataceae families were revised, causing the merger of these bacteria (*Ehrlichia phagocytophilum*, *E. equi,* and HGE agent) into a single species, *A. phagocytophilum* (Dumler et al., 2001).

1.2.1.1 Morphology

Anaplasma phagocytophilum is a small obligate intracellular rickettsial Gram-negative pleomorphic alpha-proteobacteria with size ranging from 0.2 - 2.0 µm (Rikihisa, 2011). This bacterium resides in early endosomes in granulocytic neutrophils and monocytes-macrophages (Lin and Rikihisa, 2003; Rikihisa, 1991), obtain nutrients for

bacterial fission and grow to form micro-colony/clusters known as morulae. These morulae have no fibrillar matrix and have no physical contact with mitochondria (Popov et al., 1998). The size of morulae can range from 2- 7 µm (Carlyon and Fikrig, 2003). The entire life of *A. phagocytophilum* is confined to these membrane-bound inclusions. These inclusions do not mature into phagolysosomes (Lin and Rikihisa, 2003), and avoid degradation by inhibition of the phagosome fusion with lysosomes (Carlyon and Fikrig, 2003). *A. phagocytophilum* exists in two distinct ultra-structures, a more substantial reticulate core (RC) form containing homogeneous loose chromatin and a smaller dense core (DC) form containing condensed chromatin and protoplasm as shown in Figure 1 (Battilani et al., 2017; Popov et al., 1998). RC forms are usually identified *in vivo* and DC forms are usually found during *in vitro* propagation, both of these forms are known to replicate by binary fission (Battilani et al., 2017). Figure 1 shows an electron micrograph of a dividing *A. phagocytophilum* in morulae with both DC and RC forms, in human promyelocytic leukemia cell lines (HL-60) cells.

1.2.1.2 Genomic Features

Anaplasma phagocytophilum (HZ strain isolated from New York) has a small single circular double-stranded genome of 1.47 Mb size with 1369 ORFs (Dunning Hotopp et al., 2006) which is about one-fourth of an *Escherichia coli* genome. *A. phagocytophilum* has no detectable plasmids, intact prophage or transposable elements (Rikihisa, 2010), thus making the genetic study in this bacteria very challenging. *A. phagocytophilum* genome consists of more than 12% repetitive sequences. These repeats consist of over 100 genes of *msp2*/*p44* (major surface protein), eight genes of type IV secretion system (T4SS) and many genes responsible for vitamin/co-factor biosynthesis (Dunning Hotopp et al., 2006; Rikihisa, 2010). The high number of repetitive sequences especially for immunodominant Msp2 protein can cause new antigenic variations due to chromosomal inversions during multiplication of the bacterium (Battilani et al., 2017; Dunning Hotopp et al., 2006). The expansion of this *msp2/p44* may allow *Anaplasma* variants to escape the host immune system which may enable the bacterium to survive in many vertebrate reservoir hosts with an increased tick to host bacterial transmission (Dunning Hotopp et al., 2006).

Anaplasma phagocytophilum genome lacks genes for biosynthesis of lipopolysaccharide and peptidoglycan (Dunning Hotopp et al., 2006; Rikihisa, 2010). In order to grow, *A. phagocytophilum* needs to incorporate host cholesterol into its own membranes for membrane integrity and stability (Rikihisa, 2010). *A. phagocytophilum* is unable to utilize glucose as a carbon or energy source due to lack of genes encoding for intermediary metabolism (Rikihisa, 2010) and also auxotrophic for over 15 amino acids and can only synthesize four amino acids (glycine, glutamine, glutamate and aspartate) (Battilani et al., 2017; Rikihisa, 2010). All these genomic features make *A. phagocytophilum* highly dependent upon the host for its survival.

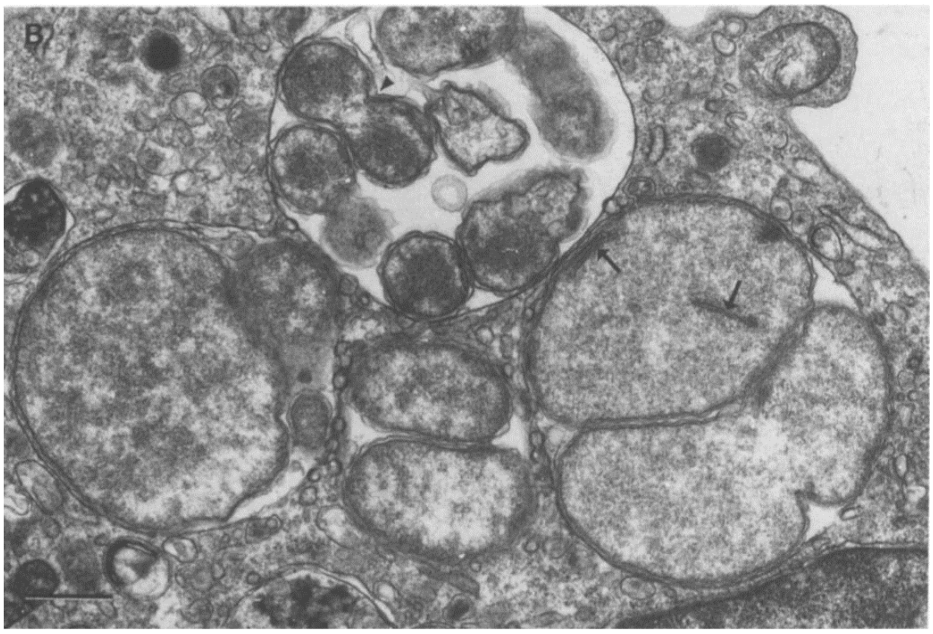

Figure 1. Electron micrographs showing *Anaplasma phagocytophilum* in promyelocyte HL-60 cell
Upper morula contains DC form with wavy cell-wall membrane, the arrowhead shows a dividing cell. Lower morulae show dividing RC, the black arrows show intracytoplasmic membrane invaginations. This image is reproduced from a published journal article (Popov et al., 1998, by permission from The Pathological Society of Great Britain and Ireland, see permissions sections for more detail).

1.2.1.3 Vector

The primary vector for *A. phagocytophilum* in the United States is *Ixodes scapularis* (deer tick or black-legged tick, found predominantly in the northeastern part of the United States) and *I. pacificus* (western black-legged tick, found in the western part of the United States) (Barlough et al., 1997; Eisen, 2018). In Europe, the primary vector is *Ixodes ricinus*, commonly known as Castor bean tick or sheep tick (Kowalec et al., 2018; Stuen et al., 2013). *A. phagocytophilum* has also been found in other ticks such as *Haemaphysalis punctata*, *H. concinna*, and *Rhipicephalus bursa* (Barandika et al., 2008), *I. persulcatus* (taiga ticks) *(*Alekseev et al*.,* 2004), *I. trianguliceps* (Perez et al., 2017), *Amblyomma americanum*, *Dermacentor variabilis*, and *D. occidentalis* (Stuen et al., 2013) and *Riphicephalus sanguineus* (Alberti et al., 2005). The prevalence of *A. phagocytophilum* in *I. scapularis* ticks is highly variable and ranges from 1 up to 50%, from 1 to ~10% in *I. pacificus* ticks, and about 1 to ~20% in *I. ricinus* ticks in Europe (Stuen et al., 2013). Ticks acquire *A. phagocytophilum* when they feed on infected hosts. The bacteria enter into the tick midgut epithelium and replicates and then migrates to tick salivary glands and undergoes secondary replication cycle (Battilani et al., 2017).

1.2.1.4 Reservoirs and other animal hosts

Several mammals can be reservoir host for *A. phagocytophilum* provided that, a reservoir host must be fed by an infected tick. The infected reservoir host must acquire a critical amount of pathogen to sustain infection till the next tick feeding cycle. Viable *A. phagocytophilum* bacteria have been isolated from various hosts such as cattle, sheep, horse, red-deer (Petrovec et al., 2002) and whitetail deer, *Odocoileus virginianus* (Stuen et al., 2013). In the United States, white-tail deer and white footed mice (*Peromyscus leucopus*) (Bunnell et al., 1998) are known to be primary natural reservoirs for *A. phagocytophilum* (Belongia et al., 1997). A study published in 2005 suggested that birds can be a potential reservoir host for *A. phagocytophilum* and may aid the bacterial dispersal (De La Fuente et al., 2005). Other animals such as wild boar (*Sus scrofa*), and domestic animals such as cats, dogs, goats, donkey, and cattle (De La Fuente et al., 2005) has been implicated as *A. phagocytophilum* hosts. Figure 2 shows the proposed

life cycle of various strains of *A. phagocytophilum* in multiple hosts. *A. phagocytophilum* can infect multiple host species, but different strains are selective and cannot infect all the hosts and show host specificity (Battilani et al., 2017).

1.3 LYME DISEASE

Lyme borreliosis is a multi-organ zoonotic disease caused by spirochetes belonging to the genospecies complex Borrelia burgdorferi sensu lato (s.l.), and is transmitted by Ixodes spp. ticks. In humans, the spirochete is not naturally involved in the life cycle of the spirochete between vertebrate host and the arthropod vector, thus humans are considered as accidental dead-end hosts. Lyme disease is named after Lyme, a town in Connecticut, USA, where the first incidence of this disease was reported in 1975. This report mentioned 51 cases of residents having symptoms of Lyme disease since 1972 (Steere et al., 1977). Lyme Borreliosis is considered as the most prevalent tick-borne disease in the world (Escudero et al., 2000). In the United States, 30,000 cases of Lyme disease are reported, however recent estimates by Center for Disease Control (CDC) using alternative methods, suggest that about 300,000 people may get Lyme disease annually (CDC, 2019c). CDC – MMWR (Morbidity and Mortality Weekly Report) reported 275,589 total Lyme disease (208,834 confirmed and 66,755 probable) cases between the years 2008 to 2015 (CDC-MMWR, 2017).

Early clinical manifestation of Lyme borreliosis is a characteristic annular rash known as erythema migrans (EM rash). The EM rash is manifested in about 70-80% cases (CDC, 2019c). In some cases, the pathogen can spread to other tissues. Thus, patients may exhibit secondary symptoms, causing more severe manifestations that can involve the skin, joints, heart, and nervous system (Stanek et al., 2012). Early symptoms may cause fever, chills, headache, fatigue, muscle pain and swollen lymph nodes (CDC, 2019c). Late disease symptoms may show up weeks to months after the initial tick bite and can cause sporadic episodes of arthritis affecting larger joints. Late stage infections can cause ‘Chronic Lyme Disease’ – a disease with varied unexplained symptorms, usually accompained by chronic arthritis, chronic encephalomyelitis, and many cardiovasucular manifestations such as atrioventicular nodal block,

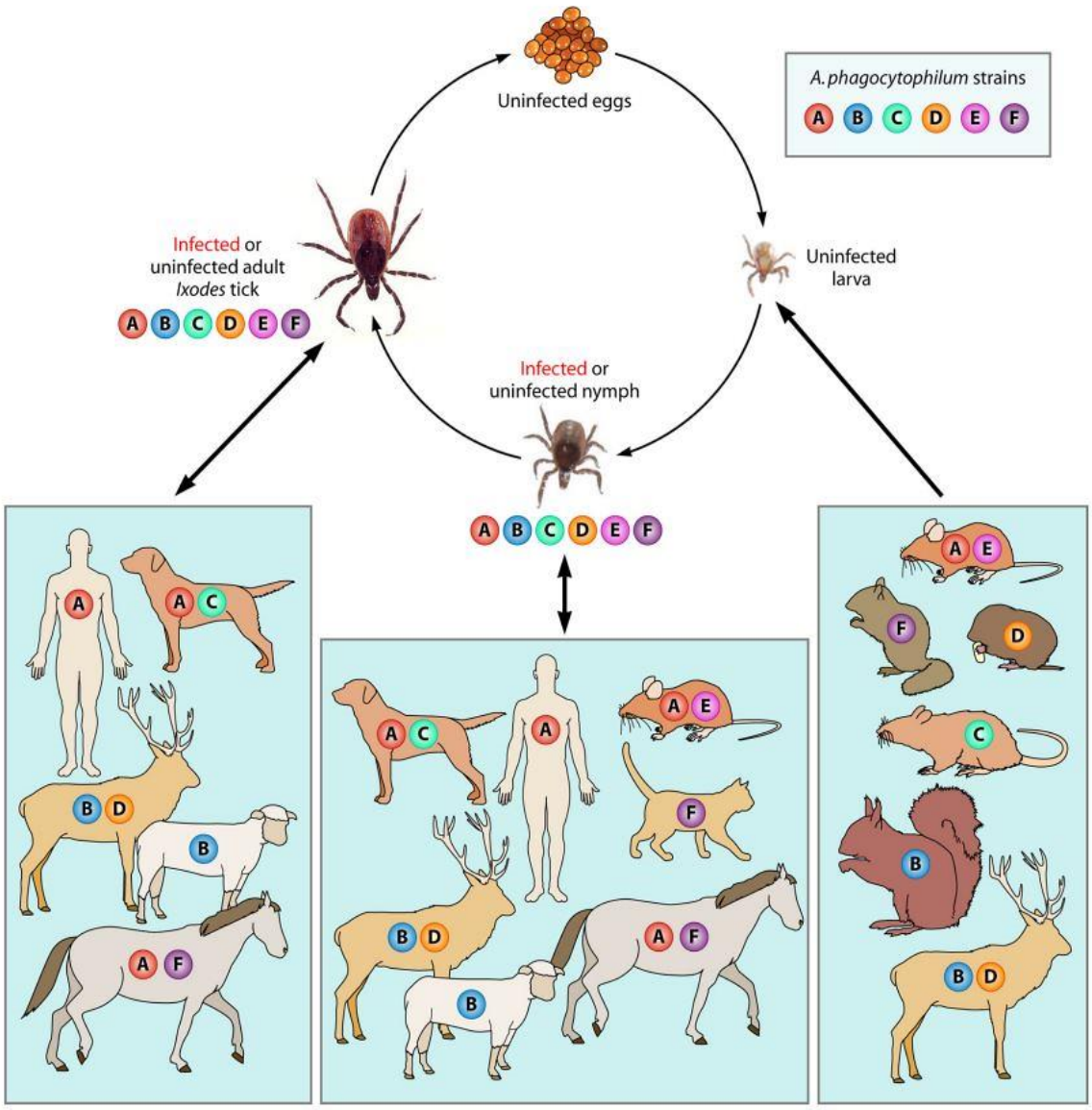

Figure 2. Proposed life cycle of *Anaplasma phagocytophilum*

Shows various strains of *A. phagocytophilum* with variable host susceptibilities. Eggs and larvae are always uninfected. Tick at any developmental stage (larvae, nymph or adults) can acquire *A. phagocytophilum* during feeding on the infected hosts. Tick maintain *A. phagocytophilum* through different molting stages and can transmit pathogen on next blood meal to susceptible host. This image is reproduced from published journal article (Rikihisa, Y. Clin. Microbiol. Rev. 2011).

myopericarditis and pancarditis (Bush et.al, 2018). Chronic neurological symptoms can lead to encephalopathy affecting mood and sleep (Tatum, 2018).

1.3.1 *Borrelia burgdorferi* sensu lato

Lyme disease agent was discovered by researcher Willy Burgdorfer in 1982 and was isolated from the midgut of *I. scapularis* (previously known as *Ixodes dammini*) ticks (Burgdorfer et al., 1982). This new species of spirochete was named as *Borrelia burgdorferi*. Four out of twenty genospecies of *B. burgdorferi* sensu stricto are known to be pathogenic for humans; this includes *B. burgdorferi*, *B. afzelii*, *B. gariniii* and *B. spielmanni* (Escudero et al., 2000; Seinost et al., 1999; Wang et al., 2014). These three species are only found in Europe. However, only *B. burgdorferi* is only pathogenic genospecies reported in the northern United States (Penza et al., 2016; Seinost et al., 1999).

1.3.1.1 Morphology

Borrelia burgdorferi is a flexible, spiral-shaped, Gram-negative, microaerophilic and motile spirochete with an internal periplasmic flagellum. The flagella resides between the outer membrane and the protoplasmic cell cylinder. About 7-10 flagella originate from the bacterial ends and overlap in the center of the bacterial cell. The cell size averages between 0.2 to 0.5 µm in diameter, the bacterial length can be variable and ranges between 4 to 30 µm. The spiral shape of the bacterium is due to complex interaction of the cell cylinder and cell wall peptidoglycan and endoplasmic flagella. Flagella is made up of primarily of one type of protein fiber, FlaB. The other flagellar protein FlaA is found in smaller amounts (Johnson, 1996; Motaleb et al., 2004; Penza et al., 2016).

Borrelia burgdorferi genome consists of a linear DNA of 9.1 kb size and consists of variable copy number of plasmids ranging from 16-21 (Casjens et al., 2012). Plasmids are found in both linear and circular configurations. The biological significance of these plasmids is not clear; however, it is suggested that these plasmids may be involved in many functions such as antigenic variation and immune invasion (Fraser et al., 1997). *Borrelia* has seven plasmid encoded outer-surface proteins (Osp), namely

OspA, OspB, OspC, OspD, OspE, OspF, and OspG. In tick gut, the bacterium OspA interacts with tick receptor of OspA (TROSPA) and helps the tick for colonization (Penza et al., 2016). Variable expression of these surface Osp proteins and bacterial motility helps the bacterium to adapt to different host tissue environments, making *Borrelia* spp. to function efficiently in the tick-vertebrate cycle (Penza et al., 2016). This cycle includes a variety of mammals, birds and reptiles (Mendoza-Roldan et al., 2019; Scott et al., 2018).

1.3.1.2 Vectors

The primary vector of transmitting *Borrelia burgdorferi* to humans are hard-bodied *Ixodidae* ticks, *I. scapularis* (in the northeastern part of the United States), *I. pacificus* (in the western part of the United States), *I. ricinus* (in Europe) and *I. persulcatus* (in Asia) (Parola and Raoult, 2001; Wang et al., 2014). Ticks acquire spirochete during feeding on the infected reservoir host; *B. burgdorferi* remains inactive till the tick molts to the next life stage (Humair and Gern, 2000). During the next developmental stage, the bacterium migrates from the midgut to other tick organs, through midgut wall and hemocoel, including salivary glands. The spirochete is transmitted to the vertebrate host through saliva by tick bite during feeding (Humair and Gern, 2000). Transovarial transmission for *B. burgdorferi* is rare, only 1% of *Ixodes ricinus* females can transmit *B. burgdorferi* transovarially (Humair and Gern, 2000). The infection rates of *B. burgdorferi*-infected *I. scapularis* varies on geographical regions and ranges between 12-100% in the northern United States; however, infection rates *for I. scapularis* and *I. pacificus* in western and southeastern regions of the United States show less than 3 % infection rate (Anderson, 1989).

1.3.1.3 Reservoirs and other animal hosts

There are numerous animal reservoirs for *Borrelia burgdorferi* s.l., this includes wild small mammals and birds. (Anderson, 1988, 1989). Larvae feed on small rodents especially white-footed mice (*Peromyscus leucopus*), while nymphs preferentially feed either on white-footed mice, eastern chipmunks *(Tamias striatus)* or gray squirrels *(Sciurus carolinensis)* (Salkeld et al., 2008). Adult ticks can feed on large mammals

such as cows, deer, bobcats, and hogs. However, Whitetail deer (*Odocoileus virginianus*) is the most important host for adult ticks (Anderson, 1988, 1989). *B. burgdorferi* can survive for long periods. In hamsters, the spirochete can survive up to 9 months, gray squirrels up to 14 months, and up to 13 months in white-footed mice (Salkeld et al., 2008). Long infectivity in these reservoir hosts suggests that the infection can be maintained and carried over to the next season for the transmission to the vector host. The prevalence of *B. burgdorferi* in white-footed mice is about 75 % in some areas in the northern United States (Anderson, 1989).

Domestic animals such as dogs (Greene, 1991), cats (Hoyt et al., 2018; Magnarelli et al., 1990), horses (Burgess, 1988; Burgess et al., 1986), cattle (Burgess, 1988), camel (Ben Said et al., 2016) and sheep (in Europe and China) can serve as reservoir host for *B. burgdorferi* (Ben Said et al., 2016; Li et al., 2019).

1.4 LANGAT VIRUS (LGTV)

Langat virus (LGTV, TP-21) was first isolated in 1955, in Malaysia and Thailand region from *Ixodes granulatus* ticks collected from forest rats (Smith, 1956). This isolated agent was further demonstrated to be closely related to the Russian spring-summer encephalitis virus (RSSE) (Smith, 1956; Work, 1963). LGTV is a *Flavivirus*, of family *Flaviviridae.* Related virus within the same group includes Tick-Borne encephalitis Virus (TBEV), Powassan virus (POWV) produces mild encephalitis (Gritsun et al., 2003b), Louping ill virus (LIV), Kyasanur Forest disease virus (KFDV), Omsk Hemorrhagic fever virus (OHFV), and Alkhurma Virus (ALKV). KFDV and OHFV cause hemorrhagic fever instead of encephalitis (Gritsun et al., 2003b). These viruses are genetically and antigenically related, and are known to be transmitted by *Ixodes* and *Dermacentor* ticks (Maffioli et al., 2014).

LGTV virus infects rodents in nature, mainly ground rats *(Rattus muelleri validus*) and the noisy rat or long-tailed rat (*Rattus sabanus vociferans*) (Gritsun et al., 2003b). Under laboratory conditions, LGTV virus is non-virulent for adult mice and primates, but young laboratory mice with intracerebral injection are known to develop encephalitis (Gritsun et al., 2003a).

Langat virus has a very low virulence for humans but shares more than 74% nucleotide identity with TBEV (Maffioli et al., 2014). Till date, there is no evidence that LGTV causes any disease manifestations in humans; however specific antibodies against LGTV virus has been detected in local people in Malaysia (Gritsun et al., 2003a). LGTV is generally non-pathogenic to primates and less pathogenic to other animals in their natural environments (Gritsun et al., 2003a). In the year 1963, LGTV was suggested to be an ideal candidate for the development of live virus vaccine against TBEV (Work, 1963). The initial human trial for the live attenuated vaccine based on LGTV had significant problems such as high rate of encephalitis (1:18,500), and failure to provide adequate protection against tick-borne encephalitis (TBE) infections (Gritsun et al., 2003a; Maffioli et al., 2014).

LGTV has been widely used in research as a substitute to study TBEV due to the following reasons: LGTV is closely related to TBEV, the availability of experimental mice models (Maffioli et al., 2014), and the availability of *in-vitro* method of infection in ticks with LGTV without feeding (Mitzel et al., 2007). Thus LGTV was used as a model organism to study viral infection in ticks. LGTV virus is further discussed in Chapter 3.

1.5 ORGANIC ANION TRANSPORTING POLYPEPTIDES (OATPS)

Human transporters are divided into two major categories, ATP-binding cassette (ABC) transporters and solute carrier transporters (SLC) (Roth et al., 2012). Most transporters are capable of bi-directional transport (Roth et al., 2012). While ABC transporters are generally responsible for efflux of substrates, the SLC transporters mediate uptake of the substrate into the cell (Roth et al., 2012). SLC transporters are further divided into two gene superfamilies; *SLC21A and SLC22A.* *SLC21A* superfamily consists of organic anion transporting polypeptides (OATPs). Substrates for OATPs are mainly large hydrophobic anions (Roth et al., 2012). The second superfamily *SLC22A* is further subdivided into organic anion transporters (OATs) and organic cation transporters (OCTs). OATs and OCTs are known to transport smaller hydrophilic anions and cation (Roth et al., 2012).

The organic anion transporting polypeptides (OATPs) is a superfamily of the plasma membrane transporters that is involved in uptake of wide variety of endogenous

and exogenous substrates, usually large (greater than 350 Daltons) hydrophobic organic anions, such as bile salts, thyroid hormones, steroid conjugates, anionic oligopeptides, toxins, neurotransmitters, anticancer drugs, antibiotics, anti-viral drugs and other xenobiotics (Hagenbuch and Meier, 2003; Roth et al., 2012; Taank et al., 2017).

Individual members of OATP superfamily are expressed on most epithelial cells throughout the human body (Roth et al., 2012). Human genome encodes 11 different OATPS, OATP1A2,OATP1B1, OATP1B3, OATP1C1, OATP2A1, OATP2B1, OATP3A1, OATP4A1, OATP4C1, OATP5A1 and OATP6A1 (Lai, 2013; Zhang and Lauschke, 2019). Structurally all human and rodent OATPs isoforms are made up of 643-722 amino acids with both N-terminus and C-terminus facing intracellularly (Roth et al., 2012). The OATP polypeptide consists of 12 transmembrane helix structure, with a characteristic large fifth extracellular loop (EL5), with a 13 amino acid signature (between transmembrane region 9 and 10) and 11 extracellular cysteine residues (Hagenbuch and Meier, 2003; Lai, 2013). The border between extracellular loop 3 (EL3) and transmembrane region 6, consists of a very characteristics conserved domain D-X-RW-(I,V)-GAWW-X-G-(F,L)-L (Radulovic et al., 2014). Various putative conserved glycosylation sites are present in loop EL2 and EL5, which are responsible for the plasma membrane localization of the OATPs (Lai, 2013).

The mechanism of OATP transporters is yet not fully understood. However, it is well known that the transport is carried in an ATP- and sodium-independent fashion through a positively charged central pore in a rocker-switch mechanism (Roth et al., 2012). Individual OATPs are capable of bi-directional transport. It has also been suggested that they work as electroneutral exchangers, for example in case of OATP1, by using cellular bicarbonate or glutathione conjugates (Li et al., 1998; Roth et al., 2012). Mechanism of transport for individual OATPs can vary; OATP1B1 and OATP1B3 are not affected by glutathione (Mahagita et al., 2007; Roth et al., 2012). It is reported that the activity of OATP2B1 is affected by pH; where at acidic pH it shows higher activity (Kobayashi et al., 2003).

The distribution of OATPs is tissue-specific, OATP1A2 is present in all tissues with the highest mRNA expression in brain, liver, lung, kidney, and testis (Roth et al.,

2012). A predicted structure of OATP1A2 using TOPO2 Transmembrane protein display software (available at http://www.sacs.ucsf.edu/cgi-bin/open-topo2.py) is shown in Figure 3. It is believed that OATP1A2 is associated with xenobiotics distribution and absorption. OATP1B1 and OATP1B3 both are expressed in the liver, OATP1B3 is also expressed around the central vein. OATP1C1 is localized mainly to brain and testis (Roth et al., 2012). A recent study reported that Xanthurenic Acid (XA) is transported by OAT 1 and OAT 3 (Uwai and Honjo, 2013).

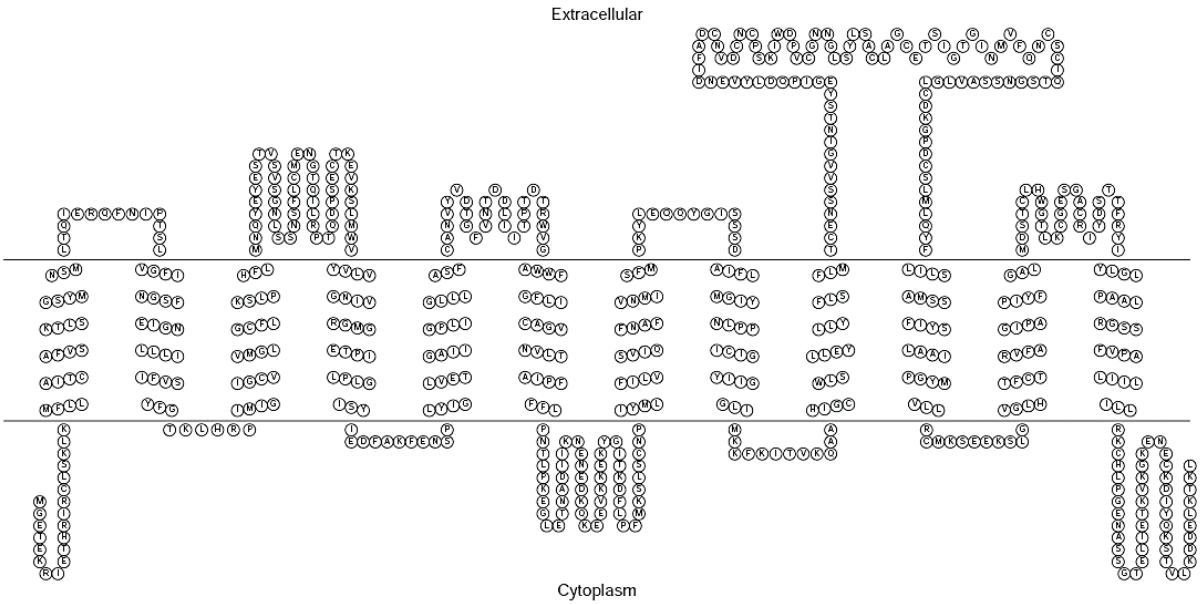

Figure 3. Predicated structure of human OATP1A2

The predicted structure shown in here is generated using TMHMM 2.0 and TOPO2 Transmembrane protein display software (available at http://www.sacs.ucsf.edu/cgi-bin/open-topo2.py, retrieved on 04/09/2019) showing 12 transmembrane domains and an enlarged extracellular loop.

1.5.1 Arthropod OATPs

Organic anion transporting polypeptides (OATPs) are an essential part of detoxification machinery in both vertebrates and invertebrates. Oatps from various arthropods has been previously reported (Radulovic et al., 2014). Nine oatps have been identified in *I. scapularis*, four in *Ripicephalus pulchellus and Pediculus humanus corporis*, six in *Aedes aegypti, Culex quinquefaciatus* and *Anopheles gambiae* and twelve in *Amblyomma americanum (*Radulovic et al., 2014). Tick Oatps show low homology to mammalian Oatp sequences and ranges between 20-33%, but show some of the oatps specific characteristic feature such as presence of 12 transmembrane domains, a larger extracellular loop (EL5), Kazal-type serine protease inhibitor domain in EL5, and presence of 11 highly conserved cysteine residues in EL5 except for *Isoatp4056* in *I. scapularis* ticks (Radulovic et al., 2014). Additionally, *I. scapularis* oatps have been shown to be differentially expressed and has a physiological role during blood feeding (Radulovic et al., 2014).

1.6 XANTHURENIC ACID

Xanthurenic acid (XA) or xanthurenate is also known as 8-hydroxykynurenine (4,8-dihydroxyquinoline-2-carboxylic acid) (Molecular weight = 205.169 g/mol) (NCBI PubChem, accession number CID5699) is a member of quinoline carboxylic acid class of compounds. The chemical structure of XA is shown in Figure 4. XA can be found in all eukaryotes ranging from yeast to humans (NCBI PubChem, accession number CID5699). XA is also present in blood (0.7 µM), urine (5 – 10 µM) (Malina et al., 2001) , feces and human epidermis tissue. Within the cell, XA is located primarily in the membranes. XA has been shown to be present in many mice neuronal cells (Roussel et al., 2016). XA is produced as a metabolite from oxidative metabolism of tryptophan (Human Metabolome Database, accession number HMDB0000881; NCBI PubChem, accession number CID5699).

Xanthurenic acid was isolated from urine of pyridoxine-deficient rats in 1942 (Lepkovsky et al., 1974). Since XA is excreted in the urine of vitamin B6 deficient

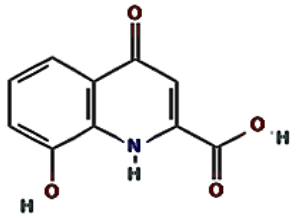

Figure 4. Chemical structure of xanthurenic acid

patients, this led to the development of XA-test. XA-test measures the disorder in tryptophan and vitamin B6 metabolism as an indicator of hypersecretion of glucocorticosteroids, this test helps in the detection of anxiety and depression (Hoes and Sijben, 1981). Various studies show that XA can be involved in many human diseases. Recent reports suggest that XA can interact and activate mGlu2 and mGlu3 receptors (Fazio et al., 2017) and may play diverse roles in neuronal pathophysiology. Experimental studies show that XA can interfere with the production, release, and biological activity of insulin (Oxenkrug et al., 2013). Increased XA levels are found in chronic migraine patients (Curto et al., 2015) and type-II diabetes patients (Matsuoka et al., 2017; Oxenkrug, 2015), on the contrary, serum XA levels are reduced in schizophrenia (Fazio et al., 2015), and in Alzheimer's disease (Giil et al., 2017).

Xanthurenic acid accumulation is known to induce apoptotic key events in vascular smooth muscle and retinal pigment epithelium cells by activation of caspase -3,-8 and -9. (Malina et al., 2001) In addition, XA causes mitochondrial migration and destruction, and cytochrome C release. Collectively all these events cause the destruction of mitochondria and nuclei in the cell (Malina et al., 2001). XA forms a covalent bond with proteins, denatures the proteins and can cause cell death (Malina et al., 2001).

Xanthurenic acid also plays an important role in the life-cycle of malaria pathogen (*Plasmodium spp.*) in the mosquito vector (Billker et al., 1998). The life cycle of *Plasmodium* is complex and requires human and mosquito hosts. After the acquisition of the blood meal from an infected host, both male and female gametocytes in the mosquito midgut must generate functional gametes (Billker et al., 1998). Male

gametogenesis involves a process known as exoflagellation, which is the extrusion of eight thread-like gametes. These threadlike gametes swim and fertilize the female gametes (Billker et al., 1998). Above described events depend primarily on three different conditions, first, at least 5°C drop in temperature and change in pH from 7.4 to 8.0 - 8.2 (Billker et al., 1998). These events represent the change of physiological conditions from the mammalian blood to the mosquito midgut. The most critical condition is the presence of XA. Hence, this metabolite is regarded as gametogenesis activating factor (GAF) (Billker et al., 1998; Vernick, 2004). XA activates guanylyl cyclase, which in turn activates cGMP-dependent protein kinase also known as protein kinase G (PKG) of the malarial parasite, thus maintaining high cytosolic calcium (Ca^{++}). This high Ca^{++} is required for further signaling for malaria reproduction (Yamamoto et al., 2018).

Xanthurenic acid is also implicated in the production of reactive oxygen species (ROS), in the presence of iron, the bound XA-Fe complex can activate oxygen molecule to form superoxide radical (Murakami et al., 2006). On the other hand, XA is known to be a high-affinity iron chelator, and it is demonstrated as a potent scavenger of peroxyl radicals (Lima et al., 2012). The role of XA as an antioxidant has been studied in mosquito *Aedes aegypti*, a vector of dengue and yellow fever (Lima et al., 2012). It is demonstrated that XA is produced in the digestive tract of mosquito following a blood meal and can reach up to millimolar levels during maximal digestive activity (Lima et al., 2012).

1.7 KYNURENINE AMINOTRANSFERASE (KAT)

Kynurenine pathway is the primary pathway for the degradation of tryptophan in most mammalian cells that generates various bioactive catabolites such as kynurenine, kynurenic acid (KA), xanthurenic acid (XA), and 3-hydroxykynurenine (3-HK) (Song et al., 2017). 3-hydroxykynurenine is further degraded into XA by KAT enzyme (Gao et al., 2018). KAT is dependent upon pyridoxal 5’phosphate (PLP), an active form of vitamin B6, which acts as a co-factor (Giil et al., 2017). *Ixodes scapularis* ticks encodes KAT (XM_002401267) that can catalyze both kynurenate and xanthurenate as shown in Figure 10 in Chapter 2. *I. scapularis* KAT also shares 70% identity with *Haemaphysalis*

longicornis HIKAT that can catalyze 3-hydroxykynurenine to XA (Battsetseg et al., 2009). These along with other studies suggests that *I. scapularis* KAT (XM_002401267) is responsible for intracellular production of XA (Taank et al., 2017; Taank et al., 2018).

CHAPTER 2

ANAPLASMA PHAGOCYTOPHILUM MODULATES *IXODES SCAPULARIS* ORGANIC ANION TRANSPORTING POLYPEPTIDE AND TRYPTOPHAN PATHWAY METABOLITE FOR ITS SURVIVAL IN TICKS

2.1 INTRODUCTION

Human anaplasmosis is known to be the most common arthropod-borne diseases in the United States, Europe and Asia (de la Fuente et al., 2016a; Dumler et al., 2005). It is caused by *A. phagocytophilum*, an obligate intracellular gram-negative pathogen, transmitted by *Ixodes scapularis* in the eastern and midwestern regions and *Ixodes pacificus* on the western regions of the United States (Barlough et al., 1997; Eisen, 2018). The blacklegged tick (*I. scapularis*) is a medically important vector which is responsible for transmission of various pathogens like *Borrelia burgdorferi*, *B. miyamotoi*, *A. phagocytophilum*, *Babesia microti*, *Ehrlichia muris*-like agent (EMLA) and Powassan virus (POWV) (Anderson and Armstrong, 2012; Anderson and Magnarelli, 2008; Krause et al., 2014; Pritt et al., 2011). These ticks can feed on more than 100 hosts in North America including humans, horse, cattle, deer, sheep, mice, and reindeer (Anderson and Magnarelli, 2008; Foley et al., 1999; Zeman et al., 2004). Due to a broad host range, *A. phagocytophilum* has developed various strategies for its survival and pathogenicity, such as cytoskeleton remodeling, inhibition of apoptosis and immune response manipulation (Sultana et al., 2010; de la Fuente et al., 2016a). *A. phagocytophilum* shows various strain variations due to host specificity (Rikihisa, 2010, 2011) as shown in Figure 2.

Ixodes scapularis ticks acquire *A. phagocytophilum* through blood feeding on an infected animal (Dumler et al., 2005; Hodzic et al., 1998). *A. phagocytophilum* enters into the midgut and then finally establishes itself in the tick's salivary glands (Hodzic et al., 1998). *A. phagocytophilum* inside the tick is transstadially maintained during different developmental stages, and there are no reports of transovarial transmission in *Ixodes species* (Hodzic et al., 1998). Various survival strategies that are used by *A. phagocytophilum* to persist during different arthropod developmental stages, these mechanisms are not yet fully understood. Further understanding of these survival strategies, especially in the unfed starvation state would give crucial insights into the mechanism(s) for *A. phagocytophilum* persistence during tick molting stages.

Anaplasma phagocytophilum in humans primarily infects and survives within neutrophils by delaying apoptosis, inhibiting NADPH oxidase activity, subverting phagolysosome formation and injection of type IV effector proteins to host cell signaling (Rikihisa, 2010, 2011). Much is known about survival strategies of the bacterium inside the mammalian host, but very little is known about bacterial survival strategies within the arthropod vector.

Anaplasma phagocytophilum specifically modulates several tick genes such as inhibition of apoptosis by upregulation of JAK/STAT pathway (Ayllon et al., 2015). The upregulation of antifreeze glycoprotein (IAFGP) by using arthropod transcriptional activator protein (AP1) for cold survival (Neelakanta et al., 2010; Khanal et al., 2018) is an important survival strategy used by *A. phagocytophilum*. The increased expression of *α1,3-fucosyltransferases* for colonization (Pedra et al., 2010) and *salp16* requirement for survival of the bacterium in tick salivary glands (Sukumaran et al., 2006) is noticeable. *A. phagocytophilum* is also known to alter arthropod host gene expression for its own survival by induction of phosphorylation of actin by *Ixodes* p21-activated kinase (IPAK1) signaling (Sultana et al., 2010). *A. phagocytophilum* can also interplay with Src tyrosine kinase for its colonization and survival in the arthropod vector (Turck et al., 2019).

Human organic anion/cation transporters are encoded by SLCO/SLC gene superfamily and are classified into, 1: organic anion transporting polypeptides (OATPs), 2: organic anion transporters (OATs) and 3: organic cation transporters (OCTs) (Roth et

al., 2012). These transporter protein families are highly conserved among vertebrates and play essential roles in the influx of several molecules including xanthurenic acid (XA), a metabolite from tryptophan oxidation pathway (Le Floc'h et al., 2011; Roth et al., 2012; Uwai and Honjo, 2013). In humans, eleven different OATPs have been identified that are localized to barrier epithelial cells (Roth et al., 2012). These OATPs participate in the trans-cellular movement of various signaling molecules, hormones, growth factors, toxins, drugs and xenobiotics across various body fluid compartments such as blood-urine, intestine-blood, blood-bile, blood-placenta, blood-central nervous system. (Hagenbuch and Meier, 2004; Kalliokoski and Niemi, 2009; Nigam et al., 2015). OATPs also play a potential role in inter-organ communication between liver, eyes kidneys and brain (Nigam et al., 2015). According to human OATP topology prediction, there are 12 transmembrane domains that are connected by a large intracellular loop between TM 9 and 10, and both N- and C-terminus are predicted to be intracellular (Figure 3) with several predictions for post-translational modifications (PTM) (Hagenbuch and Meier, 2004; Kalliokoski and Niemi, 2009; Nigam et al., 2015).

Recent studies have shown that OATPs among various arthropod species is conserved (Mulenga et al., 2008; Radulovic et al., 2014). *I. scapularis* encodes nine different OATPs with a variable expression with different tissues, including salivary glands (Radulovic et al., 2014). Mulenga and coworkers showed that some of these OATPs play an important role in blood feeding by ticks (Mulenga et al., 2008). The clear understanding and the participation of these OATP class of molecules in vector-pathogen interactions is lacking. In this study, using *A. phagocytophilum* as a model, for the first time it is demonstrated that tick-borne pathogens modulates these highly conserved OATPs along with tryptophan metabolism pathway for its survival in *Ixodes scapularis*, a medically important arthropod vector (Taank et al., 2017; Taank et al., 2018).

2.2 RESULTS

2.2.1 *Anaplasma phagocytophilum* Induces Expression of Specific *Ixodes scapularis* Organic Anion Transporting Polypeptides (OATPs) in Unfed Ticks

Ixodes scapularis encodes nine different organic anion transporting polypeptides (OATPs), these are expressed in unfed ticks. Unfed *A. phagocytophilum* ticks were generated as described in the experimental procedures section. The expression of all nine OATPs (*isoatp0726, isoatp2114, isoatp2116, isoatp4056, isoatp4134, isoatp4548, isoatp4550, isoatp5126 and isoatp5621)* were measured in *A. phagocytophilum* infected whole ticks (nymphs) using quantitative real-time PCR (QRT-PCR) (Figure 5). QRT-PCR analysis showed significant ($P < 0.05$) upregulation of *isoatp4056* (Figure 5D) and *isoatp5621* (Figure 5I) in the presence of *A. phagocytophilum* when compared to uninfected controls ticks. No significant differences were evident in the remaining (7 OATPs) including *isoatp0726* (Figure 5A), *isoatp2114* (Figure 5B), *isoatp2116* (Figure 5C), *isoatp4134* (Figure 5E), *isoatp4548* (Figure 5F), *isoatp4550* (Figure 5G), and *isoatp5126* (Figure 5H) between *A. phagocytophilum*-infected ticks as compared to the uninfected controls ticks. These data suggests that *A. phagocytophilum* selectively induces expression of tick OATPs (*isoatp4056 and isoatp5621*) in unfed whole nymphal ticks.

2.2.2 Expression of both *I. scapularis isoatp4056* and *isoatp5621* are Developmentally Regulated, but only *isoatp4056* is Induced upon *A. phagocytophilum* Colonization in Tick Salivary Glands

Next, the expression of *isoatp4056* and *isoatp5621* mRNA transcript levels was determined in different developmental stages of the tick by QRT-PCR (Figure 6A and 6B). The *isoatp4056* QRT-PCR analysis showed that this gene was expressed in all the developmental stages. Larvae expressed significantly higher ($P < 0.05$) transcript levels than adult male and female ticks. No significant difference ($P > 0.05$) in the expression of *isoatp4056* was seen between larvae and nymphs, or between the adult male and adult female ticks (Figure 6A). Expression of *isoatp5621* was evident in all development stages of tick (Figure 6B). Nymphs show significantly ($P < 0.05$) higher transcript levels

as compared to adult male and female ticks (Figure 6B). Comparison between larvae to nymphs, larvae to adult ticks or between male and female ticks showed no significant difference ($P > 0.05$) in the expression of *isoatp5621* (Figure 6B). It was observed that the expression of only *isoatp4056* transcripts was significantly ($P < 0.05$) increased in *A. phagocytophilum* infected tick salivary glands (Figure 6C), whereas no difference in *isoatp5621* expression was noted between *A. phagocytophilum*-infected and uninfected salivary glands (Figure 6D). No significant difference was noted in the expression of *isoatp4056* (Figure 6E) and *isoatp5621* (Figure 6F) in unfed guts tissues isolated from *A. phagocytophilum* and uninfected nymphal ticks. These results show that *A. phagocytophilum* specifically regulates expression of *isoatp4056* and not *isoatp5621* in nymphal salivary glands.

2.2.3 RNA Interference (RNAi) of *isoatp4056* Expression in Ticks has no Effect on *A. phagocytophilum* Acquisition from the Murine Host

The mRNA transcript levels of *isoatp4056* was analyzed during the acquisition of *A. phagocytophilum* into naïve nymphal ticks from *A. phagocytophilum* infected murine host. No significant ($P > 0.05$) change in the transcript level of *isoatp4056* was noted during *A. phagocytophilum* acquisition into uninfected nymphal ticks from the infected murine host when compared to uninfected controls (Fig 7A). To check if IsOATP4056 has any role in the acquisition of *A. phagocytophilum* from the infected murine host, *isoatp4056*-silenced unfed uninfected nymphs were generated by RNA interference using double-stranded RNA (dsRNA) targeting the *isoatp4056* gene. The *isoatp4056*-dsRNA or mock control was micro-injected at equal volumes into the body of the ticks. After microinjection, ticks were allowed to recover for 2-4 h or 24 h at room temperature. Post-recovery, these ticks were fed immediately on *A. phagocytophilum* infected mice. QRT-PCR analysis of these fed nymph ticks showed a significant reduction in the *isoatp4056* transcripts in the *isoatp4056*-dsRNA-injected ticks when compared to mock-injected controls (Fig 3B). However, no significant difference in *A. phagocytophilum* loads were evident between *isoatp4056*-dsRNA injected ticks in comparison to the has no role during the acquisition of *A. phagocytophilum* from the murine host to ticks.

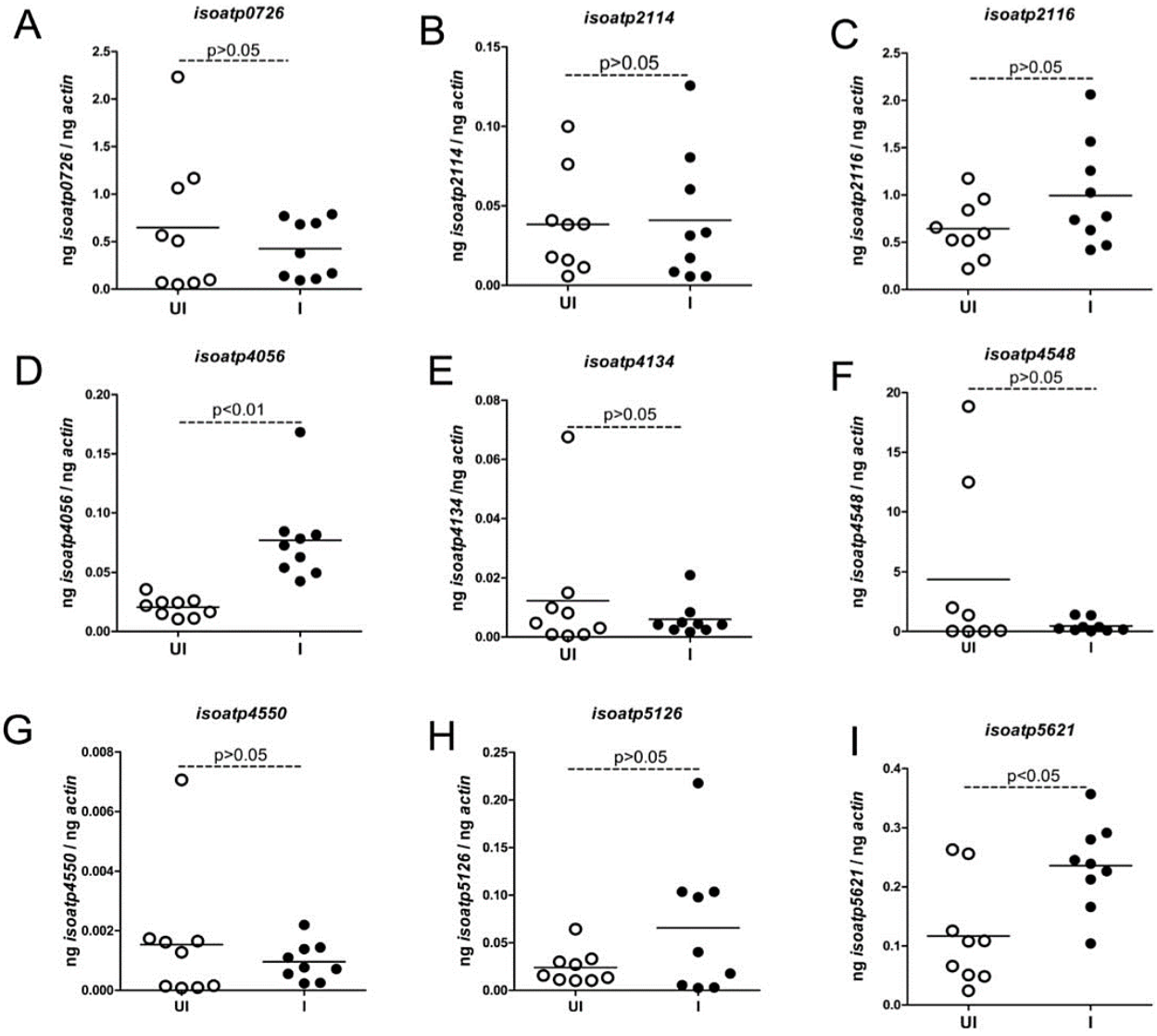

Figure 5*. Anaplasma phagocytophilum* up-regulates *isoatp4056* and *isoatp5621* in unfed *Ixodes scapularis* whole ticks (nymphs)

(A–I) Quantitative PCR analysis showing expression of nine OATPs: *isoatps*0726 (A), *isoatp*2114 (B), *isoatp2116* (C), *isoatp4056* (D), *isoatp4134* (E), *isoatp*4548 (F), *isoatp4550* (G), *isoatp5126* (H) and *isoatp5621* (I) between unfed uninfected ticks and *A. phagocytophilum*-infected ticks. Open circle represents uninfected (UI) and closed circles represent infected (I) ticks. Each circle represents one tick. The mRNA levels of OATPs are normalized to tick beta-*actin* mRNA levels. P value from non-paired Student's t-test is shown.

2.2.4 RNAi of *isoatp4056* Expression Affects *A. phagocytophilum* Survival in ISE6 Tick Cells

The effect of *isoatp4056*-silencing was analyzed on the *A. phagocytophilum* survival in tick cells. Transcript levels of *isoatp4056* transcript levels were significantly ($P < 0.05$) increased in tick cells upon *A. phagocytophilum* infection when compared to the uninfected controls (Fig. 8A). Further experiments were performed to study if gene silencing of *isoatp4056* (by using dsRNA in tick cells) has any impact on *A. phagocytophilum* survival. It was found that *isoatp4056*-dsRNA transfected tick cells showed a significant ($P < 0.05$) decrease of *isoatp4056* transcripts in *isoatp4056*-dsRNA-treated cells when compared to mock-treated control cells (Fig. 8B). In addition, no change in cell morphology was noticed at 4 and 24 h post-transfection and 48 h post transfection (24 h post infection) in comparison to mock-treated control cells (Figure 9). RNAi-mediated silencing of *isoatp4056* expression in *A. phagocytophilum*-infected-*isoatp4056*-dsRNA-treated tick cells showed significant ($P < 0.05$) reduction in the *A. phagocytophilum* burden in comparison to the *A. phagocytophilum*-infected mock-treated controls (Figure 8C). To further confirm results from RNAi analysis, the effects of commercially available OATP inhibitor SPZ (± -sulfinpyrazone) on *A. phagocytophilum* burden in tick cells was tested. Tick cells were either treated with 100 µM of ± -sulfinpyrazone or mock control and then were infected by *A. phagocytophilum*. This experiment showed that *A. phagocytophilum* burden was significantly ($P < 0.05$) reduced within the OATP inhibitor ± -sulfinpyrazone-treatment group in comparison to the control group (Figure 8D). These results further suggest that IsOATP4056 play an important role in the survival of *A. phagocytophilum* in tick cells.

2.2.5 *Anaplasma phagocytophilum* Up-Regulates Kynurenine Aminotransferase (*kat*), a Gene Involved in the Synthesis of Xanthurenic Acid (XA), in Salivary Glands of Unfed Ticks

The upregulation of *isoatp4056* gene in tick cells and salivary glands of unfed ticks suggested a very crucial role for this gene in *A. phagocytophilum* colonization and

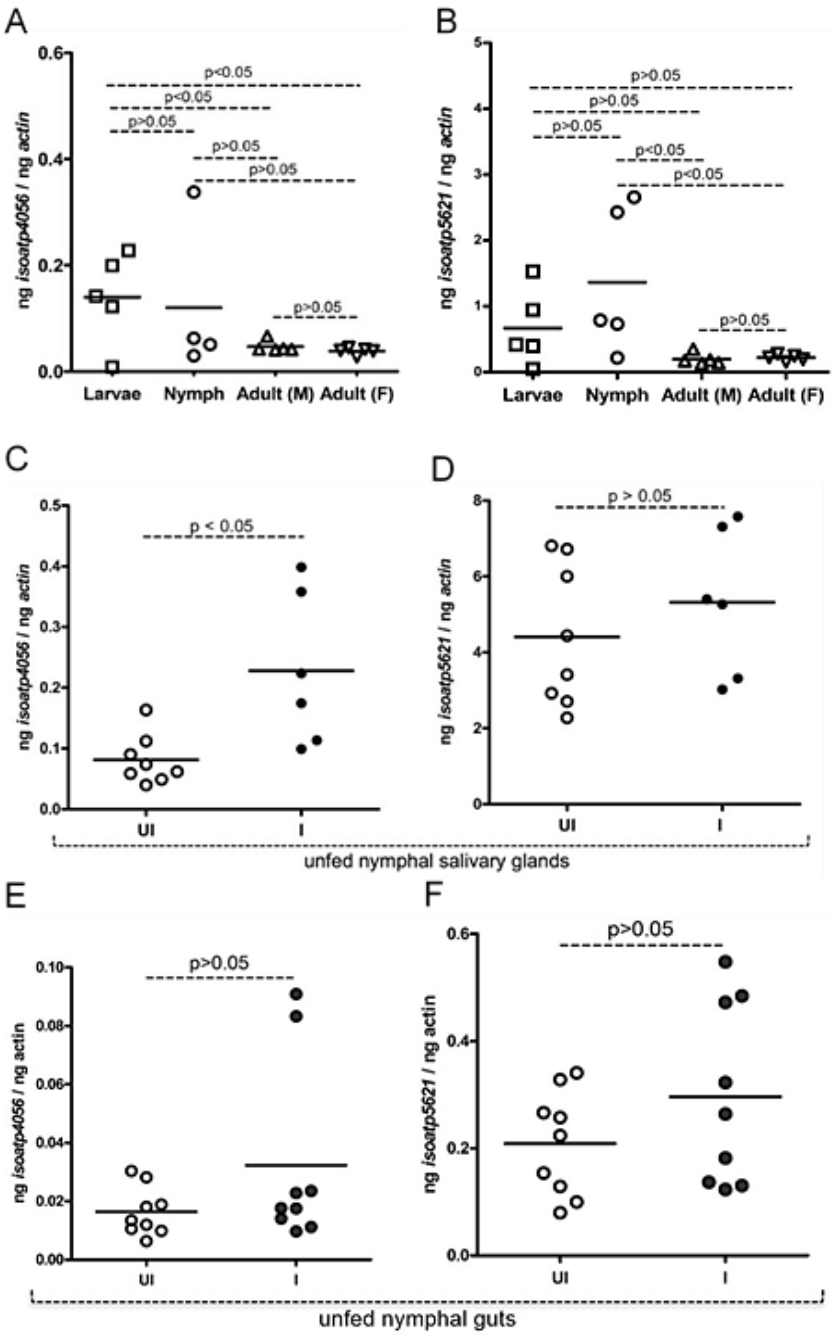

Figure 6. Transcripts of i*soatp4056* is upregulated in salivary glands of unfed *A. phagocytophilum*-infected *I. scapularis* nymphal ticks

QPCR analysis showing transcript level expression of *isoatp4056* (A) and *isoatp5621* (B) at different tick development stages in unfed uninfected ticks. Expression of *isoatp4056* (C) and *isoatp5621* (D) in unfed salivary glands of uninfected and *A. phagocytophilum* infected tick. Expression of *isoatp4056* (E) and *isoatp5621* (F) in unfed guts of uninfected and *A. phagocytophilum* infected ticks.

survival in tick cells. It has been experimentally shown that human OAT, which is structurally similar to OATPs, can transport xanthurenic acid (XA) (Uwai and Honjo, 2013). Ticks encode an enzyme kynurenine aminotransferase (KAT) that could participate in the synthesis of xanthurenic acid and kynurenic acid. Figure 10 shows the tryptophan catabolism pathway adopted and simplified from KEGG Pathways online database (KEGG:IscW_ISCW005441). Table 1 lists the VectorBase / GenBank accession numbers of *I. scapularis* putative genes that are involved in tryptophan metabolism, which suggests the presence of multiple enzymes in *I. scapularis* genome that are involved in tryptophan metabolism. Further, experiments were performed to understand whether *A. phagocytophilum* has any effect on the expression of kynurenine aminotransferase (KAT, EC 2.6.1.7). First, the transcript levels of *kat* were compared

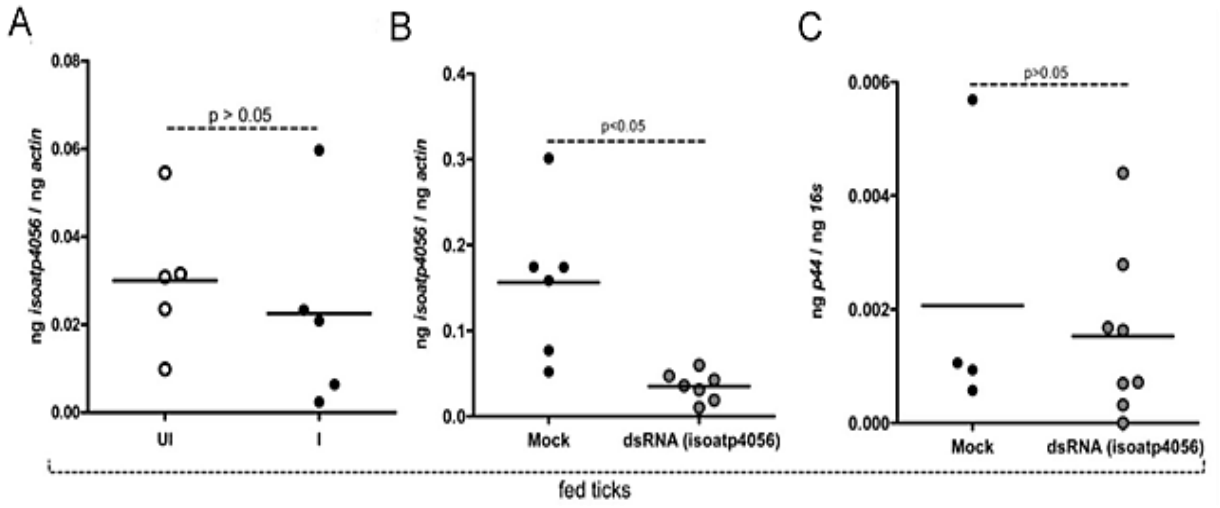

Figure 7. Isoatp4056 has no role in *A. phagocytophilum* acquisition from murine host to ticks

(A) QRT-PCR analysis showing expression of *isoatp4056* in ticks during acquisition in uninfected and *A. phagocytophilum*-infected nymphal ticks. (B) The *isoatp4056* mRNA transcript levels in ticks treated with mock or *isoatp4056*-dsRNA during acquisition is shown. (C) *A. phagocytophilum* burden in mock or dsRNA-treated ticks during acquisition (48 h post repletion) is shown. The mRNA levels of *oatps* were normalized to tick beta-*actin* mRNA levels and levels of P44 (*A. phagocytophilum* gene) were normalized to tick 16S levels. Open circle represents uninfected (UI) and closed circles represent infected (I) ticks in panel A. In panels B and C, closed black circle represents infected -mock-treated and closed gray circle represents infected-*isoatp4056*-dsRNA- treated ticks. Each circle represents one tick. P value from non-paired Student's t-test is shown.

during different tick developmental stages. QRT-PCR analysis revealed that *kat* expression is evident in all stages of tick developmental life cycle (Figure 11A). Larvae showed significant *kat* gene expression ($P < 0.05$) when compared to nymphs and male and female adults (Figure 11A). Also, nymphs showed significantly increased ($P < 0.05$) mRNA transcript levels than adult males but not adult females (Figure 11A). Adult females show significantly ($P < 0.05$) higher levels of KAT when compared with adult males (Figure 11A). Next, *kat* expression was analyzed in salivary glands isolated from *A. phagocytophilum* infected unfed nymphs and uninfected controls. It was noticed that *kat* mRNA transcript expression is significantly increased ($P < 0.05$) in *A. phagocytophilum*-infected salivary glands in comparison to its expression in salivary glands from uninfected control (Figure 11B). These results suggest that KAT is involved in *A. phagocytophilum* colonization in the salivary glands of unfed ticks.

2.2.6 RNAi of *kat* Expression Affects *A. phagocytophilum* Burden and Expression of *isoatp4056* in Tick Cells

Since results in the previous section noted that *kat* mRNA transcripts were increased upon *A. phagocytophilum* infection, *kat*-silencing experiments were performed in tick cells by RNA interference using double-stranded RNA targeted against *kat* gene. QRT-PCR analysis revealed significant ($P < 0.05$) decrease in *kat* mRNA levels in the *A. phagocytophilum*-infected *kat*-dsRNA-treated tick cells in comparison to the mock-treated controls tick cells (Figure 12A). No morphological differences were noted between *kat*-dsRNA or mock-treated cells at both 4 and 24 h post-transfection treatment and 24 h post-*A. phagocytophilum* infection (48 h post-transfection) (Figure 13).

It was also noticed that significant ($P < 0.05$) low levels of *isoatp4056* expression was evident in *kat*-ds-RNA transfected cells when compared to the mock controls (Figure 12B). Simultaneous silencing of *kat* and *isoatp4056* revealed significantly ($P < 0.05$) reduced levels of both *kat* (Figure 12C), and *isoatp4056* (Figure 12D) transcript levels. No significant morphological changes were noted in cells that had double

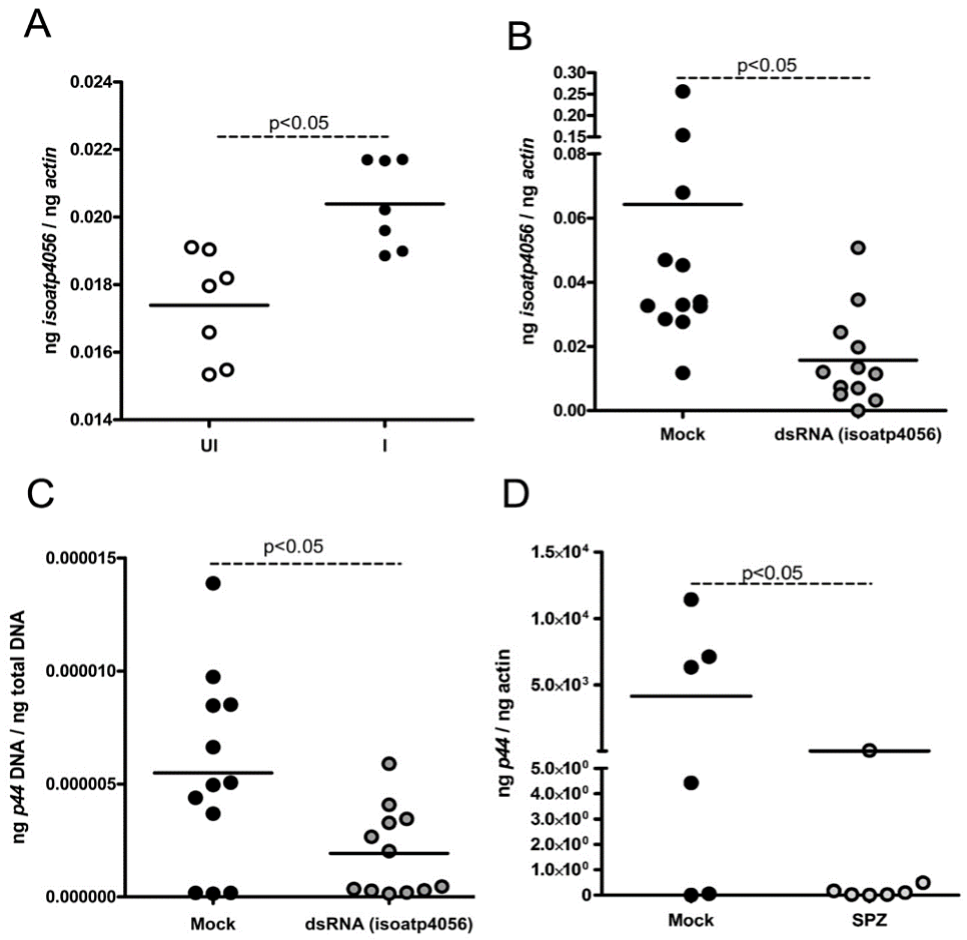

Figure 8. RNAi-mediated silencing of *isoatp4056* or OATP-inhibitor treatment in tick cells affects *A. phagocytophilum* growth and survival

(A) QRT-PCR analysis showing expression of *isoatp4056* upon *A. phagocytophilum* infection (A) or upon treatment of tick cells with mock or *isoatp4056*-dsRNA (B) is shown. UI indicates uninfected and I indicate *A. phagocytophilum* infected tick cells. (C) *A. phagocytophilum* burden in mock or *isoatp4056*-dsRNA-treated tick cells is shown. The data in (B) and (C) are from *A*. *phagocytophilum*-infected ISE6 tick cells treated with mock or *isoatp4056*-dsRNA. Each circle represents data from one independent culture plate well. The mRNA levels of *isoatp4056* are normalized to tick beta-*actin* levels and the levels of P44 (*A. phagocytophilum* burden) were normalized to tick total DNA levels. (D) *A. phagocytophilum* burden in mock or 100 µM of OATP inhibitor ± -sulfinpyrazone treated (SPZ) tick cells is shown. P value from non-paired Student's t-test is shown.

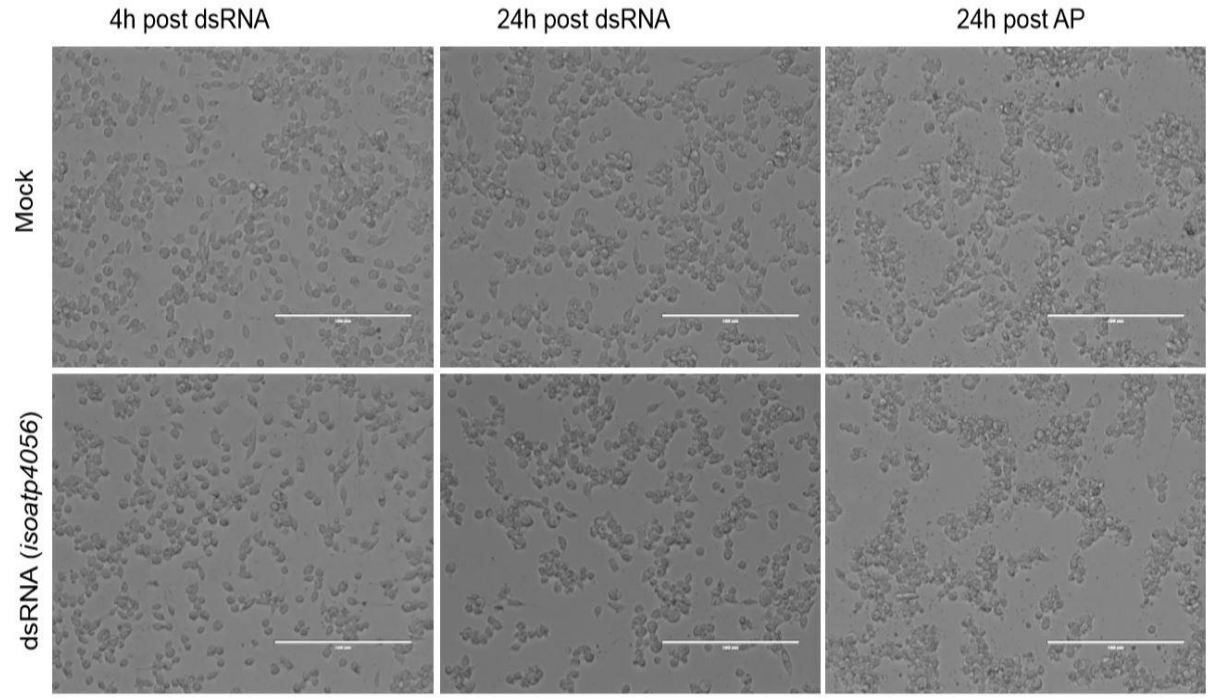

Figure 9. Tick cell treatment with *isoatp4056*-dsRNA showed no morphological changes

Representative images of *A. phagocytophilum*-infected mock treated or *A. phagocytophilum*-infected *isoatp4056*- dsRNA treated ticks cells at 4 h and 24 h before infection and 24 h post-infection is shown. Scale on each image indicates 200 µm.

silencing for *kat* and *isoatp4056* expression when compared to mock-treated cells (Figure 13). In addition, significant ($P < 0.05$) reduction in the bacterial burden was noted in both groups of *A. phagocytophilum*-infected tick cells treated with either *kat*-dsRNA alone (Figure 12E) or in combination with *isoatp4056*-dsRNA (Figure 12F). Collectively these results suggest an interesting interplay between KAT and IsOATP4056 signaling that is critical for the survival and colonization of *A. phagocytophilum* in ticks cells.

2.2.7 Exogenous Addition of XA Induces *isoatp4056* Expression and *A. phagocytophilum* Growth in Tick Salivary Glands

This study further determined, whether addition of exogenous xanthurenic acid (XA) has any impact on *isoatop4056* expression and *A. phagocytophilum* burden in tick cells. Tick cells were either treated with XA alone or Ro-61-8048 (inhibitor of XA biosynthesis (Lima et al., 2012; Rover et al., 1997)) or a combination of both in an increasing dose (1,10, and 100 µM) and infected with *A. phagocytophilum* (refer experimental procedures section). QRT-PCR analysis shows that expression of *isoatp4056* (Figure 14A) and *A. phagocytophilum* burden (Figure 14B) were significantly ($P < 0.05$) increased in tick cells with 100 µM treatment of XA when compared to the mock controls. No significant difference was observed in *isoatp4056* expression levels (Figure 14C) and *A. phagocytophilum* burden (Figure 14D) in infected-tick cells treated with XA and inhibitor XA biosynthesis (Ro-61-4048). Expression of *isoatp4056* did not show any difference with Ro-61-8048 treatment alone on tick cells (Figure 14E). To confirm the previous observations, tick cells were treated with either XA (100 µM) or mock solutions in equal volumes and infected these cells with GFP-*A. phagocytophilum.* Tick cells were processed after 48 h post-treatment and were processed for fluorescence microscopy and fluorometer measurements. Fluorometry analysis detected significantly ($P < 0.01$) increased fluorescence in XA-treated (100 µM) tick cells when compared to mock-treated tick cells (Figure 15A). Further, an immunoblotting analysis was performed that shows increased GFP protein levels in XA-treated tick cells in comparison to mock-treated controls. Total protein profile (Ponceau S stain) images serves as a loading control (Figure 15B). Tick cells treated with XA showed numerous GFP-positive cells as compared to control mock-treated cells (Figure 15C). Excitation and emission spectrum data for tick cells treated with XA or mock and infected with GFP-*A. phagocytophilum* (Figure 15D) shows consistent wavelengths for excitation (470 nm) and emission (510 nm) respectively for the GFP signal.

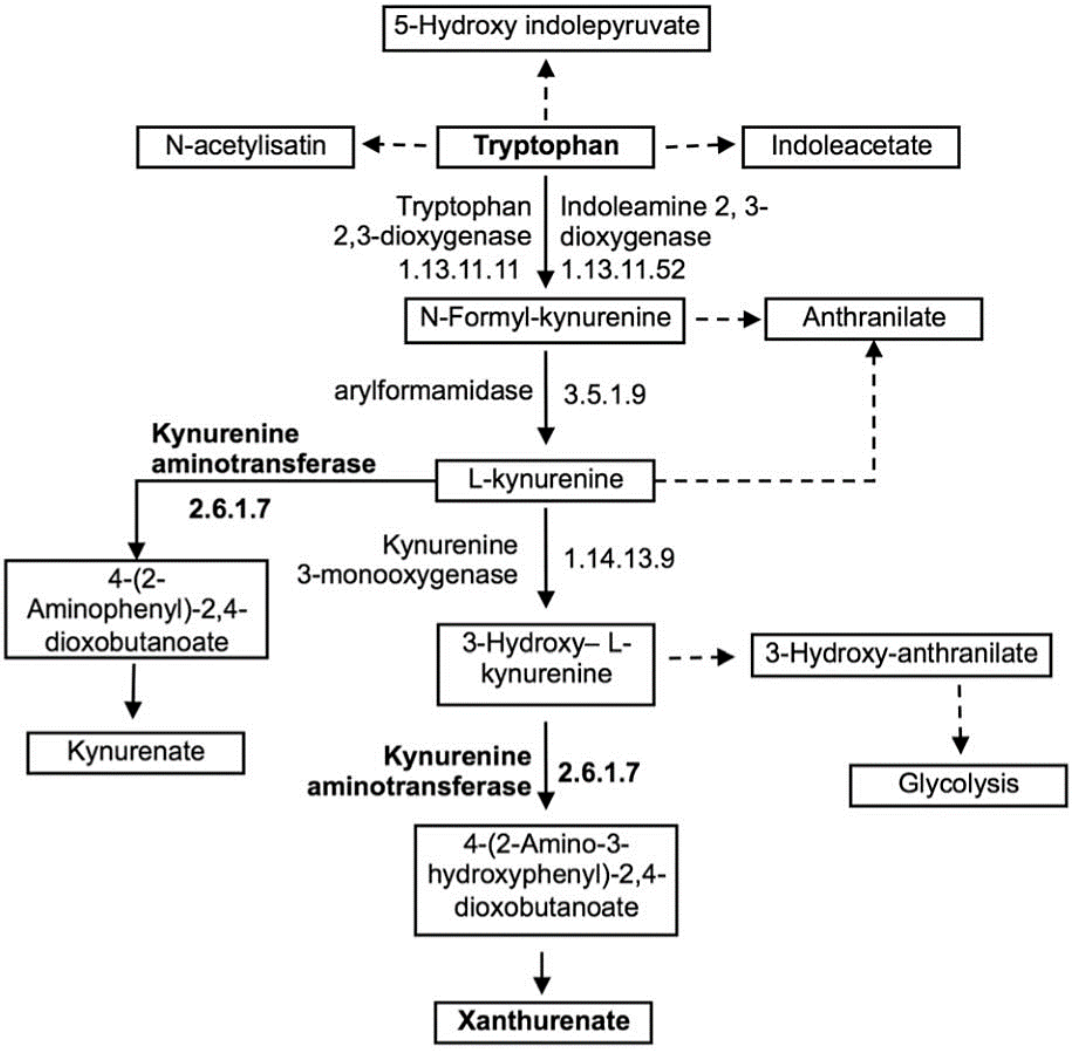

Figure 10. Putative tryptophan metabolism pathway in *Ixodes scapularis* ticks

Tryptophan pathway was modified to simple format from KEGG pathway: isc00380 for the purpose of this study. Xanthurenate and kynurenate are some of the products that are produced from this pathway. Kynurenine aminotransferase (kat), xanthurenate and tryptophan are shown in "bold" text.

Table 1. VectorBase / GenBank accession numbers for *I. scapularis* putative genes involved in tryptophan metabolism

Enzyme Number	Enzyme Name	Accession Number	
		VectorBase	**GenBank**
EC:1.13.11.11	Tryptophan 2,3-dioxygenase	ISCW02183	XM_002408230
EC:1.13.11.52	Indoleamine 2,3-dioxygenase	Not found	Not found
EC:3.5.1.9	Arylformamidase	ISCW007881	XM_002408230
EC:1.14.13.9	Kynurenine 3-monooxygenase	ISCW011595	XM_002411632
EC:2.6.1.7	Kynurenine aminotransferase	ISCW012663	XM_002401267

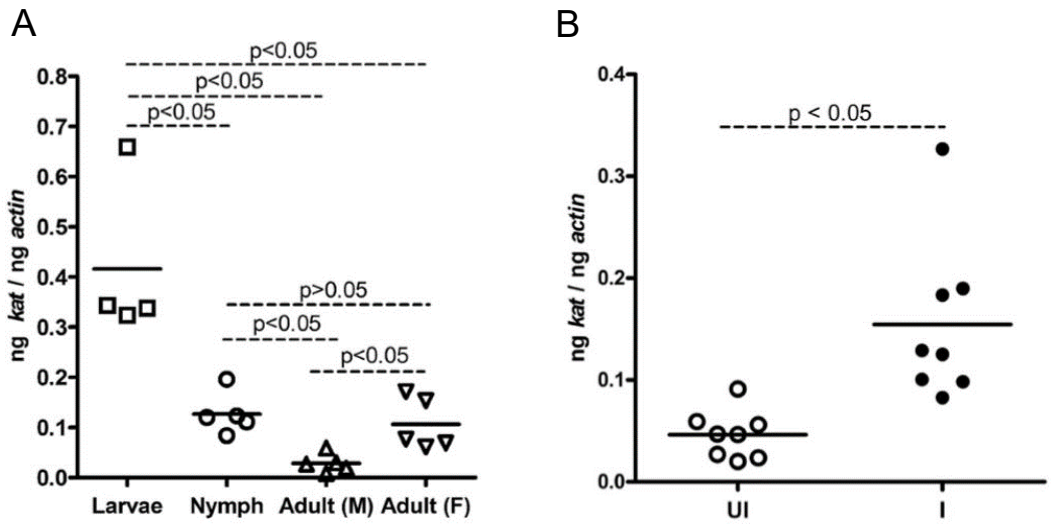

Figure 11. *Anaplasma phagocytophilum* up-regulates kynurenine aminotransferase (*kat*) gene expression in unfed *I. scapularis* salivary glands

Quantitative RT-PCR analysis showing expression of *kat* in different developmental stages in uninfected unfed ticks (A) or in the salivary glands (B) of uninfected (UI) and *A. phagocytophilum*-infected (I) unfed nymphs is shown. In panel A, data for larvae samples was obtained from 5–7 pooled ticks. Open circle represents uninfected (UI) and closed circles represents infected (I) ticks. Each circle represents one tick. Expression of *kat* mRNA was normalized to tick beta-*actin*. P value from non-paired Student's t-test is shown.

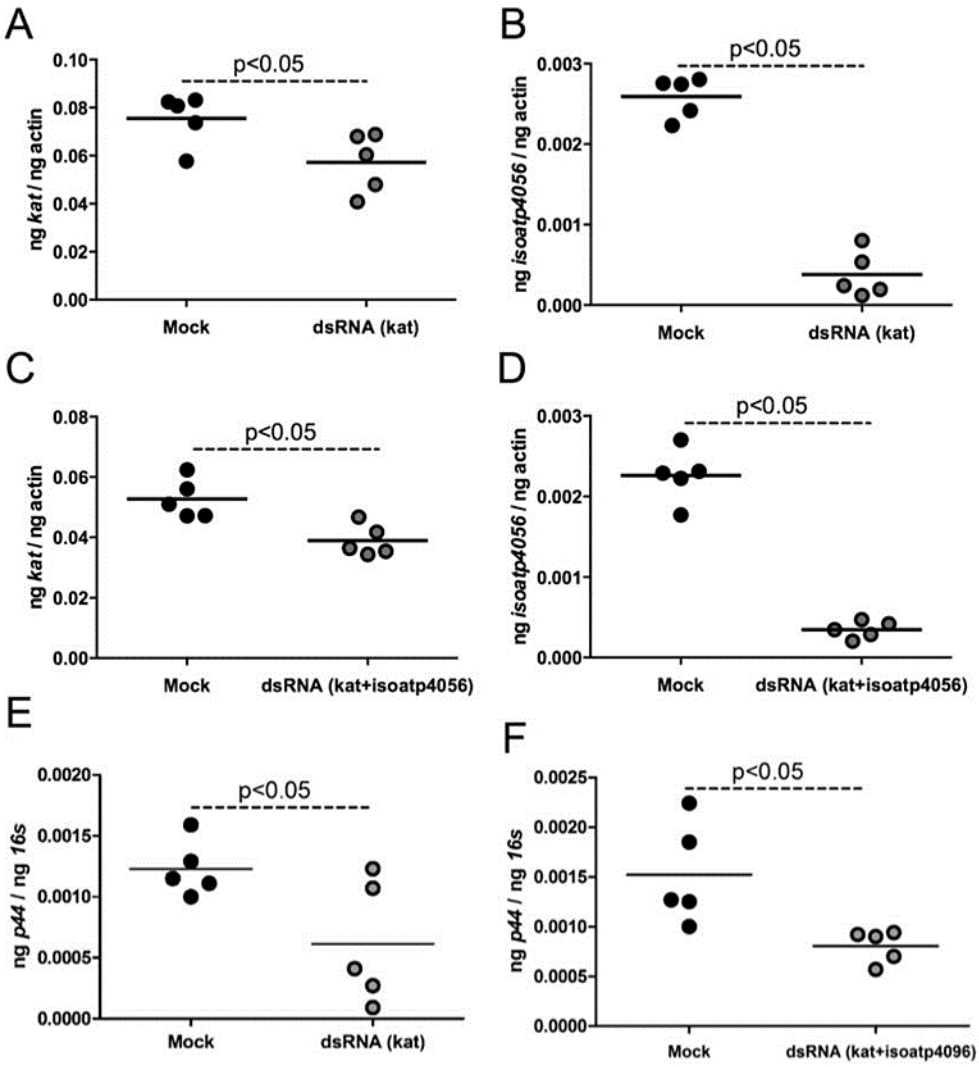

Figure 12. RNAi-mediated silencing of *kat* gene in tick cells affects *A. phagocytophilum* growth and *isoatp4056* expression

QRT-PCR analysis showing expression of *kat* (A and C) or *isoatp4056* (B and D) in *A. phagocytophilum*-infected mock or *kat*- (A and B) or *kat* + *isoatp4056*-dsRNA-treated (C and D) tick cells is shown. *A. phagocytophilum* burden in mock or *kat*- (E) or *kat* + *isoatp4056*-dsRNA-treated (F) tick cells is shown. Each circle represents data from one independent culture plate well. Black circles indicate data from mock-treated and gray circles represents data from either *kat*-dsRNA-treated or *kat* + *isoatp4056*-dsRNAtreated tick cells. The mRNA levels of *kat* or *isoatp4056* are normalized to tick beta-*actin* levels and the levels of P44 (*A. phagocytophilum* burden) were normalized to tick 16S levels. P value from non-paired Student's t-test is shown.

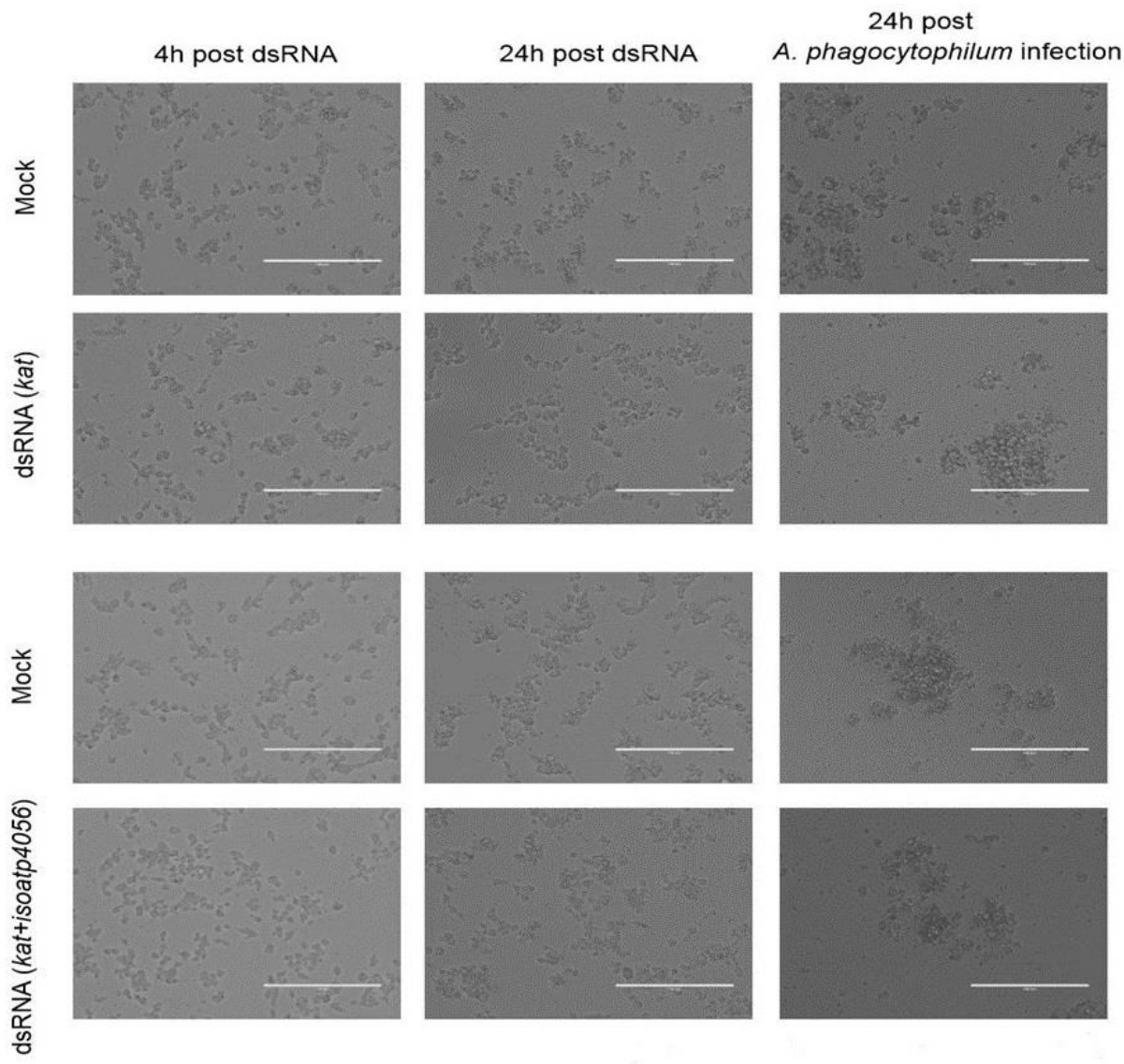

Figure 13. Silencing of *kat*- or *kat+isoatp4056*-dsRNA treatment showed no morphological changes in ISE6 tick cells

Representative images (3 images for each group) of *A. phagocytophilum*-infected mock treated or *A. phagocytophilum*-infected *kat*- (A) or *kat+isoatp4056*-dsRNA (B) treated at 4 h and 24 h before infection and 24 h post- infection is shown. Scale on each image indicates 200 µm.

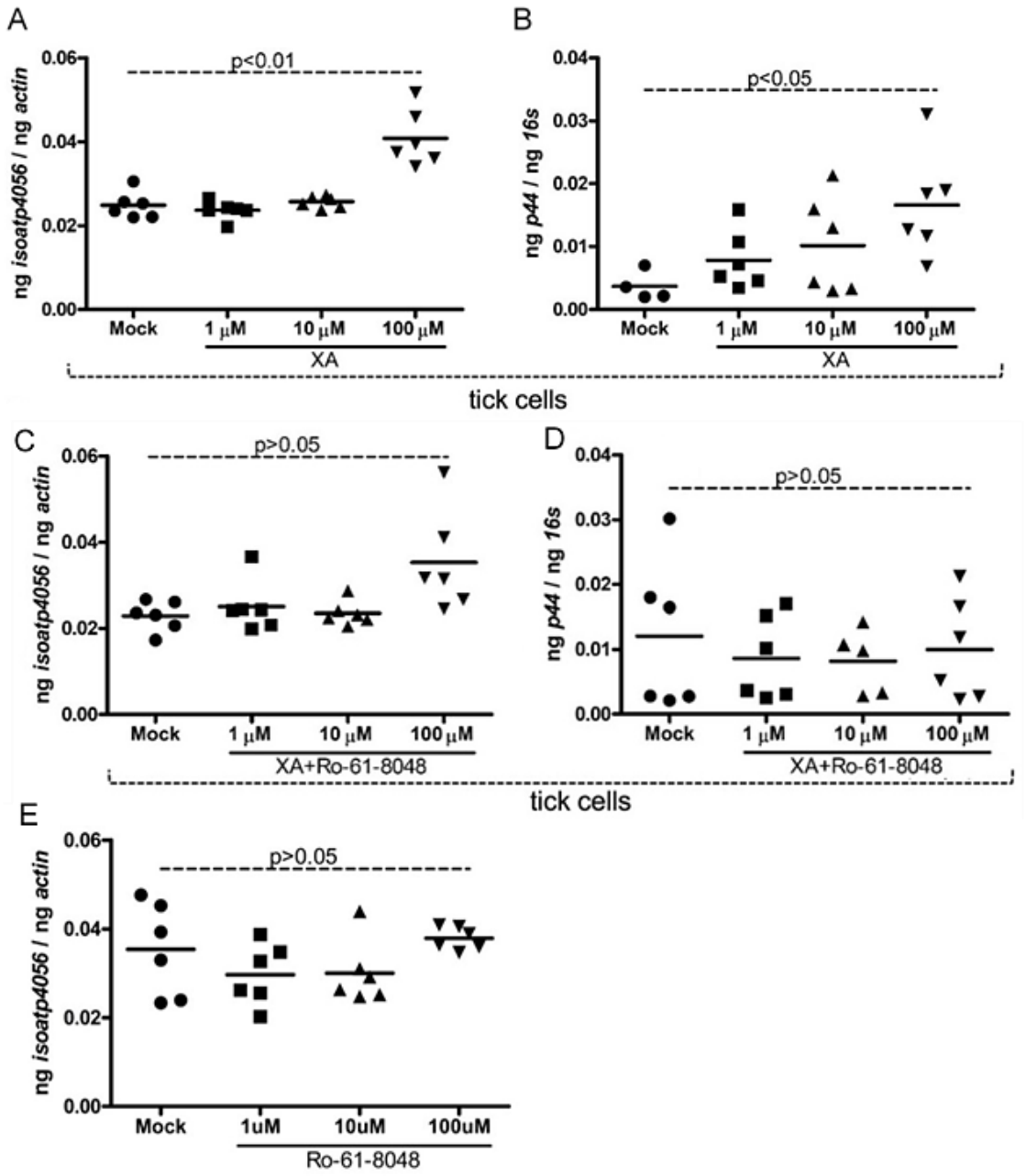

Figure 14. Exogenous treatment with XA induces *isoatp4056* expression and *A. phagocytophilum* burden in tick cells

QRT-PCR analysis showing expression of *isoatp4056* (A and C) and bacterial loads (B and D) upon treatment with xanthurenic acid (A and B) or xanthurenic acid plus Ro-61-8048 (C and D) or with only Ro-61-8048 (E) (an inhibitor of XA biosynthesis) at different doses in *A. phagocytophilum*-infected tick cells is shown. Each circle/square/triangle/inverted triangle represents data from one independent well of the culture plate performed in duplicates. The mRNA levels of kat or *isoatp4056* are normalized to tick beta-*actin* levels and the levels of P44 (*A. phagocytophilum* burden) were normalized to tick 16S levels. P value from non-paired Student's t-test is shown.

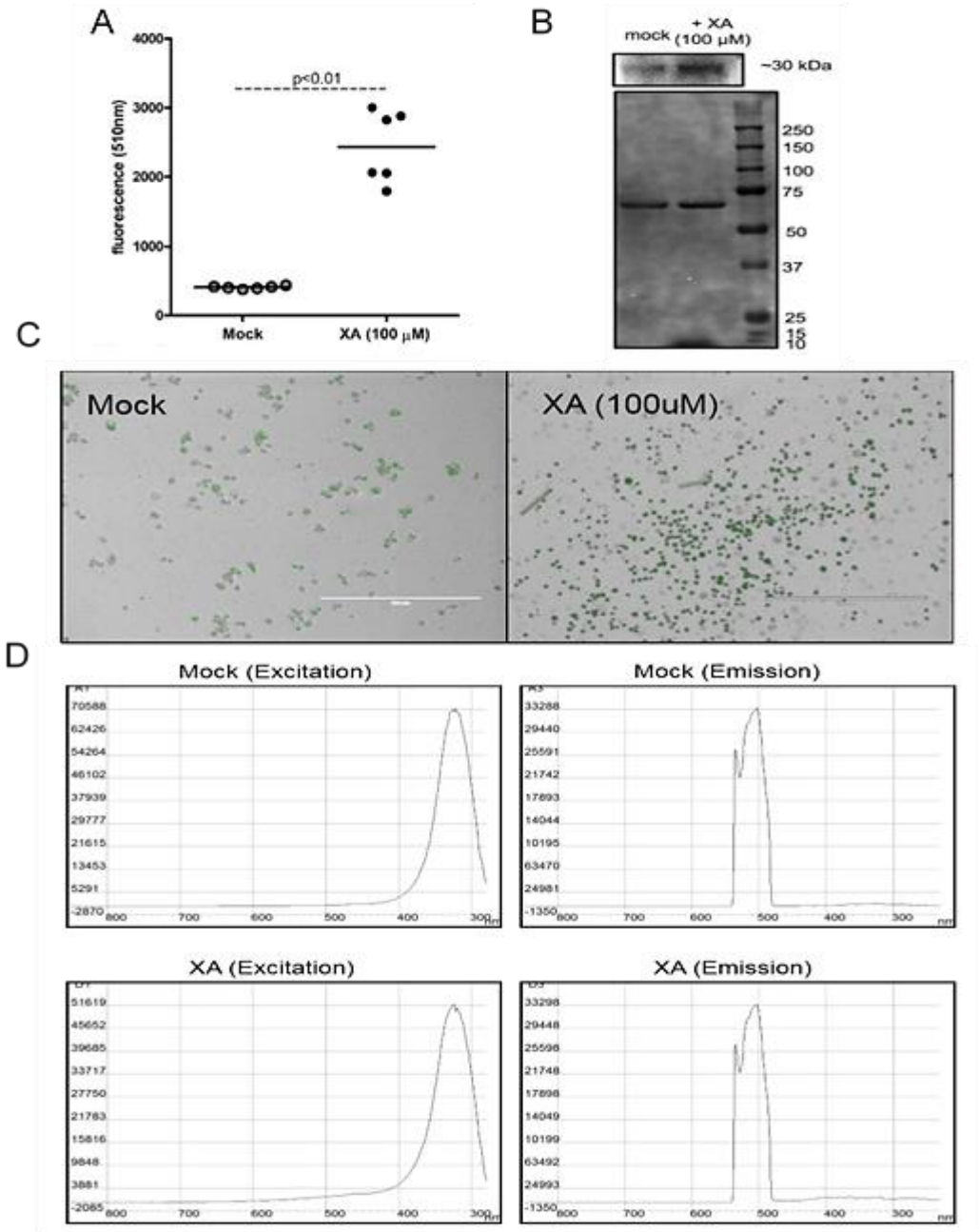

Figure 15. Exogenous treatment with XA increases *A. phagocytophilum* burden in tick cells

(A) Fluorometer measurements of tick cells infected with GFP-*A. phagocytophilum* treated with either mock or 100 µM XA at 510 nm is shown. Each circle represents data from one independent well of the culture plate performed in duplicates. (B) Immunoblotting analysis with anti-GFP antibody showing levels of GFP protein in tick cells infected with GFP-*A. phagocytophilum* treated with either mock or XA (100 µM). Levels of proteins observed on Ponceau stained membrane (used for immunoblotting analysis) serves as a loading control. (C) Representative images of tick cells infected with GFP-*A. phagocytophilum* treated with mock or XA (100 µM) is shown. Scale bar represents 400 µm. GFP fluorescence is evident as green color in the image. (D) spectrum data for both excitation (384 nm) and emission (510 nm) from fluorometer for tick cells infected with GFP-*A. phagocytophilum* treated with mock or XA (100 µM) is shown.

To further test whether *isoatp4056* expression and *A. phagocytophilum* burden are impacted by XA in ticks, microinjection into the body of *A. phagocytophilum*-infected unfed ticks (nymphs) was performed with either 100 µM of XA or mock control. After 24 h post-microinjection, these recovered ticks were dissected for salivary glands and then processed for QRT-PCR analysis. The expression levels of *isoatp4056* (Figure 16A) and *A. phagocytophilum* burden (Figure 16B) were significantly ($P < 0.05$) increased in the salivary glands of XA-injected ticks when compared to mock-injected ticks. Collectively, these results indicate that XA plays an important role in the regulation of *isoatp4056* expression and is essential for the colonization of *A. phagocytophilum* in the tick salivary glands.

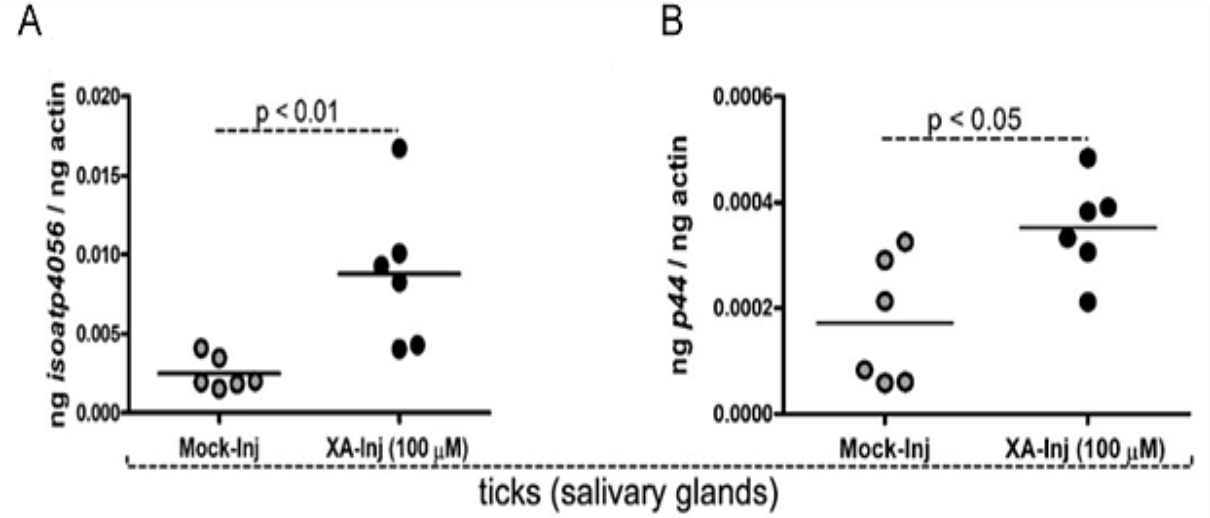

Figure 16. Exogenous treatment with XA induces *isoatp4056* expression and *A. phagocytophilum* burden in tick salivary glands

QRT-PCR analysis showing levels of *isoatp4056* (A) or *A. phagocytophilum* bacterial burden (B) after 24 h post-microinjection in mock- or XA-injected *A. phagocytophilum*-infected tick salivary glands is shown. Each circle represents data from pair of salivary glands isolated from individual unfed nymphal ticks. The mRNA levels of *isoatp4056* are normalized to tick beta-*actin* levels and the levels of P44 (*A. phagocytophilum* burden) were normalized to tick *actin* levels. P value from non-paired Student's t test is shown.

2.2.8 *Anaplasma phagocytophilum* and XA Influences *isoatp4056* Promoter

Previous results showed that the presence of *A. phagocytophilum* and the addition of XA increased the expression of *isoatp4056*. To further understand if these factors effect *isoatp4056* gene at promoter level, a putative *isoatp4056* promoter region in *I. scapularis* genome from the NCBI GenBank sequence DS922985 was identified and characterized. The position of −191 and −142 is labeled considering + 1 for the first nucleotide of exon 1 (E1) as shown in Figure 17. Electrophoretic mobility shift assay (EMSA) with nuclear extracts prepared from *A. phagocytophilum* infected and uninfected ticks was performed. Figure 18A shows an increased binding/interaction of biotinylated labeled *isoatp4056* DNA promoter probe with proteins in the nuclear extracts prepared from *A. phagocytophilum*-infected nymphal ticks in comparison to the proteins in the nuclear extracts prepared from uninfected nymphal ticks. This data demonstrates the impact of *A. phagocytophilum* infection in the regulation of *isoatp4056* gene expression at the promoter level. No shift/interaction was noted when the same probe was incubated with XA alone and in the absence of nuclear extracts, ruling out the possibility of direct interaction of XA with the promoter region of the *isoatp4056* gene (Figure 18B). However, an apparent shift of the *isoatp4056* promoter probe was evident when nuclear extracts prepared from XA (100 µM) treated *A. phagocytophilum* infected ticks cells (Figure 18B). Also, no shift was observed when the *isoatp4056*-probe is incubated with nuclear extracts prepared from *A. phagocytophilum*-infected tick cells treated with mock (Figure 18C). These results indicate that *A. phagocytophilum* and XA play a crucial role in mediating *isoatp4056* gene expression important for *A. phagocytophilum* survival in the ticks.

Figure 17. Schematic representation of the *isoatp4056* genomic region comprising of 11 exons

Exons indicated as E1-11 and a putative promoter and a TATA-binding region is shown. DS922985 indicates the GenBank accession number for the genomic sequence. The position of −191 and −142 is labeled considering + 1 for the first nucleotide of exon 1 (E1). Figure is not to scale.

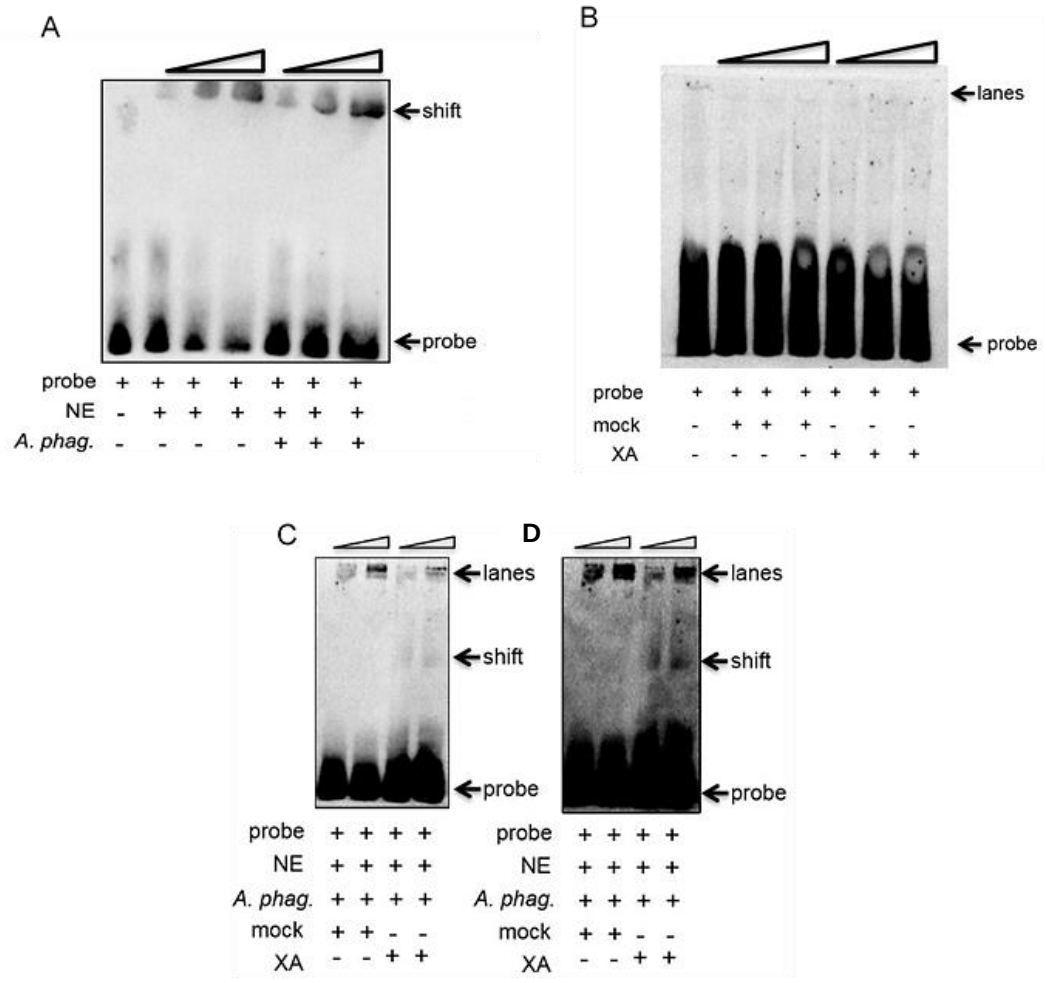

Figure 18. *Anaplasma phagocytophilum* and XA promotes increased interaction/binding of tick nuclear proteins on the *isoatp4056* promoter

(A) EMSA gel image showing increased shift of *isoatp4056* TATA-binding promoter region in the presence of *A. phagocytophilum*. EMSAs were performed with the biotin-labeled *isoatp4056* promoter TATA-binding regions and uninfected or *A. phagocytophilum*–infected ticks nuclear extract. Wedges indicate increasing amounts of nuclear extracts (1, 2, 4 µg). Probe and shifted bands are labeled. (B) EMSAs were performed with the biotin-labeled *isoatp4056* promoter TATA-binding region in the presence of mock or XA. *isoatp4056* probes are indicated with arrows. Wedges indicate increasing amount of mock or XA (1, 10, 100 µM). (C) EMSAs performed with the biotin-labeled *isoatp4056* promoter TATA-binding region and mock or XA treated *A. phagocytophilum*–infected tick cell nuclear extracts. (D) shows the image used in panel (C) with increased intensity. Wedges indicate increasing amounts of nuclear extracts (1, 1.5 µg). Gel shifts (in different intensities) and the *isoatp4056*-free probes are indicated with arrows.

2.3 DISCUSSION

To develop novel strategies for combating tick-borne diseases, it is necessary to understand how tick-borne pathogens survive the extended periods in nature during different developmental stages of a vector life cycle, including unfed starvation stage. Several studies have focused on understanding vector-host-pathogen interactions with emphasis on pathogen-associated remodeling of cytoskeleton, apoptosis inhibition, immune system manipulation (Sultana et al., 2010, de la Fuente et al., 2016a; de la Fuente et al., 2016b) and cellular resource manipulation (Nelson et al., 2008). So far, no studies have addressed the role of highly conserved OATPs in arthropod-pathogen interactions. This study provides a novel understanding on how an intracellular pathogen manipulates these highly conserved organic anion transporter polypeptides (OATPs) and tryptophan pathway for its own benefit in order to survive and colonize inside the vector host. This study provides evidence that during the unfed stage, where *A. phagocytophilum* is transstadially maintained, *isoatp4056* and *kat* gene transcripts are increased in tick salivary glands (Figure 19). Higher levels of IsOATP4056 in the ticks can cause the targeting of these transporters to localize on the plasma membrane; this can further lead to increased import of extracellular xanthurenic acid (XA) into the *A. phagocytophilum* infected cells from extracellular fluids/environment. Increased *kat* expression will cause more production of intracellular XA that could influence *isoatp4056* promoter activity and expression of the transporter protein. Combination of these two events (higher expression of *kat* and *isoatp4056*) with an ultimate goal of production and import of higher amounts of XA into the cell results in *A. phagocytophilum* survival and colonization of tick salivary glands in unfed ticks.

It is evident from the data that out of nine OATPs only one, i.e., *isoatp4056* was specifically affected in *A. phagocytophilum* infected tick salivary glands. This observation shows the importance on the role played by this particular OATP. The upregulation of *isoatp5621* in *A. phagocytophilum* infected whole ticks but not in salivary glands suggests that this OATP may have role in other tick tissues, perhaps inter-organ communication during infection. Previous studies have reported that, during acquisition of *A. phagocytophilum,* the bacterium enters the tick gut, migrates to hemocoel and

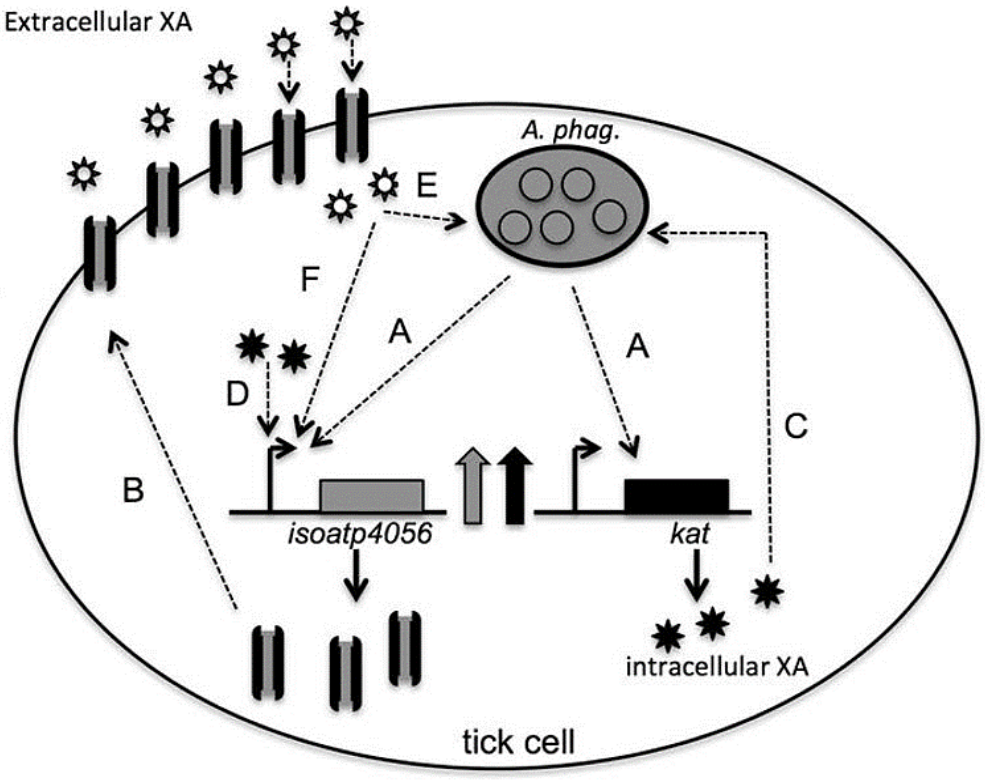

Figure 19. Model for the role of IsOATP4056 and KAT in *A. phagocytophilum* survival in tick cells

Anaplasma phagocytophilum up-regulates *isoatp4056* and *kat* genes upon entry into tick salivary gland cells (A). Which results in the increased production of IsOATP4056 that could be targeted to the plasma membrane as a transporter for intake of extracellular XA shown as open asterisk (B). Upregulation of *kat* gene results in increased production of intracellular XA (closed asterisk) that could facilitate *A. phagocytophilum* replication and colonization (C) and/ or influence *isoatp4056* promoter to make more IsOATP4056 (D). Intake of extracellular XA (open asterisk) could also participate in the increase of *A. phagocytophilum* bacterial burden (E) or regulation of *isoatp4056* promoter (F). *A. phagocytophilum* is shown as morulae in the vacuole (gray color). Picture is not drawn to the scale.

finally colonize in salivary glands (Hodzic et al., 1998). Radulovic and coworkers in 2014 have reported higher mRNA expression of *isoatp4056* in salivary glands as compared to midgut tissues (Radulovic et al., 2014). This study also noticed similar results (Figure 6C and 6E) with the expression of *isoatp4056.* RNAi and inhibitor studies collectively

suggest that *A. phagocytophilum* uses only this very specific OATP (*isoatp4056*) for colonization and survival in the tick vector host.

The *isoatp4134* mRNA transcripts are reported to be not expressed in any other tissues except salivary glands (Radulovic et al., 2014), but the results from this study did not show any changes in *isoatp4134* transcript levels upon *A. phagocytophilum* infection in whole ticks (Figure 5). Other OATPs, *isoatp0726*, *isoatp2114*, *isoatp2116*, *isoatp4548*, *isoatp4550* and *isoatp5126* are reported to be differentially and ubiquitously expressed in various tick tissues (Radulovic et al., 2014). The data showed no difference in the expression of these OATPs in the presence of *A. phagocytophilum* (Figure 5). This provides further support that *A. phagocytophilum* uses a very specific OATP (*isoatp4056*) for its colonization and survival in the tick salivary glands.

Previous studies have reported that *A. phagocytophilum* resides in a tick as a beneficial facultative micro-organism and increases tick survival at cold temperatures by increasing the expression of *I. scapularis* antifreeze glycoprotein (IAFGP) (Neelakanta et al., 2010) and induces actin phosphorylation to control arthropod *salp16* gene expression (Sultana et al., 2010). In addition, this study shows the interplay between organic anion transporting polypeptides (OATPs), xanthurenic acid (XA) and its enzyme kynurenine aminotransferase (kat) during vector-pathogen interactions. Previous studies in mosquitoes have demonstrated that XA induces gametogenesis in *Plasmodium falciparum* and is known as gametogenesis activating factor (GAF) (Arai et al., 2001; Bhattacharyya and Kumar, 2001; Billker et al., 1998; Garcia et al., 1998). The knowledge of exact interaction of XA in *Plasmodium*-mosquito remains still unclear. This study brings new insight that IsOATP4056 may act as a novel transporter for XA. The EMSA study (Figure 18) proposes that XA may play a role as a co-factor, perhaps to activate some of the transcription factor(s) that may bind to the *isoatp4056* promoter. This notion is further supported by the observation of reduced expression of *isoatp4056* mRNA transcript in *kat*-dsRNA-treated tick cells (Figure 8B) and increased expression of *isoatp4056* upon exogenous addition of XA (Figure 14A).

Xanthurenic acid is naturally present in vertebrate blood (0.7 µM) and urine (5-10µM) (Cavill, 1967; Williams et al., 1984). Ticks may acquire XA from blood while feeding on vertebrate hosts and may retain that through different developmental stages.

The role of exogenous XA from the blood of the vertebrate host, in unfed ticks, cannot be neglected and needs further investigation. This will unravel various exciting aspects of *A. phagocytophilum* survival and colonization in these ticks.

In conclusion, this work provides novel information on the modulation of the interplay between organic anion transporting polypeptide (OATPs), the tryptophan pathway metabolite, xanthurenic acid (XA), and it catalytic enzyme kynurenine aminotransferase (KAT) by *A. phagocytophilum* for its survival, replication and colonization in the tick vector host.

2.4 EXPERIMENTAL PROCEDURES

2.4.1 Bacterial Isolates, Ticks and Tick Cell Line

Anaplasma phagocytophilum isolate NCH-1 was used in the studies that involved *in vivo* work with ticks and mice. *A. phagocytophilum* isolate HZ and isolate HGE1-GFP were used in the *in vitro* cell line experiments. Wherever necessary, NCH-1 and HZ isolates are referred as *A. phagocytophilum*, and HGE1-GFP is referred as GFP-*A. phagocytophilum*. *Escherichia coli* DH5alpha strain was used as a cloning host for generating different plasmids. The laboratory-reared specimens of *I. scapularis* ticks were used throughout the study. Ticks used in this study are larvae and nymphs and were obtained from a tick colony maintained either at the Department of Epidemiology and Public Health, Yale University School of Medicine (New Haven, CT) and/or Department of Entomology, Connecticut Agricultural Experiment Station (New Haven, CT) or Department of Biological Sciences, Old Dominion University (Norfolk, VA) . The *I. scapularis* tick cell line ISE6 and HGE1-GFP *A. phagocytophilum* strain was a generous gift from Dr. Ulrike Munderloh at the University of Minnesota (St Paul, MN) and was maintained as described (Felsheim et al., 2006). *A. phagocytophilum* Isolate HZ-1 was a gift from Dr. Joao Pedra laboratory at the University of Maryland (Baltimore, MD) and was maintained as described (Severo et al., 2013).

2.4.2 Mice

C3H/HeN (female mice, 4–6 weeks old, Charles River Laboratories, USA) mice were used throughout this study. To obtain uninfected or *A. phagocytophilum*–infected

unfed nymphs, larvae were fed on either uninfected or *A. phagocytophilum*–infected C3H/HeN mice and ticks were allowed to molt. Tick rearing was carried out in an incubator maintained at 23 ± 2 °C, 95% relative humidity and at 14/10 hour light/dark photoperiod regiment. In acquisition experiments, dsRNA- or mock-treated uninfected nymphs were fed on *A. phagocytophilum*-infected mice and upon repletion ticks were processed further for RNA and DNA extractions. Animal husbandry was provided according to the Association for Assessment and Accreditation of Laboratory Animal Care (AAALAC) Program at the current institution. Prior to the handling of the animals, acepromazine tranquilizer was administered to minimize anxiety and/or discomfort, and all possible efforts were made to minimize animal suffering.

2.4.3 Ethics Statement

In this study, all animal work was carried out in strict accordance with the recommendations in the Guide for the Care and Use of Laboratory Animals of the National Institute of Health (NIH). The protocol used in this study (permit number: 16–017) was approved by the Old Dominion University Institutional Animal Care and Use Committee (IACUC) (Animal Welfare Assurance Number: A3172-01). The *in vitro* experiments in this study are performed based on protocols 15-012 and 15-014 approved by the Institutional Biosafety Committee (IBC), Old Dominion University, USA.

2.4.4 RNA or DNA Extractions and Quantitative Real-time PCR (QRT-PCR) Analysis

Total RNA from unfed or fed ticks were generated using the Aurum Total RNA mini kit (Bio-Rad, USA) following the manufacturer's instructions. RNA was converted to cDNA using the BioRAD cDNA synthesis kit (Bio-RAD, USA). The generated cDNA was used as a template for quantifying nine OATPs or KAT transcripts using the oligonucleotides mentioned in Table 2. To normalize the amount of the template, *I. scapularis* beta-*actin* was quantified as an internal control, using oligonucleotides as mentioned in Table 2. QRT-PCR was performed as described (Sultana et al., 2016) using CFX96 QRT-PCR machine (BioRad, USA) and iQ-SYBR Green Supermix (Bio-Rad, USA). To quantify bacterial burden in ticks, genomic DNA from *A.*

phagocytophilum–infected unfed or fed nymphs or tick cells was extracted using DNeasy kit (QIAGEN, USA) and processed for PCR with primers specific for the *A. phagocytophilum* p44 gene as shown in Supplementary Table 2. In QRT-PCR reactions, the standard curve was obtained by using 10-fold serial dilutions starting from 1 ng to 0.00001 ng of known quantities of the respective fragments.

2.4.5 dsRNA Synthesis and Tick Microinjections

The dsRNA synthesis was performed as described (Neelakanta et al., 2010; Sultana et al., 2010). Briefly, the *isoatp4056*- or *kat*-dsRNA fragments were generated by PCR using gene-specific primers containing BglII (forward primer) and KpnI (reverse primer) restriction enzyme sites using oligonucleotides mentioned in Table 2. The fragments containing *isoatp4056* or *kat* sequences were purified and cloned into BglII-KpnI sites of the L4440 double T7 Script II vector. The dsRNA's complementary to *isoatp4056* or *kat* gene sequences were synthesized using the MEGAscript RNAi Kit (Ambion Inc.) following the manufacturer's instructions. Microinjections of mock (buffer alone) or mock-DNA and *isoatp4056*-dsRNAs were performed as described (Neelakanta et al., 2010; Sultana et al., 2010). Briefly, 1 µg of L4440 vector containing *isoatp4056* sequence template, was used to prepare dsRNA. The prepared dsRNA was eluted in 50 µl of elution buffer (Ambion Inc.). Microinjections were performed (~4.2 nl/tick, 1×10^{12} molecules/µl) into the bodies of uninfected unfed nymphs. Microinjected ticks were incubated at room temperature for 2–3 hours for acclimatization in a desiccator and fed on *A. phagocytophilum*–infected or naïve mice. Repleted ticks were then analyzed for *isoatp4056* expression to determine silencing efficiency by QRT-PCR using oligonucleotides as mentioned in Table 2. Microinjections of XA into ticks were performed in a similar way. Briefly, *A. phagocytophilum*-infected unfed ticks were injected with 100 µM XA or mock solution (~4.2 nl/tick) into the tick body. Injected ticks were incubated for 24 h and then processed for salivary gland isolation followed by QRT-PCR analysis to evaluate the *isoatp4056* expression and *A. phagocytophilum* burden.

2.4.6 Tick Cell Line Experiments with Xanthurenic Acid (XA) and the Inhibitors

Anaplasma phagocytophilum HZ isolate or GFP-*A. phagocytophilum* isolate was maintained in the human promyelocytic leukemia cell line (HL-60, American Type Culture Collection, USA), and cell-free bacterial isolated from these cells were used for *in vitro* infection studies as described (Thomas and Fikrig, 2007). Both XA and Ro-61-8048, an inhibitor of XA biosynthesis (Rover et al., 1997), were purchased from Sigma (USA). OATP inhibitor (±-sulfinpyrazone) was purchased from Santa Cruz Biotechnology Inc. Stocks (10 mM) of XA or Ro-61-8048 or ± -sulfinpyrazone were made in 0.5 N NaOH solutions. A 1:10 dilution of the stocks were prepared in 1x PBS to a final concentration of 1 mM and used for all experiments. The mock solution was prepared in the same way but without XA or Ro-61-8048 or ± -sulfinpyrazone. Tick cells (1×10^5) were seeded onto 12 well plates and incubated overnight for 16–20 hours. Following incubation, tick cells were treated with different concentrations of XA or Ro-61-8048 (1, 10, 100 µM) or both or 100 µM of ± -sulfinpyrazone for 4 h followed by *A. phagocytophilum* infection. Equal volumes of mock solution (corresponding to 100 µM volume) were added to control cells. The cells were then incubated for 48 h (for XA or Ro-61-8048 treatment experiments) or 24 h (for ± -sulfinpyrazone treatment experiments) and processed further for RNA or DNA extractions to measure OATP transcripts and *A. phagocytophilum* loads.

2.4.7 Tick Cell Line Silencing Experiments

For silencing *isoatp4056* or *kat* expression in ISE6 cells, Lipofectamine transfection reagent (ThermoFisher Scientific/Invitrogen, USA) was used. Briefly, 5×10^5 tick cells were seeded in L-15B300 medium on to 12 well plates and incubated for 24 hours. At 24 h, 500 ng of dsRNA mixed with Lipofectamine reagent was added. After 6 hours of dsRNA and Lipofectamine addition, 2x L15-B300 medium was added, and plates were further incubated for an additional of 16 h. Cell-free *A. phagocytophilum* (isolated from infected HL-60 cells) was added after 24 h post transfection and cells were incubated further for another 24 h and processed for RNA or DNA extractions. Representative images (collected with EVOS FL microscope; Invitrogen/Thermo Fisher Scientific, USA) at different time points for mock or *isoatp4056*- or *kat*-dsRNA-treated tick cells are

Table 2. Oligonucleotides used in this study

Primer (5' – 3')	Gene, purpose
GGTATCGTGCTCGACTC	tick *actin*, qpcr
CAGGGCGACGTAGCAG	tick *actin*, qpcr
GCCACCCCCGCTTAGTGA	tick KAT, qpcr
CGAGATGCTCTCCCCAGITTTCT	tick KAT, qpcr
CCAGCGTTTAGCAAGATAAGAG	*Anaplasma*, qpcr
GCCCAGTAACAACATCATAAGC	*Anaplasma*, qpcr
TAAACAATTAAAAGCTTTCTT	tick 16S, qpcr
AATCGCTAAAAACGGAACITA	tick 16S, qpcr
GGGGCGACGGCTGTGT	tick, *isoap0726*, qpcr
GGGGACAGGTTGGAGGTTTCA	tick, *isoatp0726*, qpcr
GCCCAACTTACATCCTGTCCA	tick, *isoatp2114*, qpcr
CTGCACGGAGCCACAACGA	tick, *isoatp2114*, qpcr
GCGATGGGCCGTTTGTG	tick, *isoatp2116*, qpcr
GCITCCATATGCGGATGATGA	tick, *isoatp2116*, qpcr
CCGTCACGAAAACGCCTTCA	tick, *isoatp4056*, qpcr
GCTTCCACACGTCCACCTTCT	tick, *isoatp4056*, qpcr
CTCITGGAAACATCGCCGTG	tick, *isoatp4134*, qpcr
GCGATGACAGTTGCCACGA	tick, *isoatp4134*, qpcr
CATCATCTGCTCGCTAATCCCAC	tick, *isoatp4548*, qpcr
GGGCGGTTGCTTTGAGATAG	tick, *isoatp4548*, qpcr
GGACGAGAACACGCCGACA	tick, *isoatp4S50*, qpcr
CGGGGAGCGCTGTCACA	tick, *isoatp4550*, qpcr
GTGTCCGCCAGCTCCATCCT	tick, *isoatp5126*, qpcr
AGATGACGAACGGCAGAGAGGT	tick, *isoatp5126*, qpcr
GTTCATCGGAATCCTTGTGGTAGT	tick, *isoatp5621*, qpcr
GTGGCAGCITGACACAAGAAGAGT	tick, *isoatp5621*, qpcr
TGAGATCTCGCCCCTGTTGCCTGAAG	tick, *isoatp4056*, RNAi
CGGGTACCAGCACGAGGAAGATACCACA	tick, *isoatp4056*, RNAi
TGAGATCTCAAGACAGCGTCTGGGTGGAGT	tick, *kat*, RNAi
CGGGTACCGTTGTGTGGAGTGTGGTGGCA	tick, *kat*, RNAi
GCCTCGAGCTACGGCGCGAGTGTATACAAAACGAC TTTGTCCTCTTGTGC	tick, *isoatp4056*, EMSA probe
GCACMGAGGACAAAGTCGTTTTGTATACACTCGC GCCGTAGCTCGAGGC	tick, *isoatp4056*, EMSA probe

shown in Figures 9 and 13. Silencing efficiency and the bacterial burden was determined as mentioned in other sections.

2.4.8 Spectrophotometry, Fluorescence Microscopy, and Immunoblotting

Tick cells (1×10^5) were seeded onto 12 well plates (containing glass coverslips at the bottom in each well) and incubated overnight for 16–20 hours. XA treatment and/or infection with GFP-*A. phagocytophilum* procedures were followed as described in the *in vitro* cell line experiment section. After 48 h of incubation, coverslips were removed and placed in empty 12 well plate. Cells were immediately fixed with 4% paraformaldehyde at 37 °C for 15 min. Images were acquired using the EVOS cell imaging system (Invitrogen/Thermo Fisher Scientific, USA). For fluorescence spectrophotometry, cells infected with GFP-*A. phagocytophilum* were collected after 48 h post XA treatment, centrifuged and the cell pellet was re-suspended in 1x PBS. Fluorescence was measured with a fluorimeter (Infinite 200 PRO,Tecan, USA) with excitation at 384 nm and emission at 510 nm. The spectrum generated in this wavelength range is shown in Figure 15D. Immunoblotting was performed as described (Khanal et al., 2017; Sultana et al., 2010; Vora et al., 2017). Total lysates from ISE6 tick cells were prepared in modified RIPA buffer (BioExpress/VWR, USA) supplemented with EDTA-free protease inhibitor cocktail (Sigma, USA). Protein concentrations were determined by using BCA protein assay kit (Pierce/ThermoScientific, USA). Primary and secondary antibodies were obtained from Santa Cruz Biotechnology Inc. (USA). Thirty micrograms of total protein lysates from each group were loaded onto a 12% reducing stain-free SDS-PAGE gels (NuPAGE) for immunoblotting.

2.4.9 Preparation of Nuclear Extracts and Electrophoretic Mobility Shift Assay (EMSA)

Nuclear extracts from uninfected or *A. phagocytophilum*-infected ticks or tick cells were prepared using NE-PER nuclear and cytoplasmic extraction kit (Pierce/Thermo Fisher Scientific, USA) according to manufacturer instructions. EMSA assays were performed as described (Sultana et al., 2010). Briefly, complementary oligonucleotides consisting of *isoatp4056* putative promoter TATA-binding region were annealed and

biotin-labeled according to Pierce Biotin 3’ End DNA labeling kit (Pierce/Thermo Fisher Scientific, USA). The labeled oligonucleotides were added to a 20 µl reaction mix consisting of reagents from LightShift EMSA optimization and control kit (Pierce/Thermo Fisher Scientific, USA) and nuclear extracts prepared from either nymphal ticks or ISE6 tick cells. In some cases, nuclear lysates prepared from tick cells treated with 100 µM XA or mock (corresponding to an equal volume of 100 µM XA) were used. The entire reactions were incubated at room temperature for 25 minutes and loaded onto 6% native DNA polyacrylamide gel. The gel was initially pre-run at 100 V with 0.5% Tris-Borate-EDTA and again run with samples at the same settings and conditions. Later, the gel was transferred and processed following Chemiluminescent nucleic acid detection module recommendations (Pierce/Thermo Fisher Scientific, USA). Images were captured using BioRad ChemiDoc MP imager (BioRad, USA).

2.4.10 Tick Salivary Gland and Gut Isolation

Pairs of salivary glands or whole gut tissues from individual unfed nymphal ticks were dissected in sterile 1X phosphate buffered saline (PBS) and processed for homogenization in Lysis buffer (Aurum Total RNA kit, Bio-Rad, USA) for RNA extractions following manufacturer’s recommendations. The extracted RNA samples were later converted to cDNA and used for QRT-PCR analysis.

2.4.11 GenBank Accession Numbers for *I. scapularis* OATPs and KAT

The following are the GenBank accession numbers for the nine OATPs and kat genes: XM_002400726 (*isoatp0726*), XM_002412114 (*isoatp2114*), XM_002412116 (*isoatp2116*), XM_002414056 (*isoatp4056*), XM_002434134 (*isoatp4134*), XM_002404548 (*isoatp4548*), XM_002404550 (*isoatp4550*), XM_002415126 (*isoatp5126*), XM_002435621 (*isoatp5621*) and *kat* (XM_002401267).

2.4.12 Statistics

Statistical significance in the data sets was analyzed using GraphPad Prism 6 software and Microsoft Excel (2010). For data to compare two means, the non-paired

Student t-test was performed. P values of < 0.05 were considered significant in all analyses. Wherever necessary, the statistical test and P values used are reported.

CHAPTER 3

CHARACTERIZATION OF *IXODES SCAPULARIS* ORGANIC ANION TRANSPORTING POLYPEPTIDES UPON *BORRELIA BURGDORFERI* AND LANGAT VIRUS INFECTIONS

3.1 INTRODUCTION

Most important infectious diseases of the world require an intermediate blood-sucking arthropod vector host, such as ticks, mosquitos, fleas or lice (Hill et al., 2005).Total disease burden calculations based on Disability-Adjusted Life Year (DALY) statistics estimate that about one-sixth of the human population infectious diseases pathogenic agents are transmitted by these vectors (Neelakanta and Sultana, 2015). Various strategies to control the arthropod vector are limited due to the ineffectiveness of acaricides (George, 2008; McNair, 2015). Progress in the development of transmission-blocking vaccines that are aimed to target conserved vector molecules to interrupt the transmission of the pathogen from arthropod to mammalian hosts is very much essential (Neelakanta and Sultana, 2015). One of the vaccine, TickGARD^{PLUS} was developed in the 1990s and is based on recombinant *Rhipicephalus microplus* (cattle tick) gut glycoprotein BM86, which was found to be effective over many generations (Billingsley et al., 2008; de la Fuente and Merino, 2013). The only limitation is that this vaccine is specific to only *R. microplus* and does not work against other ticks (de la Fuente and Merino, 2013). Therefore, development of new vaccines that could affect pathogen transmission to human and animals populations to reduce the risk of vector-borne disease is important.

Previous studies show that organic anion transporting polypeptides (OATPs) are conserved among arthropod and vertebrate species that play important roles in various aspects of the physiology of these organisms (Stieger and Hagenbuch, 2014; Taank et al., 2017). In humans, OATPs are critical determinants of the transmembrane passage of many pharmaceutically important drugs (Kalliokoski and Niemi, 2009). Hard ticks belonging to the *Ixodidae* family transmit tick-borne encephalitis virus (TBEV). Langat virus (LGTV) is a biosafety level 2 model virus closely related to TBEV, is widely used as a model to study of infection dynamics of TBEV (Zhou et al., 2018; Mitzel et al., 2007; Mlera et al., 2016). LGTV easily infects *I. scapularis* ticks as well as ISE6 tick cells (Mitzel et al., 2007; Mlera et al., 2016; Zhou et al., 2018). Previously, nine distinct OATPs were reported from *I. scapularis* ticks. These OATPs are reported to cluster phylogenetically with various orthologs from other medically important blood-feeding arthropod vectors such as lice and mosquitos (Radulovic et al., 2014).

Previous study reported the involvement of a specific *I. scapularis* OATP in the tick-rickettsial pathogen interactions (Taank et al., 2017). This study showed that *A. phagocytophilum* specifically modulates *isoatp4056*, kynurenine aminotransferase (*kat*), a gene involved in intracellular production of xanthurenic acid (XA) a tryptophan metabolite, for its survival within the ticks. RNA interference studies (Chapter 2) using double-stranded RNA (dsRNA) showed that silencing of either *isoatp4056*, *kat* or combination of both dsRNA affects *A. phagocytophilum* growth and survival in *I. scapularis* ticks. This study noticed very interesting cross-talk between tick OATP and XA in the survival of *A. phagocytophilum* in the vector host. XA in arthropods is also known to mediate gametogenesis in malarial parasite in mosquitoes (Arai et al., 2001; Bhattacharyya and Kumar, 2001). Conclusively, these studies suggest that OATPs participates in vector-pathogen interactions in addition to their role in normal physiological processes.

In view for the development of an effective anti-vector vaccine, it is necessary to understand the role of conserved proteins such as OATPs in vector biology with different pathogens. In this study, a detailed molecular analysis of OATPs was performed in the interactions of ticks with an extracellular bacterial pathogen (*Borrelia burgdorferi*) and an intracellular tick-borne virus LGTV.

3.2 RESULTS

3.2.1 *Borrelia burgdorferi* has no Effect on the Expression of any of the *I. scapularis* OATPs in Unfed Ticks

Previous studies have reported nine distinct oatps in *I. scapularis* unfed ticks (Radulovic et al., 2014; Taank et al., 2017). As described in chapter 2, and previously published study, a specific OATP (*isoatp4056*) and *kat* gene were noted to be upregulated in unfed ticks in the presence of *A. phagocytophilum* infection (Taank et al., 2017). To further study if similar observations were evident with an extracellular pathogen, *B. burgdorferi*-infected unfed ticks were used and analyzed for the mRNA expression of these nine tick *oatps* and *kat* genes using QRT-PCR. No significant differences were observed in the mRNA transcript levels of *isoatp-0726* (Figure 20a), *isoatp-2114* (Figure 20b), *isoatp-2116* (Figure 20c), *isoatp-4056* (Figure 20d), *isoatp-4134* (Figure 20e), *isoatp-4548* (Figure 20f), *isoatp-4550* (Figure 20g), *isoatp-5126* (Figure 20h) and *isoatp-5621* (Figure 20i) between *B. burgdorferi*-infected and uninfected unfed ticks (Figure 20 , Table 3). Also, no significant difference were noticed in the expression of *kat* gene between *B. burgdorferi*-infected and uninfected unfed ticks (Figure 20j, Table 3). Figure 20k shows the presence of *B. burgdorferi-flaB* as expected only in infected ticks and not in uninfected ticks. These results show that extracellular pathogen *B. burgdorferi,* unlike intracellular pathogen *A. phagocytophilum* as previously reported in the study (Taank et al., 2017), does not impact the expression of any of the arthropod OATPs or *kat* genes.

3.2.2 Synchronous Infection of LGTV in Ticks does not Impact OATP Expression in Unfed Ticks

It was reported earlier, that *I. scapularis* can be readily infected by LGTV (Mitzel et al., 2007). Using an *in vitro* method, synchronously infected LGTV ticks were generated, as described in the experimental procedure section (3.4.2). Experiments were performed to understand whether tick-borne viruses have any effect on the

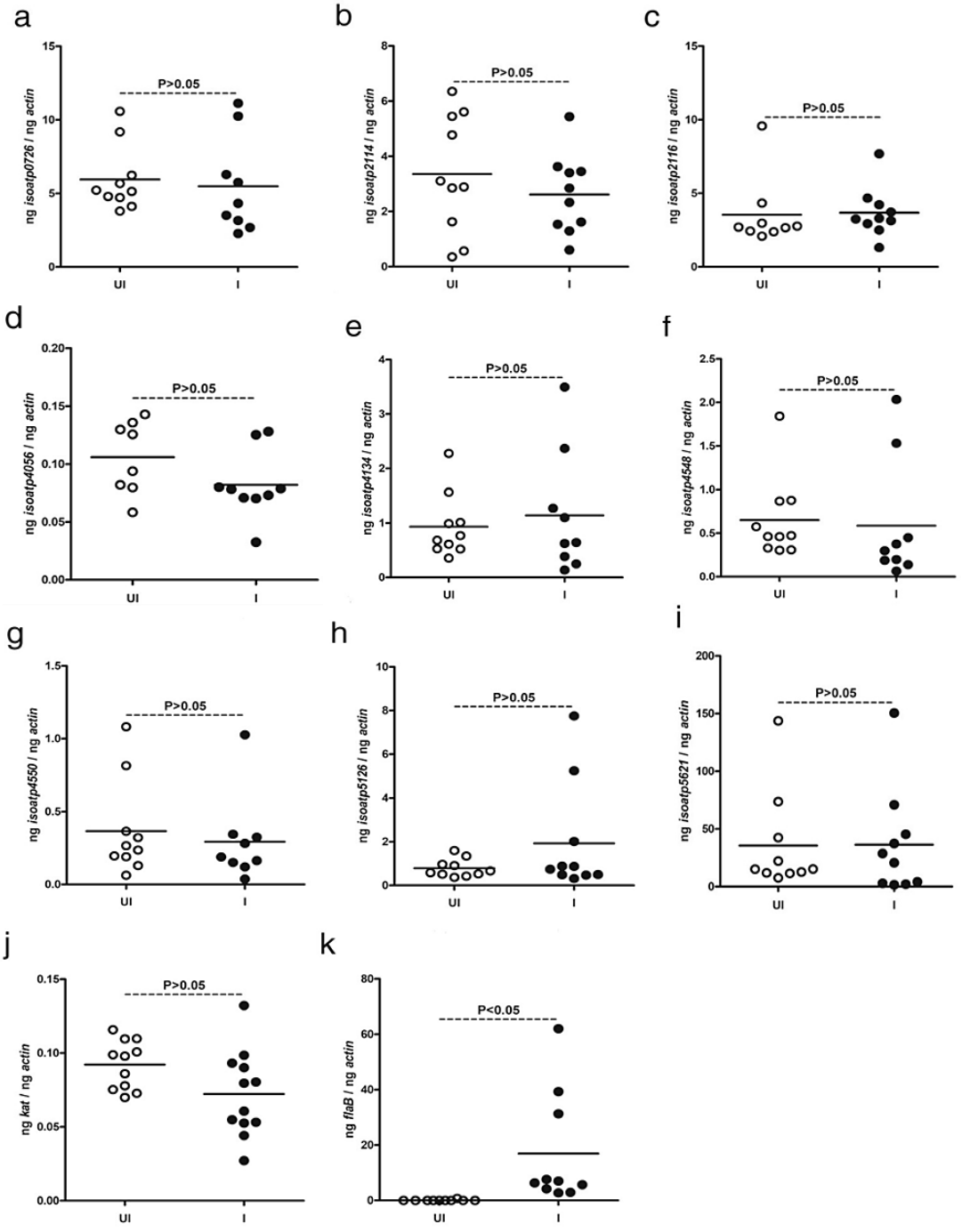

Figure 20. *Borrelia burgdorferi* has no impact on the expression of nine *I. scapularis oatps* in unfed nymphal ticks

Results from QRT-PCR assays are shown in all panels. a-i) Expression of nine *I. scapularis* OATPs: *isoatp0726* (a), *isoatp2114* (b), *isoatp2116* (c), *isoatp4056* (d), *isoatp4134* (e), *isoatp4548* (f), *isoatp4550* (g), *isoatp5126* (h) and *isoatp5621* (i) in unfed uninfected or *B. burgdorferi*-infected ticks. Levels of tick *kat* (j) or spirochete *flaB* (k) mRNA in *B. burgdorferi*-infected unfed nymphal ticks are also shown. Open circles represent data from uninfected (UI) and closed circles represent data from infected (I) ticks. Each circle represents data from one tick. The amount of mRNA levels of *flaB* or OATPs or *kat* was normalized to the amount of tick beta-*actin* mRNA levels.

Table 3. Summary of statistical test outcomes between uninfected and *B. burgdorferi* infected ticks

Gene	Samples	Student's t-test (P value)	Mann Whitney test (P value)
*Isoatp*0726	Uninfected, *Borrelia burgdorferi* infected	0.4881	0.7959
Isoatp2114		0.3707	0.4359
Isoatp2116		0.8931	0.2428
Isoatp4056		0.5938	0.0753
Isoatp4134		0.6086	1.0000
Isoatp4548		0.4358	0.2799
Isoatp4550		0.5152	0.4967
Isoatp5126		0.1765	0.7959
Isoatp5621		0.9685	0.7959
kat		0.0571	0.0605
flaB		**0.0175**	**< 0.0001**

expression of tick OATPs. No significant (P > 0.05) differences were noticed (Table 4) in the mRNA expression levels of *isoatp0726* (Figure 21a), *isoatp2114* (Figure 21b), *isoatp2116* (Figure 21c), *isoatp4056* (Figure 21d), *isoatp4134* (Figure 21e), *isoatp4548* (Figure 21f), *isoatp4550* (Figure 21g), *isoatp5126* (Figure 21h) and *isoatp5621* (Figure 21i) between unfed uninfected ticks or LGTV-infected ticks. No significant (P > 0.05) difference (Table 4) in the *kat* gene expression was noted between unfed uninfected ticks or LGTV-infected ticks (Figure 21j). As expected, both positive (Figure 21k) and negative (Figure 21l) strands of LGTV virus were evident in only in LGTV- infected ticks not in uninfected control ticks. (Figure 21k and 21l). These results indicate that LGTV infection does not have any impact on the expression of any tick *oatps* or *kat* in the unfed stage of the tick lifecycle.

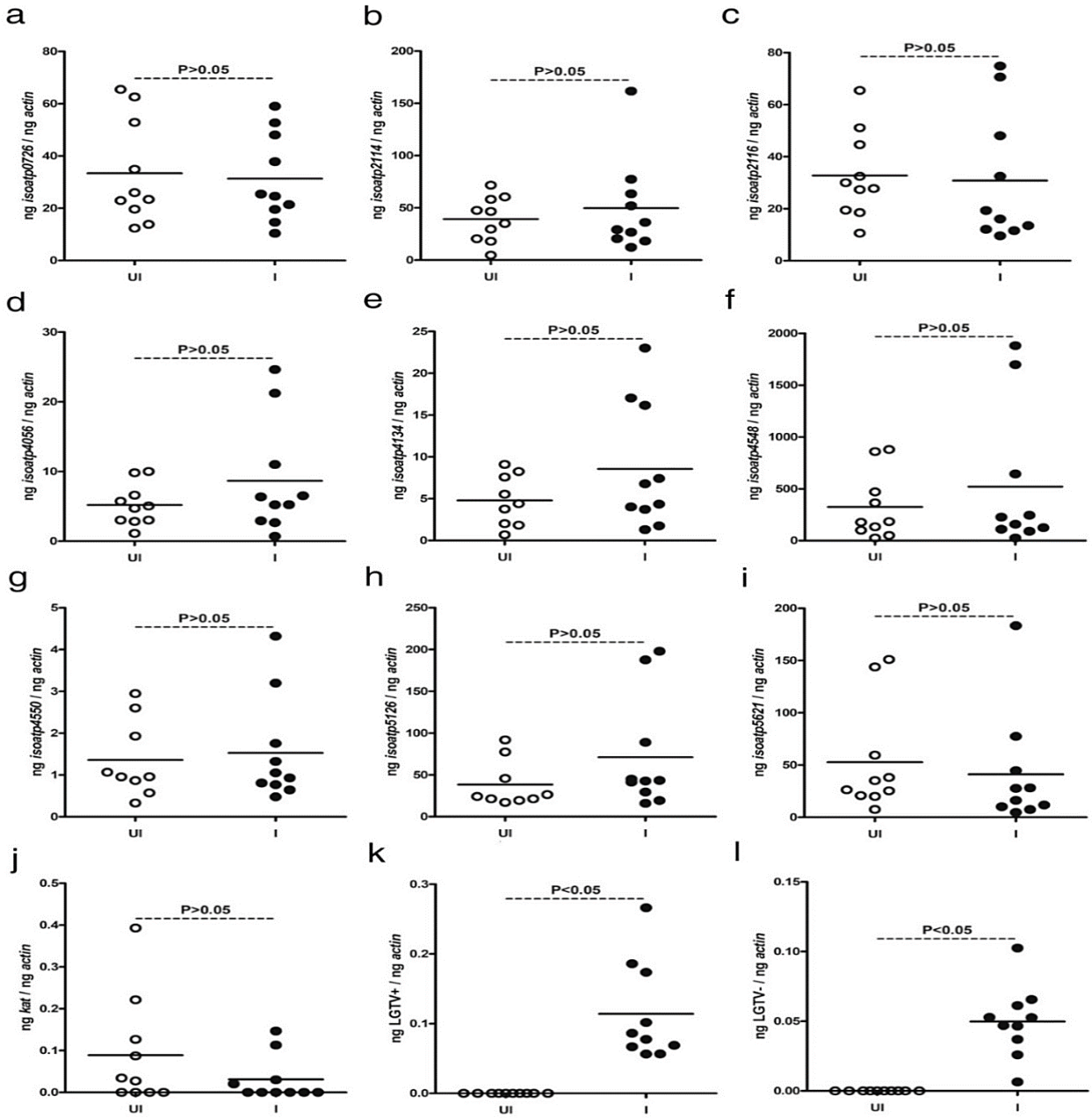

Figure 21. LGTV has no impact on the expression of nine *I. scapularis* oatps in synchronously-infected unfed nymphal ticks

Data from QRT-PCR assays are shown in all panels. a-i) Expression of nine *I. scapularis* OATPs: *isoatp0726* (a), *isoatp2114* (b), *isoatp2116* (c), *isoatp4056* (d), *isoatp4134* (e), *isoatp4548* (f), *isoatp4550* (g), *isoatp5126* (h) and *isoatp5621* (i) in unfed uninfected or LGTV-synchronously-infected ticks is shown. j) Levels of tick *kat* mRNA in unfed uninfected or LGTV synchronously-infected ticks. Levels of viral positive-sense strand (k) or negative sense strand (l) in LGTV-synchronously-infected ticks are shown. Uninfected ticks were used as controls in all panels. In all panels, open circles represent data from uninfected (UI) and closed circles represent data from LGTV synchronously-infected (I) ticks. Each circle represents data from one tick. The amount of mRNA levels of LGTV positive- or negative-sense strands or *oatps* or *kat* was normalized to the amount of tick beta-*actin* mRNA levels.

Table 4. Summary of statistical test outcomes between uninfected and LGTV infected ticks

Gene	Samples	Student's t-test (P value)	Mann Whitney test (P value)
*Isoatp*0726	Uninfected, LGTV infected	0.8088	0.7959
Isoatp2114		0.5110	0.8534
Isoatp2116		0.8414	0.4813
Isoatp4056		0.2193	0.5288
Isoatp4134		0.1787	0.6038
Isoatp4548		0.4263	0.9188
Isoatp4550		0.7449	1.0000
Isoatp5126		0.1912	0.3562
Isoatp5621		0.6316	0.3930
kat		0.2064	0.2756
LGTV + strand		**< 0.0001**	**< 0.0001**
LGTV - strand		**< 0.0001**	**< 0.0001**

3.2.3 Expression of Specific OATP Transcripts from *I. scapularis* was Downregulated upon LGTV Infection in Tick Cells

Previous studies has shown that ISE6 tick cells are permissible to LGTV infection in vitro at an MOI (Multiplicity of infection) of 1-2 (Zhou et al., 2018). To test, whether LGTV infection in ticks cells has any impact on the expression of *oatps* transcript levels in tick cells. Two experimental timepoints, 24 h and 72 h were selected to represent the early and late stages of LGTV infection. All nine *oatps* transcript levels were analyzed using QRT-PCR. The data revealed no significant differences ($P > 0.05$) (Table 5) in the expression levels of *isoatp0726* (Figure 22a), *isoatp2116* (Figure 22c), *isoatp4056* (Figure 22d), *isoatp4134* (Figure 22e) and *isoatp5621* (Figure 22i) in the LGTV infected

Table 5. Summary of statistical test outcomes from uninfected and LGTV infected ticks cells at 24 and 72 h post infection

Gene	Samples	Student's t-test (P value)	Mann Whitney test (P value)
*Isoatp*0726	24 h, Uninfected, LGTV infected tick cells	0.1813	0.1797
Isoatp2114		**0.0010**	**0.0022**
Isoatp2116		0.1255	0.1320
Isoatp4056		0.0960	0.0931
Isoatp4134		0.1180	0.1320
Isoatp4548		**0.0059**	**0.0152**
Isoatp4550		**0.0325**	**0.0411**
Isoatp5126		**0.0191**	**0.0152**
Isoatp5621		0.5253	0.8182
kat		0.5463	0.8182
LGTV + strand		**< 0.0001**	**0.0022**
*Isoatp*0726	72 h, Uninfected, LGTV infected tick cells	0.0767	0.0931
Isoatp2114		0.6696	0.6991
Isoatp2116		0.0946	0.1320
Isoatp4056		0.0963	0.0931
Isoatp4134		0.2200	0.2403
Isoatp4548		0.2021	0.1255
Isoatp4550		0.1999	0.3939
Isoatp5126		0.2964	0.6991
Isoatp5621		0.2257	0.9372
kat		0.9894	0.6991
LGTV + strand		**< 0.0001**	**0.0022**

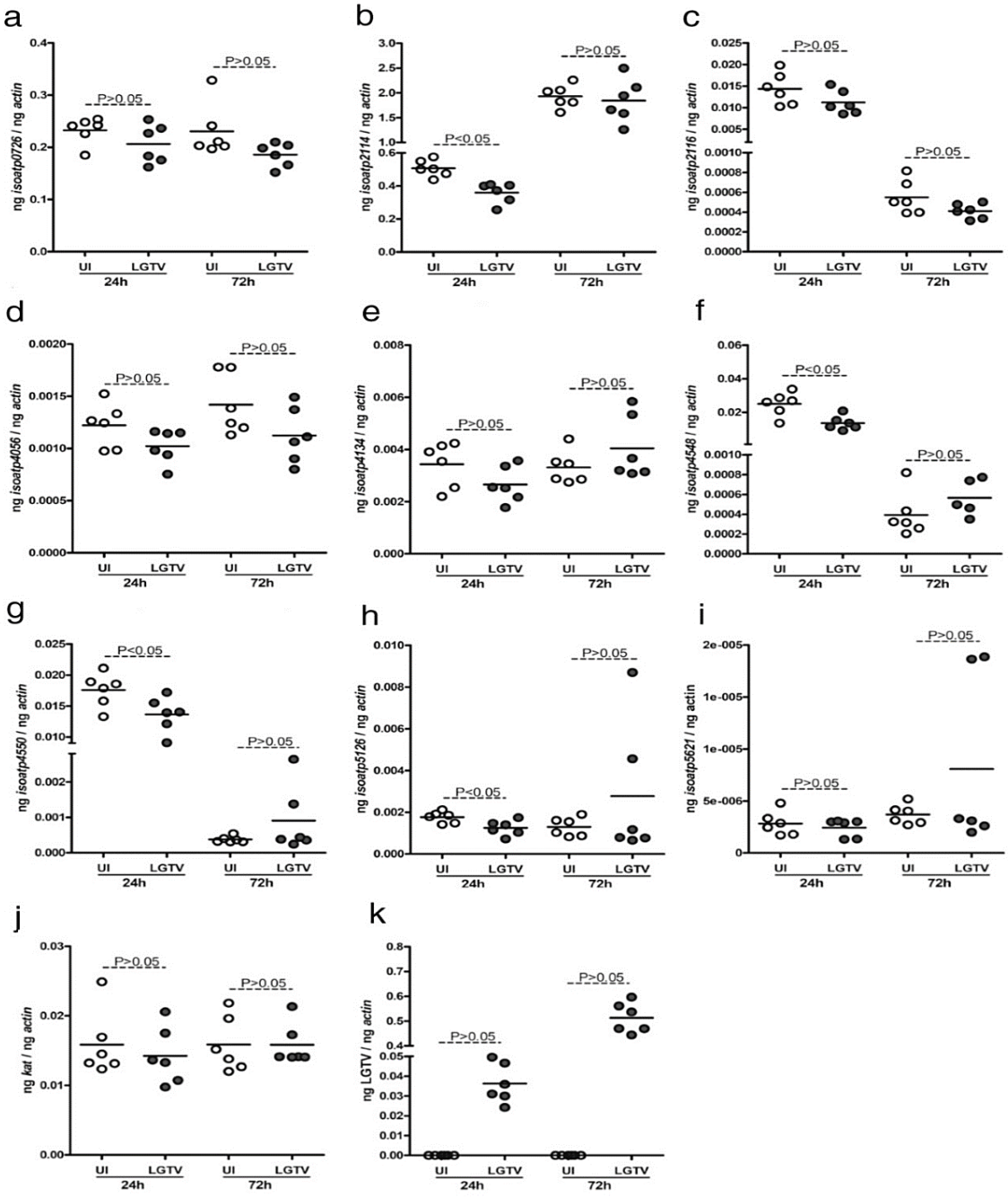

Figure 22. LGTV infection of tick cells *in vitro* affects expression of *isoatp2114*, *isoatp4548*, *isoatp4550* and *isoatp5126*

Data from QRT-PCR assays are shown in all panels. a-i) Expression of nine *I. scapularis* OATPs: *isoatp0726* (a), *isoatp2114* (b), *isoatp2116* (c), *isoatp4056* (d), *isoatp4134* (e), *isoatp4548* (f), *isoatp4550* (g), *isoatp5126* (h), *isoatp5621* (i) and *kat* mRNA (j) in unfed uninfected ticks and LGTV-infected tick cells at 24 and 72 h p.i. is shown. k) Levels of viral RNA in LGTV-infected ISE6 tick cell line (LGTV) at 24 and 72 h p.i. is shown. Uninfected (UI) cells were used as controls in all panels. In all panels, open circles represent data from uninfected (UI) and closed circles represent data from LGTV-infected (LGTV) tick cells. Each circle represents data from one cell culture well. LGTV loads or oatps or *kat* mRNA levels was normalized to the amount of tick beta-*actin* mRNA levels. The P-values indicate the results from statistical analyses.

ticks cells as compared with uninfected control at 24 h p.i. However, the significant decrease in expression of *isoatps2114* (Figure 22b), *isoatp4548* (Figure 22f), *isoatp4550* (Figure 22g) and *isoatp5126* (Figure 22h) was evident in LGTV-infected tick cells as compared to uninfected control at 24 h p.i. Also, No significant ($P > 0.05$) differences (Table 5) were noticed in the expression of all nine *oatps* between LGTV-infected tick cells and uninfected controls at 72 h p.i. In addition, no significant ($P > 0.05$) difference was noticed in expression of *kat* gene (Figure 22j) between LGTV-infected tick cells at both 24 h and 72 h p.i. Further it was noticed that LGTV infected tick cells with an increase of virus load at 72 h p.i. (Figure 22k) and as evident in the published study (Zhou et al., 2018). No morphological differences were evident between uninfected or LGTV-infected tick cells at both 24 h and 72 h time points (Figure 23). These results suggest that specific tick cell *oatp* genes are modulated at an early time point (24 h p.i.) of viral replication but not at later stages (72 h p.i.) of LGTV infection.

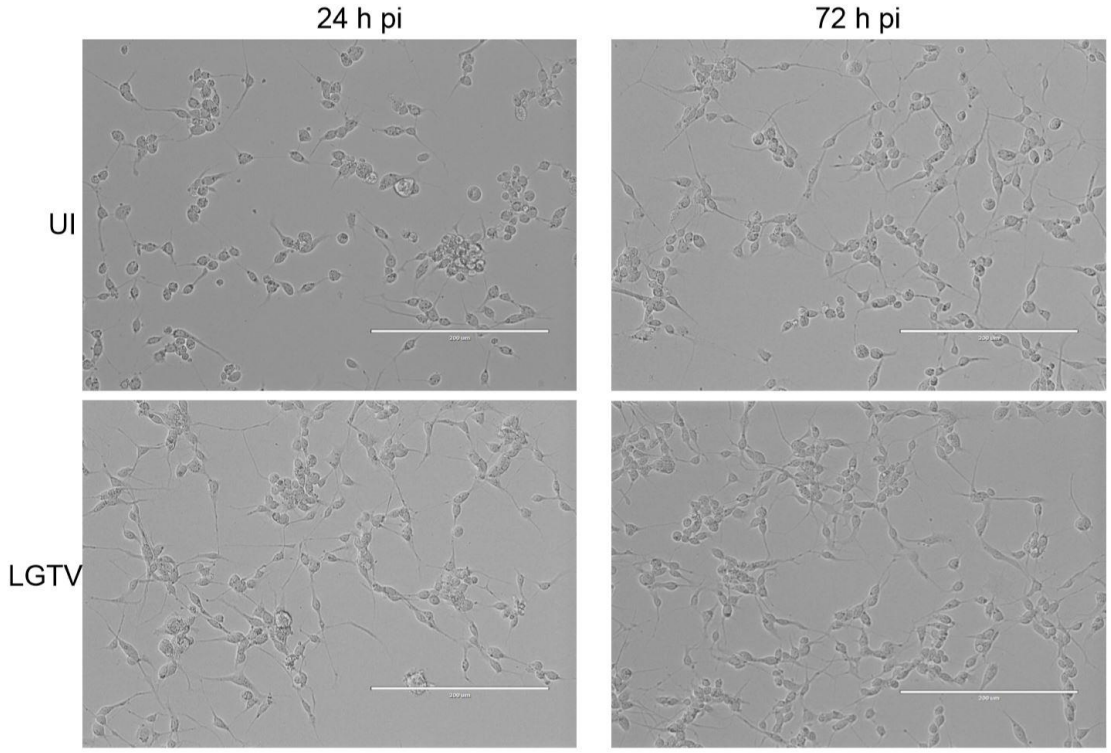

Figure 23. LGTV infection has no impact on tick cell morphology at tested dose

A) Representative phase contrast images of uninfected or LGTV-infected tick cells at 24 and 72 h p.i. UI indicates uninfected and LGTV indicates LGTV-infected tick cells. Scale bars on each image indicates 200 µm.

3.2.4 Inhibition of OATPs in Tick Cells Affects LGTV Burden

In the previous set of experiments, downregulation of specific *oatps* upon LGTV infection was noticed, suggesting an important role of these *oatps* at early LGTV-tick interactions. To study whether inhibition of tick cell OATPs at an early stage (24 h p.i.) cause any impact on LGTV infection, tick cell were treated with 100 µM of SPZ, a general inhibitor of OATP (Taank et al., 2017) and equal volume of mock solution. No morphological differences were observed in the tick cells either treated with the mock solution or 100uM of SPZ inhibitor solution at 4 h or 24 h post-treatment followed by LGTV-infection (Figure 24a). In addition, no cytotoxicity was observed after the treatment of uninfected tick cells with 100 µM of SPZ inhibitor at 4, 24, 48, and 72 h post-treatment (Figure 25). However, at 24 h p.i. significantly ($P < 0.05$) reduced loads of LGTV virus (Figure 24b) was observed after SPZ inhibitor-treatment in LGTV-infected tick cells in comparison to mock-treated control (Figure 24b). These results suggest that OATPs play significant roles in the survival of LGTV in tick cells.

3.2.5 LGTV- Infection in Tick Cells Treated with OATP Inhibitor (SPZ) Affects the Expression of Several OATPs and *kat* Gene

This study then tested whether treatment of tick cells with OATP inhibitor (SPZ) has any effect on the transcript levels of the *oatps* (Figure 26). By QRT-PCR analysis, at 24 p.i., significant ($P < 0.05$) (Table 6) downregulation of four oatps, *isoatps0726* (Figure 26a), *isoatps4056* (Figure 26d), *isoatps4134* (Figure 26e) and *isoatps5621* (Figure 26i) in SPZ inhibitor-treated LGTV-infected tick cells was observed in comparison to mock-treated controls. However, a significant ($P < 0.05$) increase of *isoatp4550* in SPZ inhibitor-treated-LGTV-infected tick cells was noted as compared to mock-treated control at 24 h p.i. (Figure 26g). No significant ($P > 0.05$) differences in the mRNA expression levels of *isoatps2114* (Figure 26b), *isoatps2116* (Figure 26c), *isoatps4548* (Figure 26f), and *isoatps5126* (Figure 26h) was noted between SPZ inhibitor-treated-LGTV-infected tick cells when compared to mock-treated controls at 24 h p.i. Previous report suggested that KAT is an upstream molecule that impacts tick *isoatp4056* expression (Taank et al., 2017). QRT-PCR analysis revealed a significant ($P < 0.05$) reduction in *kat* transcripts (Table 6) in SPZ-treated LGTV-infected tick cells in

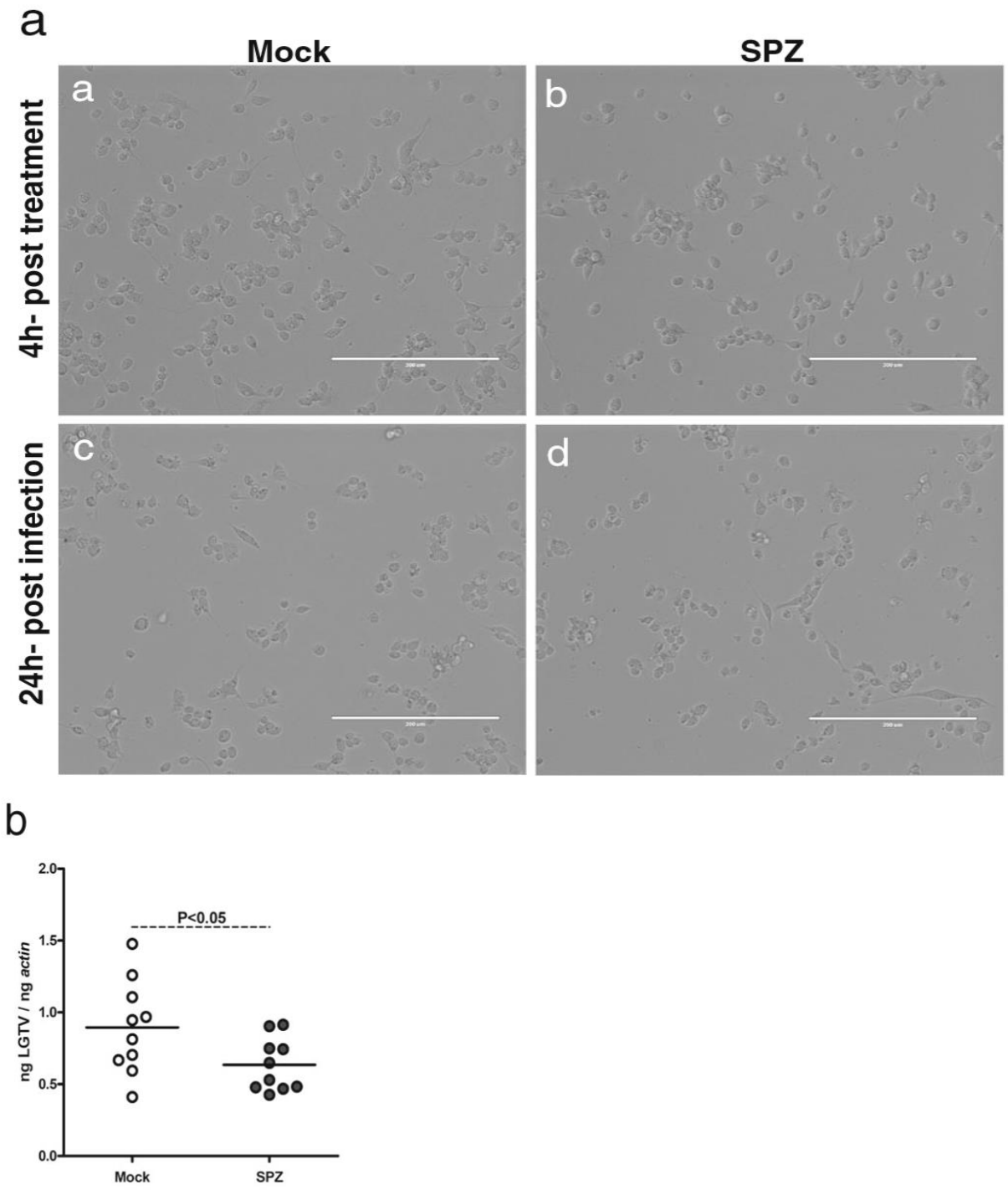

Figure 24. Inhibition of OATPs affects LGTV loads in tick cells

a) Representative phase-contrast images of LGTV-infected mock-treated or SPZ-treated tick cells (4 h post-treatment of the inhibitor, before infection) followed by 24 h post-LGTV-infection. b) QRT-PCR analysis showing levels of viral RNA in LGTV infected mock- or SPZ-treated tick cells at 24 h p.i. Open circles represent data from LGTV-infected mock-treated and closed circles represent data from SPZ-treated tick cells at 24 h p.i. Each circle represents data from one cell culture well. LGTV loads were normalized to the amount of tick beta-*actin* levels. In b, the P-value indicates the result from statistical

comparison to the mock-treated control at 24 h p.i. (Figure 26j). These results strongly suggest an important role for many OATPs, including IsOATP4056, and KAT in the early stages of LGTV infection in tick cells.

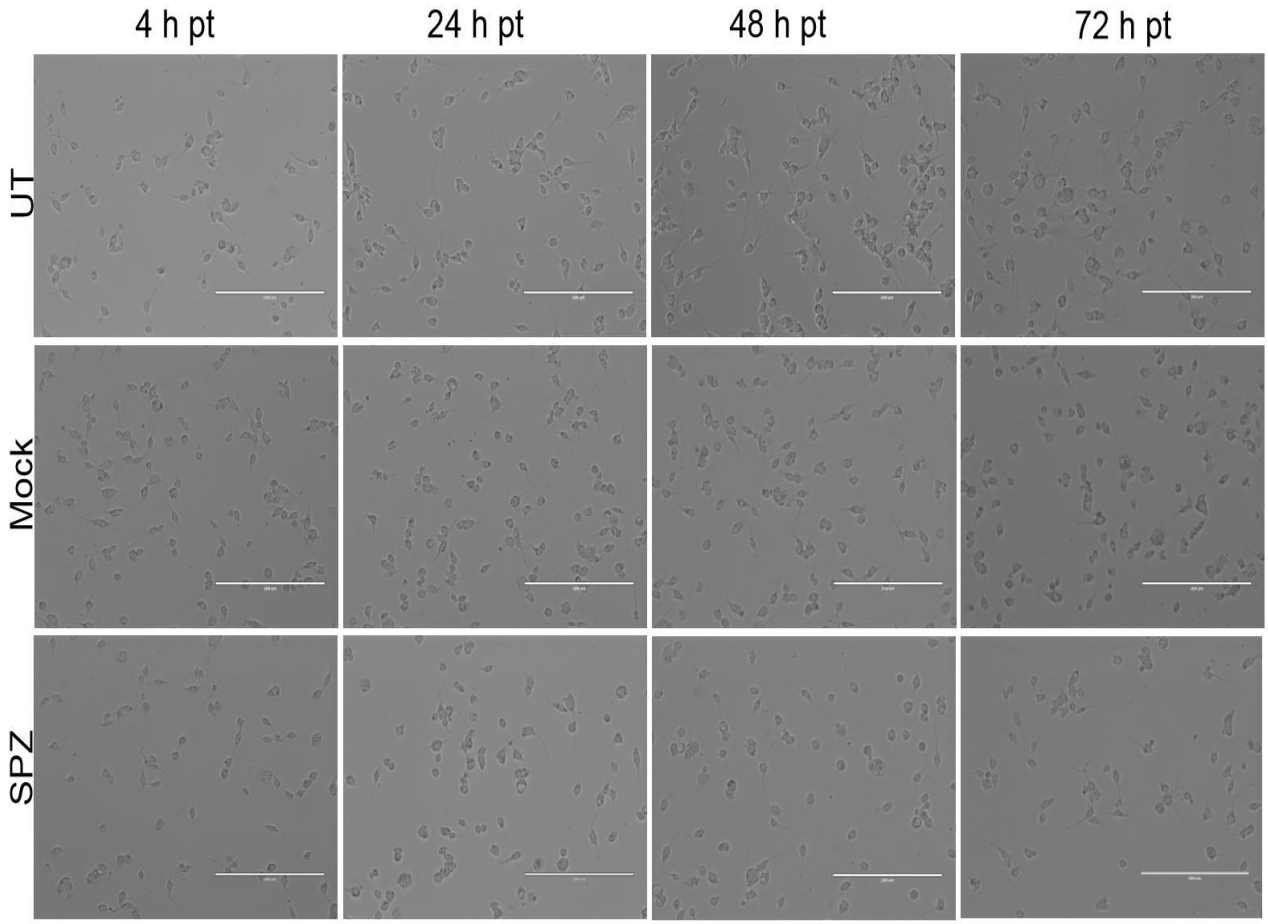

Figure 25. SPZ treatment has no cytotoxic effects on the tick cells

Representative phase contrast images of untreated or mock- or 100 µM of SPZ uninfected tick cells at 4, 24, 48 and 72 h post treatment (p,t,) are shown. Scale bars on each image indicates 200 µm.

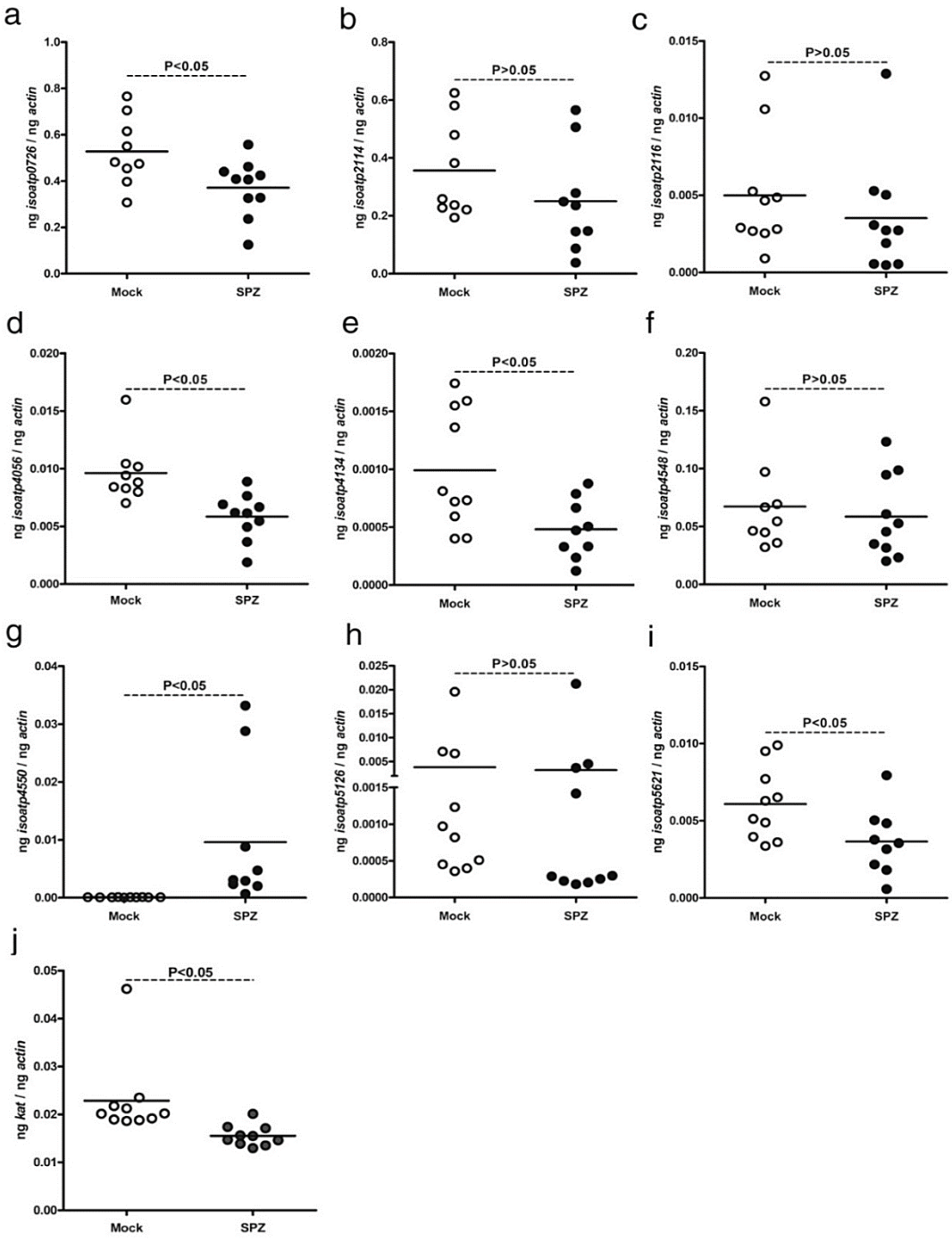

Figure 26. Treatment of tick cells with OATP inhibitor affects *oatps* and *kat* gene expression

Data from QRT-PCR assays are shown in all panels. Expression of nine *I. scapularis* OATPs: *isoatps0726* (a), *isoatp2114* (b), *isoatp2116* (c), *isoatp4056* (d), *isoatp4134* (e), *isoatp4548* (f), *isoatp4550* (g), *isoatp5126* (h), *isoatp5621* (i) and *kat* (j) mRNA levels in LGTV-infected mock- or OATP-inhibitor (SPZ)-treated tick cells at 24 h p.i. In all panels, open circles or closed circles represent data from LGTV-infected mock- or SPZ-treated tick cells at 24 h p.i., respectively. Each circle represents data from one cell culture well. The *oatps* and *kat* mRNA levels were normalized to the tick beta-*actin* mRNA levels. The P-values indicate the results from statistical analyses.

Table 6. Summary of statistical test outcome for LGTV, *kat* and *oatps* between mock and SPZ inhibitor treated tick cells

Gene	Samples	Student's t-test (P value)	Mann Whitney test (P value)
*Isoatp*0726	Mock, SPZ treated tick cells	**0.0216**	**0.0350**
Isoatp2114		0.2141	0.2224
Isoatp2116		0.3904	0.3527
Isoatp4056		**0.0024**	**0.0006**
Isoatp4134		**0.0159**	**0.0279**
Isoatp4548		0.6194	0.4967
Isoatp4550		**0.0259**	**< 0.0001**
Isoatp5126		0.8399	0.1655
Isoatp5621		**0.0311**	**0.0279**
kat		**0.0151**	**< 0.0001**
LGTV		**0.0252**	**0.0418**

3.2.6 Bioinformatic Analysis of OATPs from Ticks, Mosquitoes, and Lice

Post-translational modification (PTM) of proteins provides a versatile tool to regulate the activity of critical proteins. PTM is a key strategy used by pathogens to modulate host cell signaling proteins (Ribet and Cossart, 2010). Previous finding shows that a rickettsial pathogen can interplay with OATP-KAT pathway (Taank et al., 2017). Similarly, this study further supports modulation of the tryptophan pathway with another intracellular tick-borne pathogen, LGTV. These two studies suggest that OATP-KAT signaling plays a crucial role in vector-pathogen interactions. It is known that post-translational modifications are essential for the proper functioning of the OATPs (Alam et al., 2018; Powell et al., 2014; Yao et al., 2012). Therefore, knowledge of post-translational modification sites on OATPs is important.

OATPs are present in many arthropod species (Mulenga et al., 2008; Radulovic et al., 2014). Therefore, a comparative analysis of *I. scapularis* OATPs with orthologs of medically important vectors along with the fruit fly (*Drosophila melanogaster*) was performed. OATPs primary amino acid sequences were obtained from the National Center for Biotechnology Information (NCBI) database. These amino acid sequences were screened for a specific OATP signature sequence (–WxGxWWxG--). The sequences containing this signature were retained (37 total sequences), eight sequences from *I. scapularis* OATPs, five from *Aedes aegypti* OATPs, five from *Anopheles gambiae* OATPs, four from *Culex quinquefasciatus* OATPs, four from *Pediculus humanus corporis* OATPs, four from *Rhipicephalus pulchellus* OATPs, one from *Amblyomma americanum* OATP and six from *D. melanogaster.* Variable length of amino acid sequences was observed among various OATP sequences (Figure 27, Table 7, 8, 9, 10, 11, and 12).

Each OATP amino acid sequence was individually analyzed at TMHMM server v2.0 for the prediction of transmembrane helices. Regions of amino acid sequence that are either exposed outside the plasma membrane (extracellular) or regions that are inside the plasma membrane (intracellular) were selected for further analysis (Table 7, 8, 9, 10, 11, and 12). Only internally or externally exposed regions were considered for prediction of conserved domains and or unique post-translation modification (PTM) sites in the OATP amino acid sequences. Figure 28 shows an example of *I. scapularis* OATP4056 amino acid sequence analyzed for the presence of different post translational modification and domains. Similar analysis was carried to analyze all the other OATPs in the study.

Based on the analysis, it was noticed that all but two OATP sequences were predicted to carry at least two N-glycosylation sites (Figure 29 and Table 7). OATP sequences from *Aedes aegypti* (GenBank: XP_001660407) were predicted to carry the highest number (14 sites) of N-glycosylation sites, while, *Ixodes. scapularis* (GenBank: XP_002435666), *Amblyomma americanum* (GenBank: ACH98103), *Rhipicephalus pulchellus* (GenBank: JAA59396) and *Culex quinquefasciatus* (GenBank: EDS26845) were predicted to carry the lowest (2 sites) number of N-glycosylation sites (Figure 29a

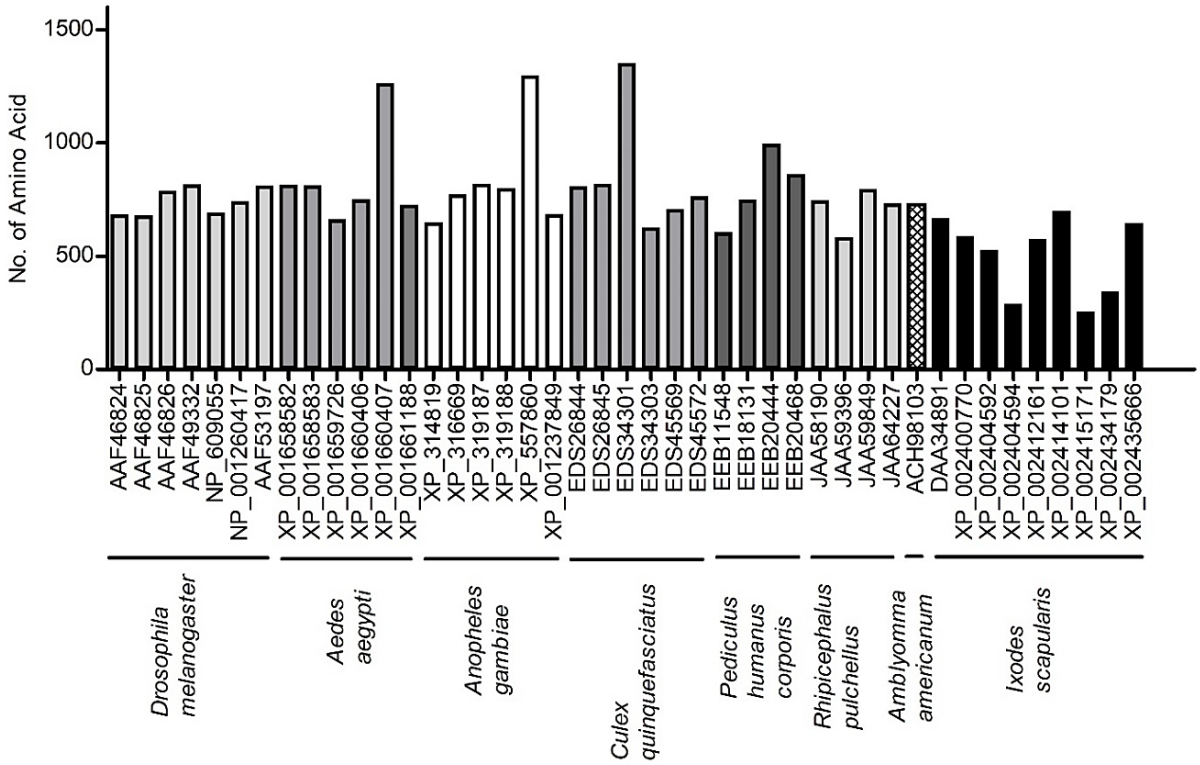

Figure 27. Amino acid sequence variation as obtained from NCBI database

Amino acid sequences of several OATPs were obtained from NCBI. Histograms represent the number of amino acids on each OATP. GenBank accession numbers and organism names are shown at the bottom of the figure.

and Table 7). Figure 30a represents the relative position of all the N-glycosylation sites on the *Ixodes scapularis* amino acid sequences, including transmembrane regions.

All of the 37 OATPs were predicted to carry at least two myristoylation sites (Figure 29b and Table 8), where OATP sequence from *Anopheles gambiae* (XP_557860) was predicted to carry the highest number (24 sites) of myristoylation sites, and *Ixodes scapularis* OATPs (DAA34891, XP_002400770, XP_002404592, XP_002415171) were predicted to carry the lowest (3 sites) number of myristoylation sites. Figure 30b shows the relative position and distribution of all the predicted myristoylation sites on *Ixodes scapularis* OATPs, including transmembrane regions.

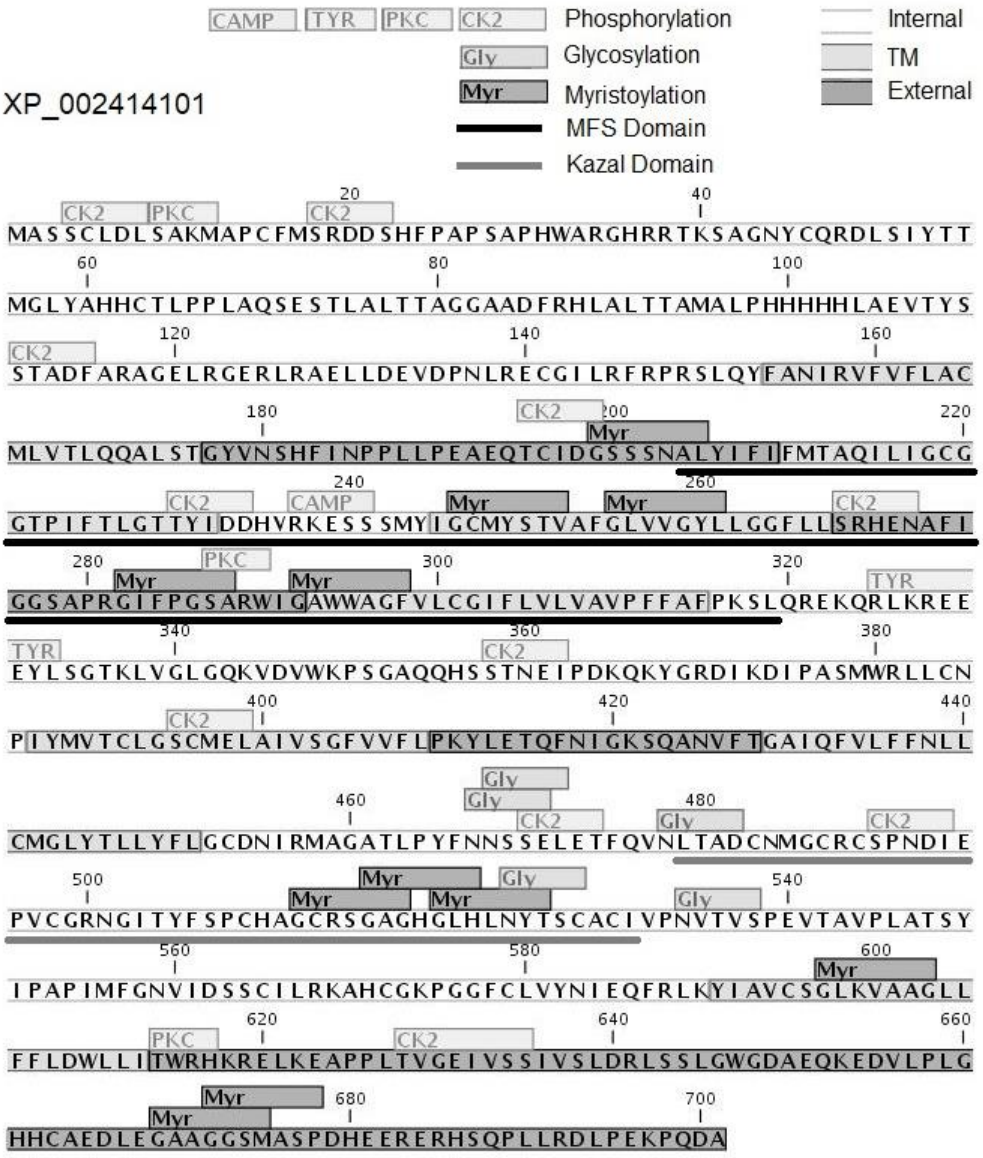

Figure 28. Detailed Post translational modification analysis of *Ixodes scapularis* tick OATP (Isoatp4056)

Amino acid sequences of OATPs were individually analyzed at Biology Workbench, NCBI conserved domain search and PROSITE databases for prediction of glycosylation, phosphorylation and myristoylation sites, these sites are shown in box over the sequence. TMHMM v2.0 server was used to predict the transmembrane regions and are shown as Internal (on sequence, clear), transmembrane (on sequence, light grey) and external regions (on sequence, dark grey). MFS (major facilitator transporter superfamily) domain and Kazal domain is shown below the sequence by black and grey lines respectively. Accession number for the *I. scapularis* OATP is provided on the top left of the figure.

All of the 37 OATPs analyzed in this study were predicted to carry varying numbers of PKC phosphorylation sites (Figure 31a and Table 9). The *Drosophila melanogaster* OATPs sequence (AAF46824, AAF46826) were predicted to carry the highest number (12 sites), and *I. scapularis* OATP (XP_002400770) were predicted to carry the lowest number (1 site) of PKC phosphorylation sites (Figure 31a and Table 9).

In addition, out of the 37 OATP amino acid sequences analyzed, all were predicted to carry at least one CK2 phosphorylation site (Figure 31b and Table 10). *Pediculus humanus corporis* OATP (EEB20444) was predicted to carry the highest number (19 sites) of CK2 phosphorylation sites, while *I. scapularis* OATP (XP_002404594) was predicted to carry the lowest number (1 site) of CK2 phosphorylation sites (Figure 31b and Table 10). Tyrosine phosphorylation (TYR) sites were also evident in 20 out of the 37 OATPs amino acid sequence that was analyzed (Figure 31c and Table 11). All four OATP amino acid sequences from *Pediculus. humanus corporis*, four out of six *Drosophila melanogaster* sequences, three out of four *Culex quinquefasciatus* sequences and three out of five *Anopheles gambiae* sequences contained at least one tyrosine phosphorylation site (Figure 31c).

Interestingly, out of 13 OATP sequences from the ticks, only three sequences from *I. scapularis* (XP_002412161, XP_002414101, and XP_00243 5666) were predicted to carry tyrosine phosphorylation sites (Figure 31c). Among all the OATP amino acid sequences, *Aedes aegypti* OATP (XP_001660407), *P. humanus corporis* OATPs (EEB18131, EEB20468) and *D. melanogaster* OATPs (AAF46824, AAF49332) were predicted to carry the highest number (2 sites) of tyrosine phosphorylation sites (Figure 31c and Table 11).

Out of 37 OATPs sequences, only 27 were predicted to carry at least one cAMP-dependent protein kinase phosphorylation site (Figure 31d and Table 12). The *Aedes aegypti* OATP (XP_001660407) and *Anopheles gambiae* OATP (XP_557860) were predicted to carry the highest number (4 sites) of cAMP-dependent protein kinase phosphorylation sites (Figure 31d and Table 12). Relative distribution of all the phosphorylation sites on *I. scapularis* OATP amino acid sequences including the transmembrane domain regions is shown in Figure 32.

In addition, with the exception of three *I. scapularis* OATP amino acid sequences (XP_002400770, XP_002404594, and XP_002415171) and one from *Drosophila melanogaster* OATP (AAF46825), all 33 other OATPs were predicted to carry at least one Kazal domain in their sequences (Figure 33a). Figure 33b shows the relative location of the KAZAL domain on the OATP amino acid sequence of *I. scapularis.*

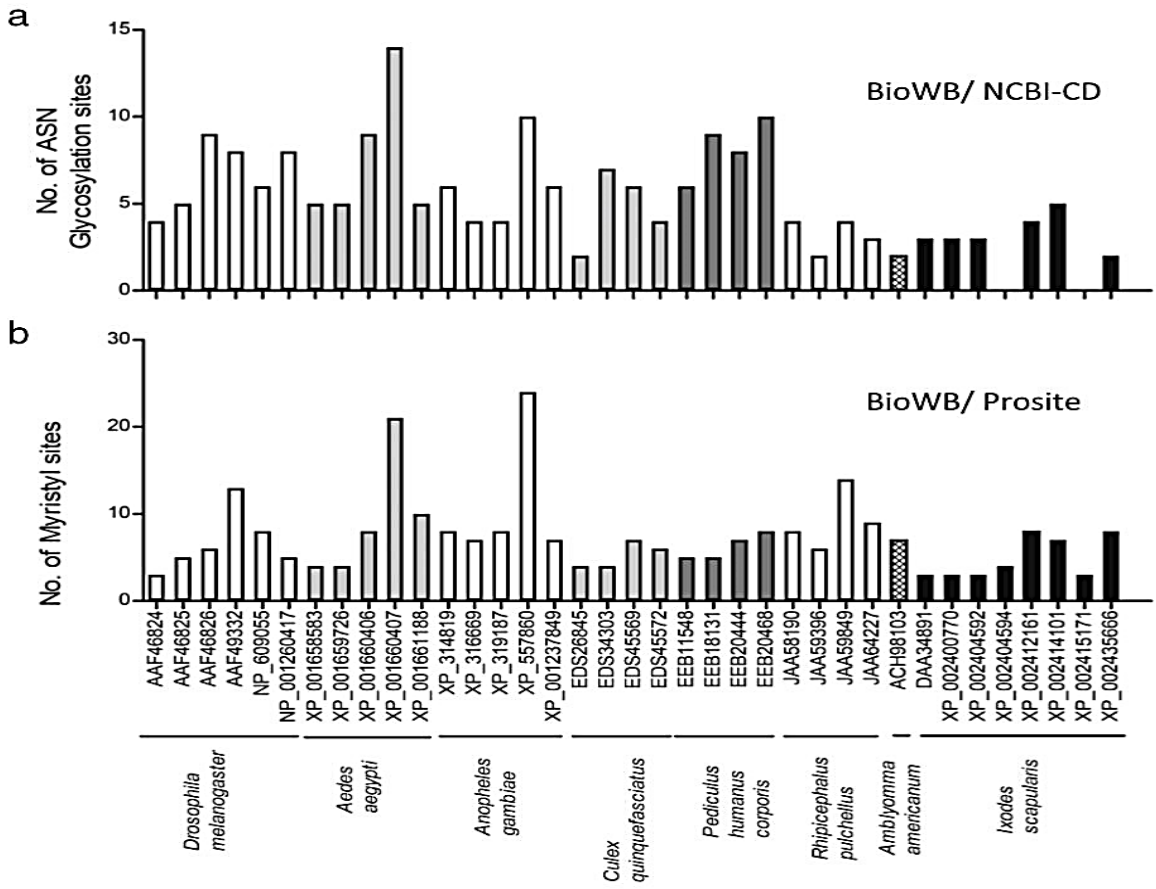

Figure 29. Analysis of glycosylation and myristoylation sites in OATPs from medically important vectors

Amino acid sequences of several OATPs were individually analyzed at Biology WorkBench (a, b), NCBI conserved domain search (a) and PROSITE (b) databases for glycosylation (a) and myristoylation (b) sites. Histograms represent the number of post-translational modification sites on each OATP. The post-translational modifications in the transmembrane regions within each OATP were not considered for histogram plots. GenBank accession numbers and organism names are shown at the bottom of the figure.

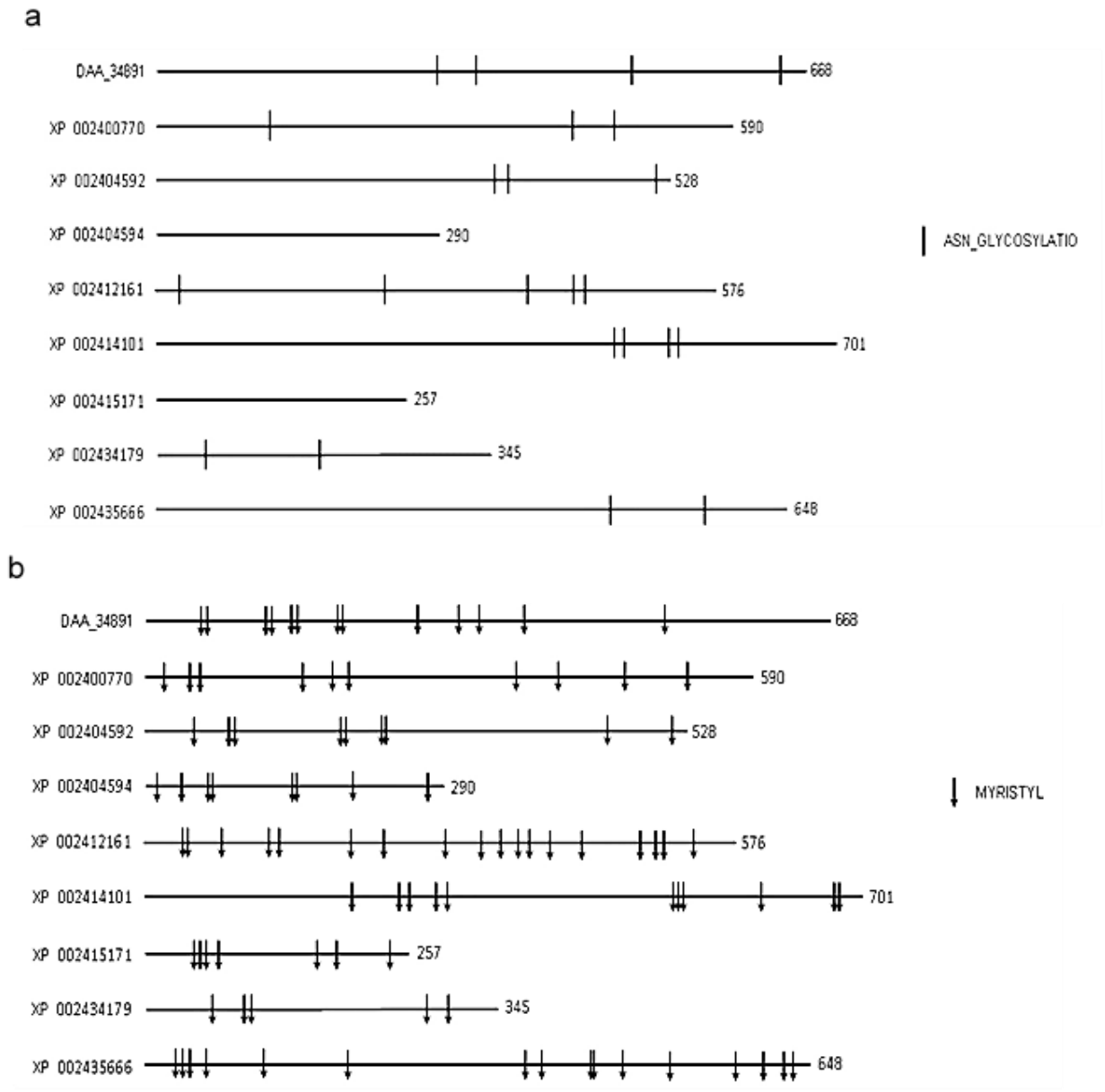

Figure 30. Relative position of glycosylation (a) and myristoylation sites (b) *on Ixodes scapularis* OATPs including the transmembrane regions

Amino acid sequences of *I. scapularis* OATPs were individually analyzed at Biology WorkBench (a, b), NCBI conserved domain search (a) and PROSITE (b) databases for glycosylation (a) and myristoylation (b) sites. The glycosylation (a) and myristoylation (b) in the full amino acid sequence including the transmembrane regions within each OATP were considered for the figure. GenBank accession numbers are shown at the left side of the figure. Figure not to scale.

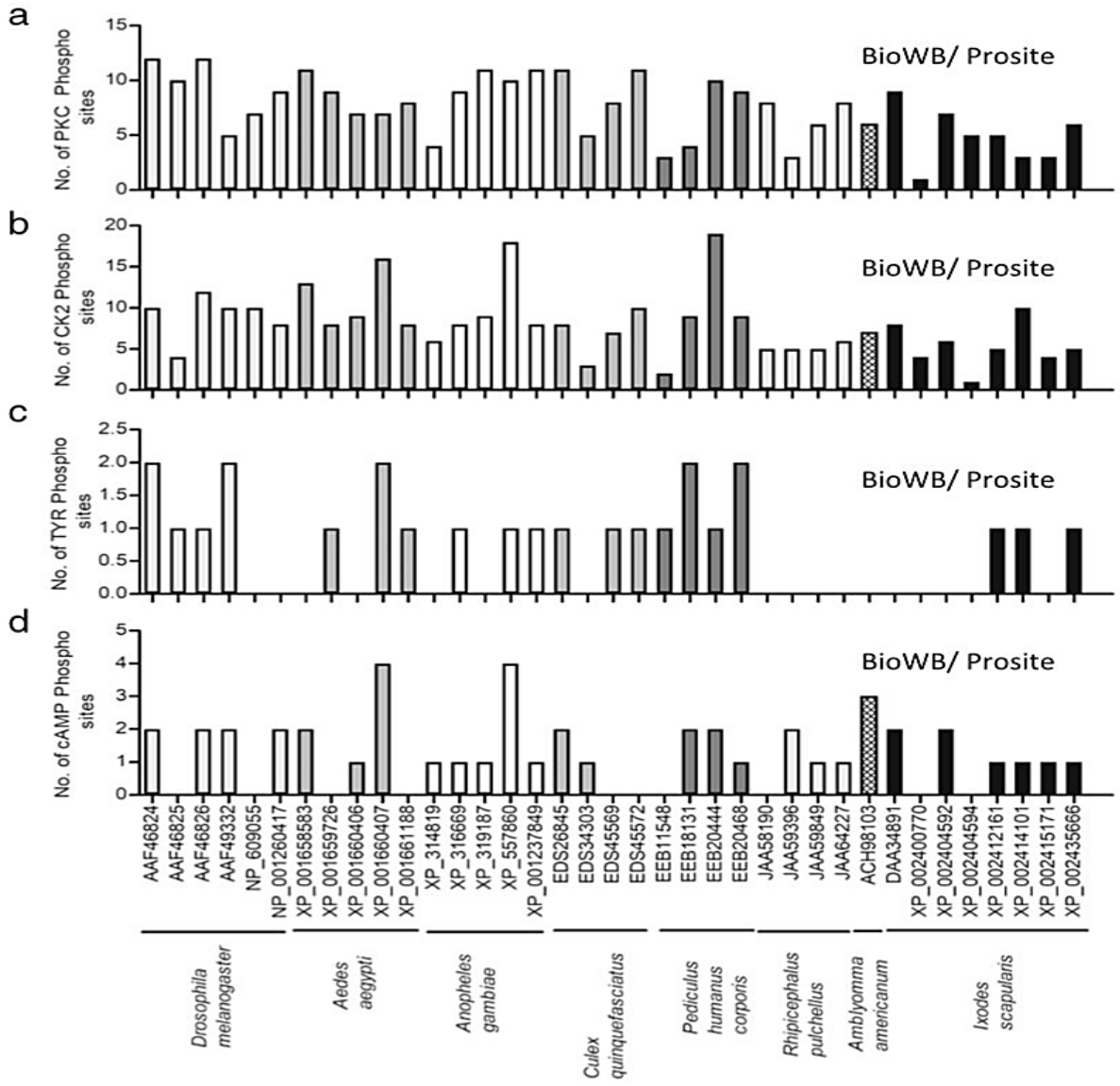

Figure 31. Analysis of phosphorylation sites in OATPs from medically important vectors

Amino acid sequences of several OATPs were individually analyzed at Biology WorkBench or PROSITE databases for PKC phosphorylation (a), CK2 phosphorylation (b), tyrosine phosphorylation (c) and cAMP-dependent phosphorylation sites (d). Histograms represent the number of post-translational modification sites for each OATP. The posttranslational modifications in the transmembrane regions within each OATP were not considered for histogram plots. GenBank accession numbers and organism names are shown at the bottom of the figure.

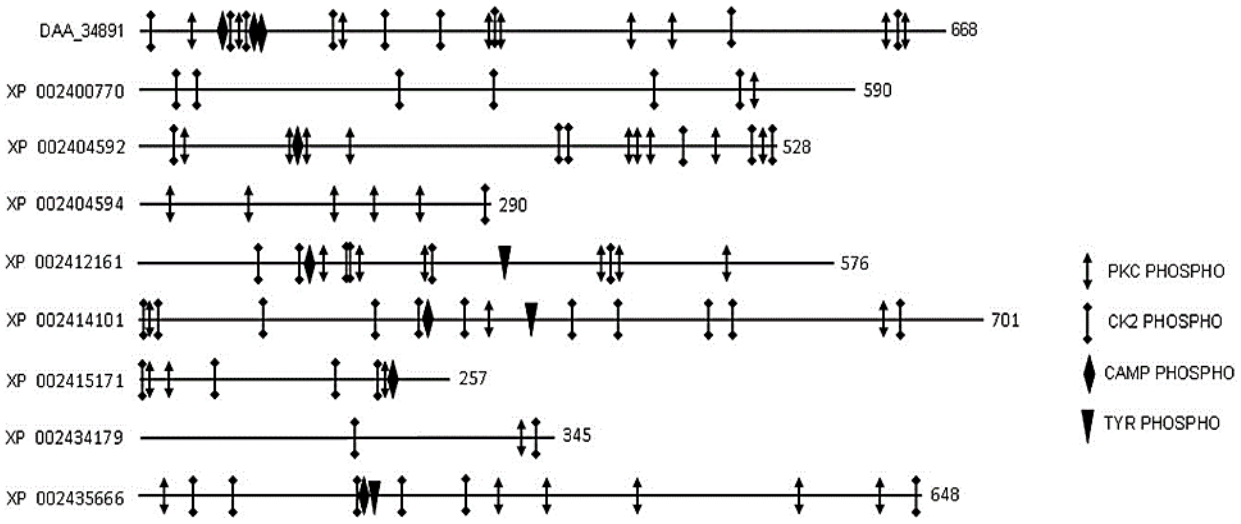

Figure 32. Position of different phosphorylation sites on *Ixodes scapularis* OATPs including the transmembrane regions

Amino acid sequences of *I. scapularis* OATPs were individually analyzed at Biology WorkBench or PROSITE databases for PKC phosphorylation, CK2 phosphorylation, tyrosine phosphorylation and cAMP-dependent phosphorylation sites (d). The figure represents the relative positions of phosphorylation sites for each OATP. The phosphorylation in the full length amino acid sequence including the transmembrane regions within each OATP were considered for this figure. GenBank accession numbers are shown at the left side of the figure. Figure not to scale.

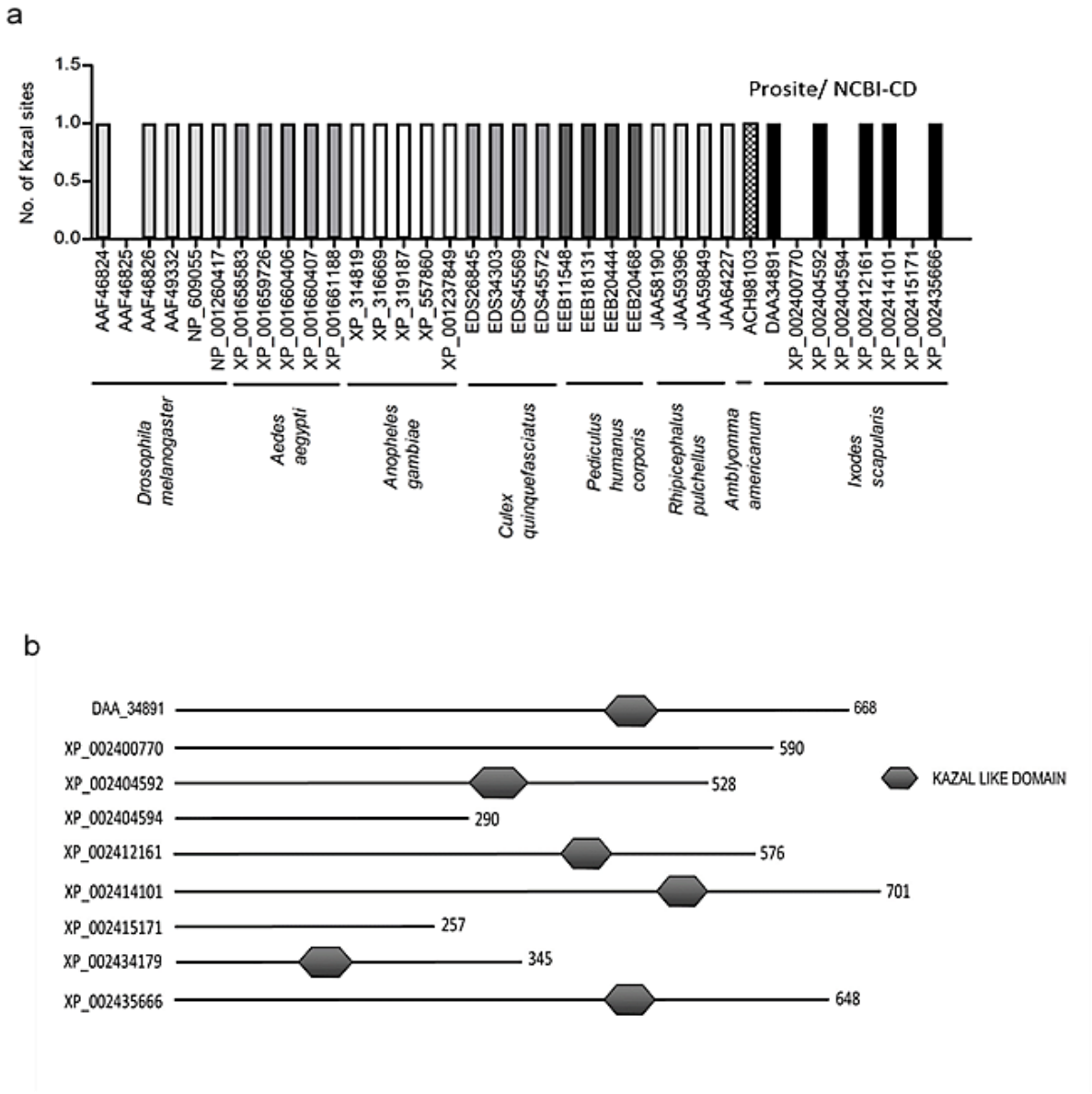

Figure 33. Analysis of Kazal domain sites in OATPs from medically important vectors

Amino acid sequences of OATPs were individually analyzed at NCBI conserved domain search and PROSITE databases for prediction of Kazal domain sites in several arthropod OATPs. (a) Histograms represent number of KAZAL sites for each OATP. (b) Relative position of the KAZAL sites in *I. scapularis* OATPs is shown. Full-length OATP sequences including the transmembrane regions were considered to determine KAZAL sites.

Table 7. Summary of the number of glycosylation sites in different arthropod OATPs

The numbers of myristoylation sites predicted from either outside (external) or inside (internal) regions of OATPs but not in the transmembrane regions are shown. Aa indicates total number of amino acids and TM indicates number of transmembrane regions.

Organism	Accession	Aa	TM	Oatp Motif	ASN Glycosylation sites		
					Internal	External	Total
Aedes aegypti	XP_001658583	815	12	+	0	5	5
	XP_001659726	664	12	+	1	4	5
	XP_001660406	752	11	+	5	4	9
	XP_001660407	1266	11	+	6	8	14
	XP_001661188	728	12	+	0	5	5
Anopheles gambiae	XP_314819	650	10	+	5	1	6
	XP_316669	772	12	+	0	4	4
	XP_319187	822	12	+	2	2	4
	XP_557860	1301	13	+	6	4	10
	XP_001237849	687	12	+	2	4	6
Culex quinque fasciatus	EDS_26845	821	12	+	0	2	2
	EDS_34303	629	9	+	4	3	7
	EDS_45569	708	12	+	1	5	6
	EDS_45572	764	11	+	0	4	4
Pediculus humanus corporis	EEB_11548	607	11	+	0	6	6
	EEB_18131	751	12	+	2	7	9
	EEB_20444	996	11	+	1	7	8
	EEB_20468	864	12	+	2	8	10
Rhipicephalus pulchellus	JAA_58190	748	12	+	1	3	4
	JAA_59396	585	10	+	0	2	2
	JAA_59849	798	12	+	0	4	4
	JAA_64227	734	11	+	3	0	3
Amblyomma americanum	ACH_98103	733	12	+	1	1	2
Ixodes scapularis	DAA_34891	668	12	+	2	1	3
	XP_002400770	590	12	+	0	3	3
	XP_002404592	528	10	+	2	1	3
	XP_002404594	290	6	+	0	0	0
	XP_002412161	576	11	+	1	3	4
	XP_002414101	701	7	+	5	0	5
	XP_002415171	257	5	+	0	0	0
	XP_002435666	648	12	+	1	1	2
Drosophila melanogaster	AAF46824	684	12	+	2	2	4
	AAF46825	680	12	+	1	4	5
	AAF46826	789	12	+	3	6	9
	AAF49332	819	12	+	2	6	8
	NP_609055	692	12	+	4	2	6
	NP_001260417	745	11	+	2	6	8

Table 8. Summary of the number of myristoylation sites in different arthropod OATPs

The numbers of myristoylation sites predicted from either outside (external) or inside (internal) regions of OATPs but not in the transmembrane regions are shown. Aa indicates total number of amino acids and TM indicates number of transmembrane regions.

Organism	Accession	Aa	TM	Oatp Motif	Myristoylation sites		
					Internal	External	Total
Aedes aegypti	XP_001658583	815	12	+	1	3	4
	XP_001659726	664	12	+	2	2	4
	XP_001660406	752	11	+	2	6	8
	XP_001660407	1266	11	+	5	16	21
	XP_001661188	728	12	+	4	6	10
Anopheles gambiae	XP_314819	650	10	+	5	3	8
	XP_316669	772	12	+	3	4	7
	XP_319187	822	12	+	2	6	8
	XP_557860	1301	13	+	4	20	24
	XP_001237849	687	12	+	4	3	7
Culex quinque fasciatus	EDS_26845	821	12	+	2	2	4
	EDS_34303	629	9	+	1	3	4
	EDS_45569	708	12	+	1	6	7
	EDS_45572	764	11	+	3	3	6
Pediculus humanus corporis	EEB_11548	607	11	+	2	3	5
	EEB_18131	751	12	+	0	5	5
	EEB_20444	996	11	+	2	5	7
	EEB_20468	864	12	+	2	6	8
Rhipicephalus pulchellus	JAA_58190	748	12	+	5	3	8
	JAA_59396	585	10	+	1	5	6
	JAA_59849	798	12	+	10	4	14
	JAA_64227	734	11	+	4	5	9
Amblyomma americanum	ACH_98103	733	12	+	2	5	7
Ixodes scapularis	DAA_34891	668	12	+	1	2	3
	XP_002400770	590	12	+	1	2	3
	XP_002404592	528	10	+	1	2	3
	XP_002404594	290	6	+	2	2	4
	XP_002412161	576	11	+	3	5	8
	XP_002414101	701	7	+	3	4	7
	XP_002415171	257	5	+	0	3	3
	XP_002435666	648	12	+	1	7	8
Drosophila melanogaster	AAF46824	684	12	+	1	2	3
	AAF46825	680	12	+	1	4	5
	AAF46826	789	12	+	1	5	6
	AAF49332	819	12	+	9	4	13
	NP_609055	692	12	+	4	4	8
	NP_001260417	745	11	+	2	3	5

Table 9. Summary of the number of PKC phosphorylation sites in different arthropod OATPs

The numbers of PKC phosphorylation sites predicted either outside or inside regions of OATPs but not in the transmembrane regions are shown. Aa indicates total number of amino acids, TM indicates number of transmembrane regions, Int. indicates number of sites in the inside region and Ext. indicates outside.

Organism	Accession	Aa	TM	OATP Motif	PKC_PHOSPHO		
					Int.	Ext.	Total
Aedes aegypti	XP_001658583	815	12	+	4	7	11
	XP_001659726	664	12	+	5	4	9
	XP_001660406	752	11	+	0	7	7
	XP_001660407	1266	11	+	3	4	7
	XP_001661188	728	12	+	6	2	8
Anopheles gambiae	XP_314819	650	10	+	1	3	4
	XP_316669	772	12	+	6	3	9
	XP_319187	822	12	+	5	6	11
	XP_557860	1301	13	+	2	8	10
	XP_001237849	687	12	+	9	2	11
Culex quinque fasciatus	EDS_26845	821	12	+	6	5	11
	EDS_34303	629	9	+	2	3	5
	EDS_45569	708	12	+	3	5	8
	EDS_45572	764	11	+	6	5	11
Pediculus humanus corporis	EEB_11548	607	11	+	2	1	3
	EEB_18131	751	12	+	2	2	4
	EEB_20444	996	11	+	5	5	10
	EEB_20468	864	12	+	6	3	9
Rhipicephalus pulchellus	JAA_58190	748	12	+	7	1	8
	JAA_59396	585	10	+	1	2	3
	JAA_59849	798	12	+	4	2	6
	JAA_64227	734	11	+	6	2	8
Amblyomma americanum	ACH_98103	733	12	+	4	2	6
Ixodes scapularis	DAA_34891	668	12	+	5	4	9
	XP_002400770	590	12	+	1	0	1
	XP_002404592	528	10	+	3	4	7
	XP_002404594	290	6	+	3	2	5
	XP_002412161	576	11	+	2	3	5
	XP_002414101	701	7	+	1	2	3
	XP_002415171	257	5	+	3	0	3
	XP_002435666	648	12	+	3	3	6
Drosophila melanogaster	AAF46824	684	12	+	7	5	12
	AAF46825	680	12	+	5	5	10
	AAF46826	789	12	+	9	3	12
	AAF49332	819	12	+	3	2	5
	NP_609055	692	12	+	2	5	7
	NP_001260417	745	11	+	4	5	9

Table 10. Summary of the number of CK2 phosphorylation sites in different arthropod OATPs

The numbers of CK2 phosphorylation sites predicted either outside or inside regions of OATPs but not in the transmembrane regions are shown. Aa indicates total number of amino acids, TM indicates number of transmembrane regions, Int. indicates number of sites in the inside region and Ext. indicates outside.

Organism	Accession	Aa	TM	OATP Motif	CK2_PHOSPHO		
					Int.	Ext.	Total
Aedes aegypti	XP_001658583	815	12	+	3	10	13
	XP_001659726	664	12	+	2	6	8
	XP_001660406	752	11	+	4	5	9
	XP_001660407	1266	11	+	7	9	16
	XP_001661188	728	12	+	6	2	8
Anopheles gambiae	XP_314819	650	10	+	5	1	6
	XP_316669	772	12	+	4	4	8
	XP_319187	822	12	+	3	6	9
	XP_557860	1301	13	+	5	13	18
	XP_001237849	687	12	+	5	3	8
Culex quinque fasciatus	EDS_26845	821	12	+	2	6	8
	EDS_34303	629	9	+	3	0	3
	EDS_45569	708	12	+	3	4	7
	EDS_45572	764	11	+	2	8	10
Pediculus humanus corporis	EEB_11548	607	11	+	1	1	2
	EEB_18131	751	12	+	4	5	9
	EEB_20444	996	11	+	7	12	19
	EEB_20468	864	12	+	5	4	9
Rhipicephalus pulchellus	JAA_58190	748	12	+	2	3	5
	JAA_59396	585	10	+	2	3	5
	JAA_59849	798	12	+	1	4	5
	JAA_64227	734	11	+	3	3	6
Amblyomma americanum	ACH_98103	733	12	+	4	3	7
Ixodes scapularis	DAA_34891	668	12	+	4	4	8
	XP_002400770	590	12	+	1	3	4
	XP_002404592	528	10	+	4	2	6
	XP_002404594	290	6	+	1	0	1
	XP_002412161	576	11	+	2	3	5
	XP_002414101	701	7	+	7	3	10
	XP_002415171	257	5	+	2	2	4
	XP_002435666	648	12	+	4	1	5
Drosophila melanogaster	AAF46824	684	12	+	6	4	10
	AAF46825	680	12	+	2	2	4
	AAF46826	789	12	+	9	3	12
	AAF49332	819	12	+	6	4	10
	NP_609055	692	12	+	5	5	10
	NP_001260417	745	11	+	2	6	8

Table 11. Summary of the number of tyrosine phosphorylation sites in different arthropod OATPs

The numbers of tyrosine phosphorylation sites predicted either outside or inside regions of OATPs but not in the transmembrane regions are shown. Aa indicates total number of amino acids, TM indicates number of transmembrane regions, Int. indicates number of sites in the inside region and Ext. indicates outside.

Organism	Accession	Aa	TM	OATP Motif	TYR_PHOSPHO		
					Int.	Ext.	Total
Aedes aegypti	XP_001658583	815	12	+	0	0	0
	XP_001659726	664	12	+	0	1	1
	XP_001660406	752	11	+	0	0	0
	XP_001660407	1266	11	+	2	0	2
	XP_001661188	728	12	+	0	1	1
Anopheles gambiae	XP_314819	650	10	+	0	0	0
	XP_316669	772	12	+	0	1	1
	XP_319187	822	12	+	0	0	0
	XP_557860	1301	13	+	1	0	1
	XP_001237849	687	12	+	0	1	1
Culex quinque fasciatus	EDS_26845	821	12	+	0	1	1
	EDS_34303	629	9	+	0	0	0
	EDS_45569	708	12	+	0	1	1
	EDS_45572	764	11	+	0	1	1
Pediculus humanus corporis	EEB_11548	607	11	+	0	1	1
	EEB_18131	751	12	+	0	2	2
	EEB_20444	996	11	+	0	1	1
	EEB_20468	864	12	+	1	1	2
Rhipicephalus pulchellus	JAA_58190	748	12	+	0	0	0
	JAA_59396	585	10	+	0	0	0
	JAA_59849	798	12	+	0	0	0
	JAA_64227	734	11	+	0	0	0
Amblyomma americanum	ACH_98103	733	12	+	0	0	0
Ixodes scapularis	DAA_34891	668	12	+	0	0	0
	XP_002400770	590	12	+	0	0	0
	XP_002404592	528	10	+	0	0	0
	XP_002404594	290	6	+	0	0	0
	XP_002412161	576	11	+	0	1	1
	XP_002414101	701	7	+	1	0	1
	XP_002415171	257	5	+	0	0	0
	XP_002435666	648	12	+	1	0	1
Drosophila melanogaster	AAF46824	684	12	+	1	1	2
	AAF46825	680	12	+	0	1	1
	AAF46826	789	12	+	0	1	1
	AAF49332	819	12	+	2	0	2
	NP_609055	692	12	+	0	0	0
	NP_001260417	745	11	+	0	0	0

Table 12. Summary of the number of CAMP phosphorylation sites in different arthropod OATPs

The numbers of CAMP phosphorylation sites predicted either outside or inside regions of OATPs but not in the transmembrane regions are shown. Aa indicates total number of amino acids, TM indicates number of transmembrane regions, Int. indicates number of sites in the inside region and Ext. indicates outside.

Organism	Accession	Aa	TM	OATP Motif	CAMP_PHOSPHO		
					Int.	Ext.	Total
Aedes aegypti	XP_001658583	815	12	+	2	0	2
	XP_001659726	664	12	+	0	0	0
	XP_001660406	752	11	+	0	1	1
	XP_001660407	1266	11	+	1	3	4
	XP_001661188	728	12	+	0	0	0
Anopheles gambiae	XP_314819	650	10	+	0	1	1
	XP_316669	772	12	+	1	0	1
	XP_319187	822	12	+	1	0	1
	XP_557860	1301	13	+	1	3	4
	XP_001237849	687	12	+	1	0	1
Culex quinque fasciatus	EDS_26845	821	12	+	2	0	2
	EDS_34303	629	9	+	1	0	1
	EDS_45569	708	12	+	0	0	0
	EDS_45572	764	11	+	0	0	0
Pediculus humanus corporis	EEB_11548	607	11	+	0	0	0
	EEB_18131	751	12	+	1	1	2
	EEB_20444	996	11	+	2	0	2
	EEB_20468	864	12	+	1	0	1
Rhipicephalus pulchellus	JAA_58190	748	12	+	0	0	0
	JAA_59396	585	10	+	1	1	2
	JAA_59849	798	12	+	1	0	1
	JAA_64227	734	11	+	1	0	1
Amblyomma americanum	ACH_98103	733	12	+	2	1	3
Ixodes scapularis	DAA_34891	668	12	+	1	1	2
	XP_002400770	590	12	+	0	0	0
	XP_002404592	528	10	+	2	0	2
	XP_002404594	290	6	+	0	0	0
	XP_002412161	576	11	+	1	0	1
	XP_002414101	701	7	+	1	0	1
	XP_002415171	257	5	+	1	0	1
	XP_002435666	648	12	+	1	0	1
Drosophila melanogaster	AAF46824	684	12	+	2	0	2
	AAF46825	680	12	+	0	0	0
	AAF46826	789	12	+	1	1	2
	AAF49332	819	12	+	2	0	2
	NP_609055	692	12	+	0	0	0
	NP_001260417	745	11	+	1	1	2

3.3 DISCUSSION

The success in the development of a broad-spectrum anti-vector vaccine to treat diseases transmitted by arthropods, such as ticks, mosquitos, and lice, largely depends on the identification and characterization of conserved proteins present in the vectors hosts. In previous chapter, the evidence on the role of the OATP family of proteins is provided in the survival of *A. phagocytophilum*, a rickettsial pathogen transmitted by ticks. In the present chapter, further evidences are provided on the role of the OATP family of proteins in the survival of LGTV, an intracellular tick-borne virus. Collectively, both studies emphasize that arthropod OATP is a potential molecular target that is modulated by intracellular vector-borne pathogens for their survival in the vector host.

For extracellular pathogen, *B. burgdorferi,* and intracellular LGTV pathogen, no changes were observed in OATP gene expression between unfed infected and uninfected control ticks. Since these LGTV infected ticks were synchronously infected and obtained in late stages of infection (17 days p.i. for LGTV), possibility of LGTV to modulate OATPs at early stages of infection in the ticks cannot be ruled out.

To understand the role of OATPs in the early stages of infection, the *in vitro* ISE6 tick cell line and LGTV as a model were used. To test this, 24 h was considered as early, and 72 h as late time points of infection. Significant downregulation of OATPS at 24 h but not at 72 h, besides a significant increase of LGTV loads from 24 to 72 h (Figure 22), suggests that modulation of OATPs is critical for initial replication of LGTV virus in the cells. It is hypothesized that downregulation of OATPs upon LGTV infection is a host response to control the viral replication. This hypothesis is further supported by the observation of a significant reduction of LGTV viral loads upon treatment of the tick cells with OATP inhibitor (SPZ) (Figure 24b). SPZ is a general OATP inhibitor, proposed to be non-selective uridine 5'-diphospho-glucuronosyltransferase (UGT) inhibitor and a substrate for ATP-binding cassette (ABC) transporters (Evers et al., 2000; Uchaipichat et al., 2006). Therefore, roles of these molecules on LGTV infection cannot be excluded. Upon treatment of LGTV infected-tick cells with SPZ, a differential expression (up-/-downregulation) of OATPs was noted. This observation suggests that the

transcriptional regulation of OATPs could be interdependent on each other. More clearly, blocking of one type of OATP could affect transcription of other OATPs.

In the previous study (Chapter 2, Figure 12b), It was noticed that the silencing of *kat* gene expression affected the expression of the *isoatp4056* gene (Taank et al., 2017). Based on this observation, it was proposed that xanthurenic acid (XA), a byproduct of the tryptophan pathway and a product of KAT enzyme is essential for gene expression of *isoatp4056.* The results from this study are consistent with *A. phagocytophilum*-infection proposed model (Taank et al., 2017), where significantly reduced expression of *isoatp4056* (Figure 26d) and *kat* (Figure 26j) was observed upon SPZ inhibitor treatment of LGTV-infected tick cells. Collectively, these studies suggest a highly inter-dependent pathway among OATPs and KAT in the presence of the pathogen.

Furthermore, in this study, putative post-translational modification (PTM) on various arthropod OATPs amino acid sequences were predicted and analyzed. Glycosylation is an essential PTM commonly observed in membrane-bound proteins (Spiro, 2002). Glycosylation could be responsible for membrane targeting or protein stability (Zhou et al., 2005). This study suggests that PTM might be necessary during the initial stages of infection with the intracellular pathogen, perhaps for entry of the pathogen. In the prediction analysis, *Aedes aegypti* (XP_001660407) was noted to contain the highest number of glycosylation sites in comparison to the other arthropods OATPs. This opens up a fascinating question: does the level of glycosylation have any impact on membrane protein targeting or stability of OATPs during vector-pathogen interactions?

It is previously reported that an intracellular pathogen can induce actin phosphorylation in the vector-host through IPAK1 mediated signaling (Sultana et al., 2010). Higher number of predicted CK2, PKC, and cAMP phosphorylation sites were observed in comparison to TYR phosphorylation sites; this suggests that serine/threonine kinases are important mediators of signaling in the medically important vectors.

It was also noted that all but four of the OATPs carry one Kazal domain in their primary amino acid sequence (Figure 33a). It was previously reported that serine

proteases containing Kazal domain play an essential role in various physiological mechanism in several organisms including blood-feeding arthropods (Laskowski and Kato, 1980; Mulenga et al., 2008). Further a detailed PTM analysis on *I. scapularis* XP_002414101.1 OATP (Figure 28) revealed presence of one CK2 phosphorylation site in addition to three myristoylation and one glycosylations site on the Kazal domain of the protein. These PTM sites could be playing a crucial role in the proper functioning of the protein. Future mutational analysis on PTM sites could reveal important therapeutic approaches. Knockdown of OATP with dsRNA in *A. americanum* ticks showed lower engorgement weight as compared to the controls ticks, suggesting a critical role of OATP in blood feeding (Mulenga et al., 2008).

The presence of kazal domain in most of the arthropod OATPs suggests that this domain region on the protein sequence could be an ideal target for the development of a broad-spectrum anti-vector vaccine against many arthropod vector species.

3.4 EXPERIMENTAL PROCEDURES

3.4.1 Bacterial and Viral Isolates, Ticks and Tick Cell Line

Borrelia burgdorferi strain B31-A3 or Langat virus (LGTV) strain (LGT-TP21) was used throughout this study. These strains are referred to as *B. burgdorferi* and LGTV, respectively. *Borrelia burgdorferi*-infected ticks were generated as described (Nogueira et al., 2012). Tick RNA extractions were performed in the laboratory of Dr. Utpal Pal at the University of Maryland (MD, USA). Uninfected nymphs used in generating LGTV-infected ticks were obtained from a tick colony maintained at the Connecticut Agricultural Experiment Station, New Haven, CT, USA. ISE6 tick cell line was provided by Dr. Ulrike Munderloh at the University of Minnesota (St Paul, MN, USA) and maintained as described (Munderloh et al., 2003; Taank et al., 2017). Both uninfected and LGTV-infected ticks used in this study were maintained in an environmental chamber (Parameter Generation and Control, Black Mountain, NC, USA) set at a temperature of 23 ± 1 °C,with 95% humidity and with a regiment of 14/10 h light / dark photo-period.

3.4.1.1 Ethics Statement

The *in vitro* experiments in this study are performed based on protocols 15-012, 15-013 and 15-014 approved by the Institutional Biosafety Committee (IBC), Old Dominion University, USA.

3.4.2 In vitro Generation of LGTV-Infected Ticks

Synchronous LGTV infection in uninfected ticks was performed as described (Mitzel et al., 2007). Briefly, about 25 ticks (nymphs) were immersed in 0.5 ml of complete Dulbecco's modified Eagle's medium (DMEM) containing 1×10^7 pfu/ml of LGTV viral stock and incubated at 34 °C for 1 h. Vials containing ticks in the medium were vortexed every 10 minutes to redistribute the medium over ticks (as ticks float over the media). After incubation, ticks were thoroughly washed five times with 1X phosphate-buffered saline (PBS) and maintained for 17 days in an environmental chamber. RNA from these ticks were extracted and tested for the presence of both positive and negative sense RNA strands of LGTV as described (Mitzel et al., 2007; Zhou et al., 2018).

3.4.3 RNA Extraction and Quantitative Real-Time PCR (QRT-PCR) Analysis

Total RNA from uninfected or LGTV-infected nymphs and tick cells was generated using an Aurum Total RNA mini kit (Bio-Rad, Hercules, USA) following the manufacturer's instructions. The cDNA was later synthesized using an iScript cDNA synthesis kit (Bio-Rad) and used for QRT-PCR reactions (Taank et al., 2017; Zhou et al., 2018). Tick beta-*actin* mRNA transcripts were used to normalize the amount of template in each reaction. QRT-PCR assays were performed using iQ-SYBR Green Supermix (Bio-Rad) and a Bio-Rad CFX96 QPCR machine. *Borrelia burgdorferi flaB* gene transcripts or LGTV positive or negative RNA strands were quantified in the cDNA samples. Serial dilutions (10-fold) were made to generate a standard curve, ranging from 1 to 0.00001 ng of the respective fragments. QRT-PCR oligonucleotides for *oatps*, *actin*, *kat*, *B. burgdorferi flaB* and for the detection of LGTV are published in our previous studies (Neelakanta et al., 2007; Taank et al., 2017; Zhou et al., 2018).

3.4.4 LGTV Infection of the Tick Cells

LGTV infection of ISE6 tick cells was performed as previously described (Zhou et al., 2018). 1 MOI of LGTV of the virus was used in all the infection experiments in the tick cells. 1 X 10^5 tick cells were plated in L-15B300 medium onto 12-well plates and incubated for 24 h followed by infection with 1 MOI of LGTV and collection of the cells at 24 and 72 h post-infection (p.i.). Collected cells were processed for RNA, cDNA synthesis, and QRT-PCR analysis.

3.4.5 Tick Cell Line Experiments with OATP Inhibitor

Inhibitor treatment was performed as described (Taank et al., 2017). 1 X 10^5 tick cells were plated into 12-well cell culture plates and incubated for 20 h. After incubation, 100 µM of ±-sulfinpyrazone (SPZ, purchased from Santa Cruz Biotechnology Inc., Dallas, USA) was added and cells were incubated for an additional of 4 h followed by LGTV infection. 0.5 N NaOH was used to prepare 10 mM SPZ inhibitor stocks. For experiments, a one-tenth dilution for the stock (with 1× PBS) solution was carried out, (final concentration 1mM SPZ) was used in all the inhibitor experiments. A mock solution was prepared in a similar way but without the presence of SPZ. An equal volume of mock solution (corresponding to 100 µM volume of SPZ) was added to control cell culture wells. After 24 h p.i., cells were processed for RNA extractions followed by cDNA synthesis and QRT-PCR analysis to measure *oatp* or *kat* transcripts and LGTV loads.

3.4.6 Bioinformatic Analysis

The amino acid sequences that contained OATP signature sequence --WxGxWWxG-- were downloaded from GenBank and individually analyzed at ExPASy PROSITE (http://prosite.expasy.org/) as described (Neelakanta et al., 2018; Sultana et al., 2016). Biology WorkBench (San Diego Supercomputer Center) available at http://workbench.sdsc.edu/ and the National Center for Biotechnology Information conserved domain search (NCBI-CD) https://www.ncbi.nlm.nih.gov/Structure/cdd/wrpsb.cgi were used to predict glycosylation, myristoylation, protein kinase C phosphorylation, casein kinase II phosphorylation, tyrosine phosphorylation,

cAMP-dependent protein kinase phosphorylation and identification of Kazal domain sites. For data analysis, the post-translational modification sites that are present either outside or inside regions of OATPs but not on the transmembrane regions were considered. TMHMM http://www.cbs.dtu.dk/services/ TMHMM/ server v.2.0 (prediction of transmembrane helices in proteins) was used to predict transmembrane and internal or external regions of the OATPs. An overview of this process is shown in Figure 34. For Kazal site prediction, full-length OATP sequences were considered.

3.4.7 GenBank Accession Numbers

The GenBank accession numbers for the OATP sequences used in the study are as follows: *D. melanogaster* (AAF46824, AAF46825, AAF46826, AAF49332, NP_609055, and NP _001260417), *Aedes aegypti* (XP_001658583, XP_001659726, XP_001660406, XP_001660407, and XP_001661188), *Anopheles gambiae* (XP_314819, XP_316669, XP_319187, XP_557860, and XP_001237849), *Culex quinquefasciatus* (EDS26845, EDS34303, EDS45569, and EDS45572), *Pediculus humanus corporis* (EEB11548, EEB18131, EEB20444, and EEB20468), *Rhipicephalus pulchellus* (JAA58190, JAA59396, JAA59849, and JAA64227), *Amblyomma americanum* (ACH98103) and *Ixodes scapularis* (DAA34891, XP_002400770, XP_002412161, XP_002414101, XP_002434179, XP_002404592, XP_002404594, XP_002415171, and XP_002435666).

3.4.8 Statistics

A non-paired two-tailed Student’s t-test and nonparametric Mann-Whitney tests from GraphPad Prism6 software and Microsoft Excel 2016 were used to calculate statistical significance. Graphs were generated using GraphPad Prism6 software. Horizontal lines in the graphs represent the mean values. $P < 0.05$ was considered significant and shown at relevant places.

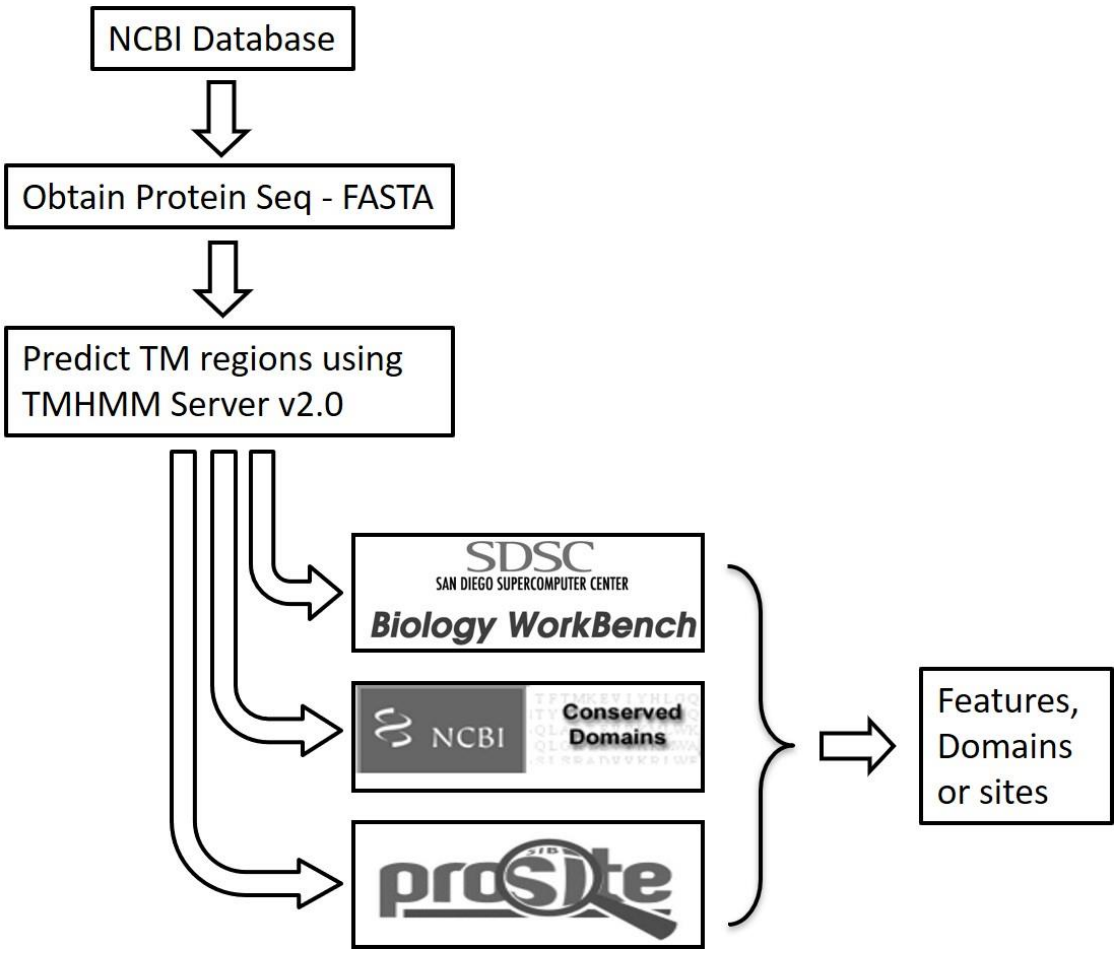

Figure 34. Workflow chart showing tools used in bioinformatics analysis for the prediction of various posttranslational modification sites and domains in oatps

Protein FASTA sequences were downloaded from NCBI GenBank Database. These sequences were analyzed to predict transmembrane regions at TMHMM server v2.0 (http://www.cbs.dtu.dk/services/TMHMM/). Transmembrane regions were removed from the sequences to obtain internally and externally exposed regions. These sequences were individually processed at Biology WorkBench, NCBI-conserved domains, and ExPASy Prosite to predict glycosylation, myristoylation, phosphorylation and Kazal sites.

CHAPTER 4

CONCLUSION

Hard bodied *I. scapularis* tick is a medically important vector, which is able to transmit many human pathogens including *A. phagocytophilum* and *Borrelia burgdorferi.* To develop new strategies to combat tick-borne diseases, both studies addressed the role of tick OATPs in the arthropod-vector-pathogen interactions. OATPs are highly conserved molecules among various arthropod species (Taank et al., 2018; Mulenga et al., 2008; Radulovic et al., 2014). The collective findings of these two studies provide novel insights into how bacterial and viral pathogen modulate a crucial pathway for their growth and survival in arthropod vectors.

The first study involving the survival of rickettsial pathogen reveals new information that xanthurenic acid (XA), a metabolite of tryptophan pathway and a specific OATPs, both are manipulated by the intracellular pathogen in the arthropod vector host. The results show that only one out of nine tick OATPs is upregulated in tick salivary gland, and this was further supported by the experiments in tick cells by higher expression of this particular OATP in *A. phagocytophilum* infected tick cells. RNA interference-mediated silencing (dsRNA studies) and OATP inhibitor experiments related to this OATP, both shows reduced bacterial survival in ticks and tick cells.

Using RNA interference, it is further shown that *isoatp4056* mRNA transcript levels were not changed during the acquisition of the pathogen into ticks (nymphs) fed on *A. phagocytophilum* infected murine host as compared to ticks fed on uninfected murine hosts. However, the possibility that OATPs can play a role during transmission of *A. phagocytophilum* to the murine host still needs to be explored.

The increased amounts of kynurenine aminotransferase (*kat*) mRNA transcripts in the salivary gland of the infected tick suggests the involvement of the tryptophan metabolic pathway for intracellular pathogen survival. RNAi mediated silencing of this gene reduced the bacterial burden in tick cells. Since *kat* is responsible for the

production of XA, further the role of XA was studied in the *A. phagocytophilum* survival in tick cells and found that exogenous addition of XA increased the bacterial survival. This is further supported by increased bacterial survival in the tick (nymph) salivary glands with the exogenous injection of XA when compared to mock-injected control ticks. EMSA studies revealed that XA promotes increased binding of nuclear proteins to the *isoatp4056* promoter. This further indicates the possibility that XA may act as a cofactor to some essential nuclear proteins, perhaps some transcription factors, and this needs to be further explored in the future.

The second study focuses on the involvement of tick OATPs in other extracellular bacterial and viral pathogen interaction with ticks, this study provides additional support on the role of the tick OATP in the interaction of viruses with tick cells at early stages of the infection. Four out of nine tick OATPs were downregulated with LGTV infection in the tick cells. This modulation of the host OATPs was found only at the early stages and not at later stages of the viral infection in the tick cells. Since *B. burgdorferi*-infected tick samples, used in this study were at later stages of the infection (unfed nymphal stage), no impact on any of the nine-tick OATPs was noted upon *B. burgdorferi* infection. The possibility that the arthropod OATPs plays a role in both LGTV and *B. burgdorferi* infections at early stages in the ticks cannot be ruled out and hence needs future attention.

The observation from OATP inhibitor studies shows therapeutic potential of this inhibitor in blocking LGTV and perhaps other tick-borne virus infection. It was also noticed that the expression of five out of nine OATPs were altered with OATP inhibitor treatment in LGTV infected tick cells. This may be due to interdependent transcriptional regulation of OATPs. The expression of both *kat* and *isoatp4056* genes were reduced upon OATP inhibitor treatment of LGTV infected tick cells. This data is consistent with the findings from the first study involving *A. phagocytophilum.* Taken together, these studies suggest highly interdependent pathways between *kat* and OATPs that are modulated by both intracellular bacterial and viral pathogens.

It is previously reported that post-translational modifications (PTM) such as glycosylation is essential and is commonly observed in membrane proteins. Glycosylation levels can impact protein targeting and stability (Spiro, 2002; Zhou et al.,

2005). It is also reported that rickettsial pathogens modulates actin phosphorylation in the host vector (Sultana et al., 2010). Various PTM on the OATPs sequences were predicted and a comparative analysis of various arthropod OATPs was performed. It is found that all arthropod OATP sequences except two from *Ixodes scapularis* carried multiple glycosylation and phosphorylation sites. Studies in the future may reveal whether glycosylation levels regulate OATP protein stability and/or membrane targeting during tick-pathogen interactions.

The observation of a reduced level of tyrosine phosphorylation sites when compared to the presence of CK2, PKC, and cAMP phosphorylation site emphasizes that serine / threonine kinases are important signaling mediators in many medically important vectors. It is further noticed that all but four out of all OATPs amino acid sequence analyzed, contained at least one Kazal type domain. Proteins with Serine protease containing Kazal domain are known to play crucial roles in various physiological mechanisms including blood-feeding in arthropods (Laskowski and Kato, 1980; Mulenga et al., 2008). Kazal motif is present in most arthropod OATPs, and this site could be considered as a desirable target for the development of a broad-spectrum anti-vector vaccine.

Collectively, these studies provides significant evidence on the role of OATP and KAT in the interactions of arthropods with bacteria and virus, especially intracellular pathogens. In the future, understanding the role of these highly conserved molecules in vector-pathogen interactions may provide novel and universal strategies to combat several tick-borne bacterial and viral diseases.

REFERENCES

Alam, K., Crowe, A., Wang, X., Zhang, P., Ding, K., Li, L., and Yue, W. (2018). Regulation of Organic Anion Transporting Polypeptides (OATP) 1B1- and OATP1B3-Mediated Transport: An Updated Review in the Context of OATP-Mediated Drug-Drug Interactions. Int J Mol Sci *19*.

Alberti, A., Addis, M.F., Sparagano, O., Zobba, R., Chessa, B., Cubeddu, T., Parpaglia, M.L., Ardu, M., and Pittau, M. (2005). *Anaplasma phagocytophilum*, Sardinia, Italy. Emerg Infect Dis *11*, 1322-1324.

Alekseev, A.N., Dubinina, H.V., and Jushkova, O.V. (2004). First report on the coexistence and compatibility of seven tick-borne pathogens in unfed adult *Ixodes persulcatus Schulze* (Acarina: Ixodidae). Int J Med Microbiol *293 Suppl 37*, 104-108.

Anderson, J.F. (1988). Mammalian and avian reservoirs for *Borrelia burgdorferi.* Ann N Y Acad Sci *539*, 180-191.

Anderson, J.F. (1989). Epizootiology of *Borrelia* in *Ixodes* tick vectors and reservoir hosts. Rev Infect Dis *11 Suppl 6*, S1451-1459.

Anderson, J.F., and Armstrong, P.M. (2012). Prevalence and genetic characterization of Powassan virus strains infecting *Ixodes scapularis* in Connecticut. Am J Trop Med Hyg *87*, 754-759.

Anderson, J.F., and Magnarelli, L.A. (2008). Biology of ticks. Infect Dis Clin North Am *22*, 195-215.

Arai, M., Billker, O., Morris, H.R., Panico, M., Delcroix, M., Dixon, D., Ley, S.V., and Sinden, R.E. (2001). Both mosquito-derived xanthurenic acid and a host blood-derived factor regulate gametogenesis of *Plasmodium* in the midgut of the mosquito. Mol Biochem Parasitol *116*, 17-24.

Ayllon, N., Villar, M., Galindo, R.C., Kocan, K.M., Sima, R., Lopez, J.A., Vazquez, J., Alberdi, P., Cabezas-Cruz, A., Kopacek, P.*, et al.* (2015). Systems biology of tissue-specific response to *Anaplasma phagocytophilum* reveals differentiated apoptosis in the tick vector *Ixodes scapularis*. PLoS Genet *11*, e1005120.

Bakken, J.S., and Dumler, J.S. (2015). Human granulocytic anaplasmosis. Infect Dis Clin North Am *29*, 341-355.

Bakken, J.S., Dumler, J.S., Chen, S.M., Eckman, M.R., Van Etta, L.L., and Walker, D.H. (1994). Human granulocytic ehrlichiosis in the upper Midwest United States. A new species emerging? JAMA *272*, 212-218.

Barandika, J.F., Hurtado, A., Garcia-Sanmartin, J., Juste, R.A., Anda, P., and Garcia-Perez, A.L. (2008). Prevalence of tick-borne zoonotic bacteria in questing adult ticks from northern Spain. Vector Borne Zoonotic Dis *8*, 829-835.

Barlough, J.E., Madigan, J.E., Kramer, V.L., Clover, J.R., Hui, L.T., Webb, J.P., and Vredevoe, L.K. (1997). *Ehrlichia phagocytophila* genogroup rickettsiae in ixodid ticks from California collected in 1995 and 1996. J Clin Microbiol *35*, 2018-2021.

Battilani, M., De Arcangeli, S., Balboni, A., and Dondi, F. (2017). Genetic diversity and molecular epidemiology of *Anaplasma*. Infect Genet Evol *49*, 195-211.

Battsetseg, B., Boldbaatar, D., Battur, B., Xuan, X., and Fujisaki, K. (2009). Cloning and molecular characterization of tick kynurenine aminotransferase (HlKAT) from *Haemaphysalis longicornis* (Acari: *Ixodidae*). Parasitol Res *105*, 669-679.

Belongia, E.A., Reed, K.D., Mitchell, P.D., Kolbert, C.P., Persing, D.H., Gill, J.S., and Kazmierczak, J.J. (1997). Prevalence of granulocytic Ehrlichia infection among white-tailed deer in Wisconsin. J Clin Microbiol *35*, 1465-1468.

Ben Said, M., Belkahia, H., Alberti, A., Abdi, K., Zhioua, M., Daaloul-Jedidi, M., and Messadi, L. (2016). First molecular evidence of [i]*Borrelia burgdorferi*[/i] sensu lato in goats, sheep, cattle and camels in Tunisia. Ann Agric Environ Med *23*, 442-447.

Bhattacharyya, M.K., and Kumar, N. (2001). Effect of xanthurenic acid on infectivity of *Plasmodium falciparum* to *Anopheles stephensi*. Int J Parasitol *31*, 1129-1133.

Billingsley, P.F., Foy, B., and Rasgon, J.L. (2008). Mosquitocidal vaccines: a neglected addition to malaria and dengue control strategies. Trends Parasitol *24*, 396-400.

Billker, O., Lindo, V., Panico, M., Etienne, A.E., Paxton, T., Dell, A., Rogers, M., Sinden, R.E., and Morris, H.R. (1998). Identification of xanthurenic acid as the putative inducer of malaria development in the mosquito. Nature *392*, 289-292.

Blanco, J.R., and Oteo, J.A. (2002). Human granulocytic ehrlichiosis in Europe. Clin Microbiol Infect *8*, 763-772.

Bunnell, J.E., Dumler, J.S., Childs, J.E., and Glass, G.E. (1998). Retrospective serosurvey for human granulocytic ehrlichiosis agent in urban white-footed mice from Maryland. J Wildl Dis *34*, 179-181.

Burgdorfer, W., Barbour, A.G., Hayes, S.F., Benach, J.L., Grunwaldt, E., and Davis, J.P. (1982). Lyme disease-a tick-borne spirochetosis? Science *216*, 1317-1319.

Burgess, E.C. (1988). *Borrelia burgdorferi* infection in Wisconsin horses and cows. Ann N Y Acad Sci *539*, 235-243.

Burgess, E.C., Gillette, D., and Pickett, J.P. (1986). Arthritis and panuveitis as manifestations of *Borrelia burgdorferi* infection in a Wisconsin pony. J Am Vet Med Assoc *189*, 1340-1342.

Bush, L.M. and M.T. Vazquez-Pertejo (2018). "Tick borne illness-Lyme disease." Dis Mon 64(5): 195-212.

Carlyon, J.A., and Fikrig, E. (2003). Invasion and survival strategies of *Anaplasma phagocytophilum*. Cell Microbiol *5*, 743-754.

Cavill, I.A. (1967). Estimation of the tryptophan metabolites xanthurenic acid, 3-hydroxykynurenine and kynurenine. Clin Chim Acta *18*, 285-289.

Casjens, S.R., Mongodin, E.F., Qiu, W.G., Luft, B.J., Schutzer, S.E., Gilcrease, E.B., Huang, W.M., Vujadinovic, M., Aron, J.K., Vargas, L.C., Freeman, S., Radune, D., Weidman, J.F., Dimitrov, G.I., Khouri, H.M., Sosa, J.E., Halpin, R.A., Dunn, J.J., Fraser, C. M. (2012). Genome stability of Lyme disease spirochetes: comparative genomics of *Borrelia burgdorferi* plasmids. PLoS One 7(3): e33280.

CDC-MMWR (2017). Surveillance for Lyme Disease — United States, 2008–2015 (Centers for Disease Control and Prevention).

CDC (2019a). Anaplasmosis (Centers for Disease Control and Prevention).

CDC (2019b). Data and Surveillance (Centers for Disease Control and Prevention).

CDC (2019c). Signs and Symptoms of Untreated Lyme Disease (Centers for Disease Control and Prevention).

Chen, S.M., Dumler, J.S., Bakken, J.S., and Walker, D.H. (1994). Identification of a granulocytotropic *Ehrlichia* species as the etiologic agent of human disease. J Clin Microbiol *32*, 589-595.

Crosby, F.L., Lundgren, A.M., Hoffman, C., Pascual, D.W., and Barbet, A.F. (2018). VirB10 vaccination for protection against *Anaplasma phagocytophilum*. BMC Microbiol *18*, 217.

Curto, M., Lionetto, L., Negro, A., Capi, M., Fazio, F., Giamberardino, M.A., Simmaco, M., Nicoletti, F., and Martelletti, P. (2015). Altered kynurenine pathway metabolites in serum of chronic migraine patients. J Headache Pain *17*, 47.

de la Fuente, J., Estrada-Pena, A., Cabezas-Cruz, A., and Kocan, K.M. (2016a). *Anaplasma phagocytophilum* Uses Common Strategies for Infection of Ticks and Vertebrate Hosts. Trends Microbiol *24*, 173-180.

de la Fuente, J., Kopacek, P., Lew-Tabor, A., and Maritz-Olivier, C. (2016b). Strategies for new and improved vaccines against ticks and tick-borne diseases. Parasite Immunol *38*, 754-769.

de la Fuente, J., and Merino, O. (2013). Vaccinomics, the new road to tick vaccines. Vaccine *31*, 5923-5929.

de La Fuente, J., Naranjo, V., Ruiz-Fons, F., Hofle, U., Fernandez De Mera, I.G., Villanua, D., Almazan, C., Torina, A., Caracappa, S., Kocan, K.M.*, et al.* (2005). Potential vertebrate reservoir hosts and invertebrate vectors of *Anaplasma marginale* and *A. phagocytophilum* in central Spain. Vector Borne Zoonotic Dis *5*, 390-401.

Dumler, J.S., Barbet, A.F., Bekker, C.P., Dasch, G.A., Palmer, G.H., Ray, S.C., Rikihisa, Y., and Rurangirwa, F.R. (2001). Reorganization of genera in the families Rickettsiaceae and Anaplasmataceae in the order Rickettsiales: unification of some species of *Ehrlichia* with *Anaplasma*, *Cowdria* with *Ehrlichia* and *Ehrlichia* with *Neorickettsia*, descriptions of six new species combinations and designation of *Ehrlichia equi* and 'HGE agent' as subjective synonyms of *Ehrlichia phagocytophila*. Int J Syst Evol Microbiol *51*, 2145-2165.

Dumler, J.S., Choi, K.S., Garcia-Garcia, J.C., Barat, N.S., Scorpio, D.G., Garyu, J.W., Grab, D.J., and Bakken, J.S. (2005). Human granulocytic anaplasmosis and *Anaplasma phagocytophilum*. Emerg Infect Dis *11*, 1828-1834.

Dunning Hotopp, J.C., Lin, M., Madupu, R., Crabtree, J., Angiuoli, S.V., Eisen, J.A., Seshadri, R., Ren, Q., Wu, M., Utterback, T.R.*, et al.* (2006). Comparative genomics of emerging human ehrlichiosis agents. PLoS Genet *2*, e21.

Eisen, L. (2018). Pathogen transmission in relation to duration of attachment by *Ixodes scapularis* ticks. Ticks Tick Borne Dis *9*, 535-542.

Escudero, R., Barral, M., Perez, A., Vitutia, M.M., Garcia-Perez, A.L., Jimenez, S., Sellek, R.E., and Anda, P. (2000). Molecular and pathogenic characterization of *Borrelia burgdorferi* sensu lato isolates from Spain. J Clin Microbiol *38*, 4026-4033.

Evers, R., de Haas, M., Sparidans, R., Beijnen, J., Wielinga, P.R., Lankelma, J., and Borst, P. (2000). Vinblastine and sulfinpyrazone export by the multidrug resistance protein MRP2 is associated with glutathione export. Br J Cancer *83*, 375-383.

Fazio, F., Lionetto, L., Curto, M., Iacovelli, L., Cavallari, M., Zappulla, C., Ulivieri, M., Napoletano, F., Capi, M., Corigliano, V.*, et al.* (2015). Xanthurenic Acid Activates mGlu2/3 Metabotropic Glutamate Receptors and is a Potential Trait Marker for Schizophrenia. Sci Rep *5*, 17799.

Fazio, F., Lionetto, L., Curto, M., Iacovelli, L., Copeland, C.S., Neale, S.A., Bruno, V., Battaglia, G., Salt, T.E., and Nicoletti, F. (2017). Cinnabarinic acid and xanthurenic acid: Two kynurenine metabolites that interact with metabotropic glutamate receptors. Neuropharmaco *112*, 365-372.

Felsheim, R.F., Herron, M.J., Nelson, C.M., Burkhardt, N.Y., Barbet, A.F., Kurtti, T.J., and Munderloh, U.G. (2006). Transformation of *Anaplasma phagocytophilum*. BMC Biotechnol *6*, 42.

Foley, J.E., Lerche, N.W., Dumler, J.S., and Madigan, J.E. (1999). A simian model of human granulocytic ehrlichiosis. Am J Trop Med Hyg *60*, 987-993.

Fraser, C.M., Casjens, S., Huang, W.M., Sutton, G.G., Clayton, R., Lathigra, R., White, O., Ketchum, K.A., Dodson, R., Hickey, E.K.*, et al.* (1997). Genomic sequence of a Lyme disease spirochaete, *Borrelia burgdorferi*. Nature *390*, 580-586.

Gao, J., Xu, K., Liu, H., Liu, G., Bai, M., Peng, C., Li, T., and Yin, Y. (2018). Impact of the Gut Microbiota on Intestinal Immunity Mediated by Tryptophan Metabolism. Front Cell Infect Microbiol *8*, 13.

Garcia, G.E., Wirtz, R.A., Barr, J.R., Woolfitt, A., and Rosenberg, R. (1998). Xanthurenic acid induces gametogenesis in *Plasmodium*, the malaria parasite. J Biol Chem *273*, 12003-12005.

George, J.E., Pound J.M., Davey R.B. (2008). Acaricides for controlling ticks on cattle and the problem of acaricide resistance. In Ticks: Biology, Disease and Control, N.P. Bowman A.S., ed. (Cambridge: Cambridge University Press), pp. 408–423.

Giil, L.M., Midttun, O., Refsum, H., Ulvik, A., Advani, R., Smith, A.D., and Ueland, P.M. (2017). Kynurenine Pathway Metabolites in Alzheimer's Disease. J Alzheimers Dis *60*, 495-504.

Gordon, W., Brownlee, A., Wilson, D. R., MacLeod, J. (1932). Tick-Borne Fever. J Comp Pathol *45*, 301-307.

Greene, R.T. (1991). Canine Lyme borreliosis. Vet Clin North Am Small Anim Pract *21*, 51-64.

Gritsun, T.S., Lashkevich, V.A., and Gould, E.A. (2003a). Tick-borne encephalitis. Antiviral Res *57*, 129-146.

Gritsun, T.S., Nuttall, P.A., and Gould, E.A. (2003b). Tick-borne flaviviruses. Adv Virus Res *61*, 317-371.

Guzman, N., and Beidas, S.O. (2018). *Anaplasma Phagocytophilum* (Anaplasmosis). In StatPearls publishing (Treasure Island (FL)).

Hagenbuch, B., and Meier, P.J. (2003). The superfamily of organic anion transporting polypeptides. Biochim Biophys Acta *1609*, 1-18.

Hagenbuch, B., and Meier, P.J. (2004). Organic anion transporting polypeptides of the OATP/ SLC21 family: phylogenetic classification as OATP/ SLCO superfamily, new nomenclature and molecular/functional properties. Pflugers Arch *447*, 653-665.

Hill, C.A., Kafatos, F.C., Stansfield, S.K., and Collins, F.H. (2005). Arthropod-borne diseases: vector control in the genomics era. Nat Rev Microbiol *3*, 262-268.

Hodzic, E., Fish, D., Maretzki, C.M., De Silva, A.M., Feng, S., and Barthold, S.W. (1998). Acquisition and transmission of the agent of human granulocytic ehrlichiosis by *Ixodes scapularis* ticks. J Clin Microbiol *36*, 3574-3578.

Hoes, M.J., and Sijben, N. (1981). Xanthurenic Acid in Depression. Journal of Orthomolecular Medicine *2*.

Hoyt, K., Chandrashekar, R., Beall, M., Leutenegger, C., and Lappin, M.R. (2018). Evidence for Clinical Anaplasmosis and Borreliosis in Cats in Maine. Top Companion Anim Med *33*, 40-44.

Humair, P., and Gern, L. (2000). The wild hidden face of Lyme borreliosis in Europe. Microbes Infect *2*, 915-922.

Johnson, R.C. (1996). Leptospira. In Medical Microbiology, S. Baron, ed. (Galveston (TX): NCBI Bookshelf).

Kalliokoski, A., and Niemi, M. (2009). Impact of OATP transporters on pharmacokinetics. Br J Pharmacol *158*, 693-705.

Khanal, S., Sultana, H., Catravas, J.D., Carlyon, J.A., and Neelakanta, G. (2017). *Anaplasma phagocytophilum* infection modulates expression of megakaryocyte cell cycle genes through phosphatidylinositol-3-kinase signaling. PLoS One *12*, e0182898.

Khanal, S., Taank, V., Anderson, J.F., Sultana, H., and Neelakanta, G. (2018). Arthropod transcriptional activator protein-1 (AP-1) aids tick-rickettsial pathogen survival in the cold. Sci Rep 8, 11409.

Kobayashi, D., Nozawa, T., Imai, K., Nezu, J., Tsuji, A., and Tamai, I. (2003). Involvement of human organic anion transporting polypeptide OATP-B (SLC21A9) in pH-dependent transport across intestinal apical membrane. J Pharmacol Exp Ther *306*, 703-708.

Kowalec, M., Szewczyk, T., Welc-Faleciak, R., Sinski, E., Karbowiak, G., and Bajer, A. (2018). Rickettsiales Occurrence and Co-occurrence in *Ixodes ricinus* Ticks in Natural and Urban Areas. Microb Ecol.

Krause, P.J., Narasimhan, S., Wormser, G.P., Barbour, A.G., Platonov, A.E., Brancato, J., Lepore, T., Dardick, K., Mamula, M., Rollend, L.*, et al.* (2014). *Borrelia miyamotoi* sensu lato seroreactivity and seroprevalence in the northeastern United States. Emerg Infect Dis *20*, 1183-1190.

Lai, Y. (2013). Organic anion-transporting polypeptides (OATPs/SLCOs) (Transporters in Drug Discovery and Development: Woodhead Publishing Series in Biomedicine).

Laskowski, M., Jr., and Kato, I. (1980). Protein inhibitors of proteinases. Annu Rev Biochem *49*, 593-626.

Le Floc'h, N., Otten, W., and Merlot, E. (2011). Tryptophan metabolism, from nutrition to potential therapeutic applications. Amino Acids *41*, 1195-1205.

Lepkovsky, S., Roboz, E., and Haagen-Smit, A.J. (1974). Nutrition classics from The Journal of Biological Chemistry 149:195-201, 1943. Xanthurenic acid and its role in the tryptophane metabolism of pyridoxine-deficient rats. Nutr Rev *32*, 338-339.

Li, L., Lee, T.K., Meier, P.J., and Ballatori, N. (1998). Identification of glutathione as a driving force and leukotriene C4 as a substrate for oatp1, the hepatic sinusoidal organic solute transporter. J Biol Chem *273*, 16184-16191.

Li, X., Li, P., Zhang, T., Zhang, P., Ren, X., and Li, G. (2019). A Serological Survey of *Borrelia burgdorferi* Infection in Sheep in Northeast China Regions Through Outer Surface Protein C-Based Enzyme-Linked Immunosorbent Assay. Vector Borne Zoonotic Dis *19*, 16-21.

Lima, V.L., Dias, F., Nunes, R.D., Pereira, L.O., Santos, T.S., Chiarini, L.B., Ramos, T.D., Silva-Mendes, B.J., Perales, J., Valente, R.H.*, et al.* (2012). The antioxidant role of xanthurenic acid in the *Aedes aegypti* midgut during digestion of a blood meal. PLoS One *7*, e38349.

Lin, M., and Rikihisa, Y. (2003). Obligatory intracellular parasitism by *Ehrlichia chaffeensis* and *Anaplasma phagocytophilum* involves caveolae and glycosylphosphatidylinositol-anchored proteins. Cell Microbiol *5*, 809-820.

Maffioli, C., Grandgirard, D., Engler, O., and Leib, S.L. (2014). A tick-borne encephalitis model in infant rats infected with langat virus. J Neuropathol Exp Neurol *73*, 1107-1115.

Magnarelli, L.A., Anderson, J.F., Levine, H.R., and Levy, S.A. (1990). Tick parasitism and antibodies to *Borrelia burgdorferi* in cats. J Am Vet Med Assoc *197*, 63-66.

Mahagita, C., Grassl, S.M., Piyachaturawat, P., and Ballatori, N. (2007). Human organic anion transporter 1B1 and 1B3 function as bidirectional carriers and do not mediate GSH-bile acid cotransport. Am J Physiol Gastrointest Liver Physiol *293*, G271-278.

Malina, H.Z., Richter, C., Mehl, M., and Hess, O.M. (2001). Pathological apoptosis by xanthurenic acid, a tryptophan metabolite: activation of cell caspases but not cytoskeleton breakdown. BMC Physiol *1*, 7.

Matsuoka, K., Kato, K., Takao, T., Ogawa, M., Ishii, Y., Shimizu, F., Masuda, J., and Takada, A. (2017). Concentrations of various tryptophan metabolites are higher in patients with diabetes mellitus than in healthy aged male adults. Diabetol Int *8*, 69-75.

McNair, C.M. (2015). Ectoparasites of medical and veterinary importance: drug resistance and the need for alternative control methods. J Pharm Pharmacol *67*, 351-363.

Mendoza-Roldan, J.A., Colella, V., Lia, R.P., Nguyen, V.L., Barros-Battesti, D.M., Iatta, R., Dantas-Torres, F., and Otranto, D. (2019). *Borrelia burgdorferi* (sensu lato) in ectoparasites and reptiles in southern Italy. Parasit Vectors *12*, 35.

Mitzel, D.N., Wolfinbarger, J.B., Long, R.D., Masnick, M., Best, S.M., and Bloom, M.E. (2007). Tick-borne flavivirus infection in *Ixodes scapularis* larvae: development of a novel method for synchronous viral infection of ticks. Virology *365*, 410-418.

Mlera, L., Melik, W., Offerdahl, D.K., Dahlstrom, E., Porcella, S.F., and Bloom, M.E. (2016). Analysis of the Langat Virus Genome in Persistent Infection of an *Ixodes scapularis* Cell Line. Viruses *8*.

Motaleb, M.A., Sal, M.S., and Charon, N.W. (2004). The decrease in FlaA observed in a flaB mutant of *Borrelia burgdorferi* occurs post-transcriptionally. J Bacteriol *186*, 3703-3711.

Mulenga, A., Khumthong, R., Chalaire, K.C., Strey, O., and Teel, P. (2008). Molecular and biological characterization of the *Amblyomma americanum* organic anion transporter polypeptide. J Exp Biol *211*, 3401-3408.

Murakami, K., Haneda, M., and Yoshino, M. (2006). Prooxidant action of xanthurenic acid and quinoline compounds: role of transition metals in the generation of reactive oxygen species and enhanced formation of 8-hydroxy-2'-deoxyguanosine in DNA. Biometals *19*, 429-435.

Neelakanta, G., Li, X., Pal, U., Liu, X., Beck, D.S., DePonte, K., Fish, D., Kantor, F.S., and Fikrig, E. (2007). Outer surface protein B is critical for *Borrelia burgdorferi* adherence and survival within *Ixodes* ticks. PLoS Pathog *3*, e33.

Neelakanta, G., and Sultana, H. (2015). Transmission-Blocking Vaccines: Focus on Anti-Vector Vaccines against Tick-Borne Diseases. Arch Immunol Ther Exp (Warsz) *63*, 169-179.

Neelakanta, G., Sultana, H., Fish, D., Anderson, J.F., and Fikrig, E. (2010). *Anaplasma phagocytophilum* induces *Ixodes scapularis* ticks to express an antifreeze glycoprotein gene that enhances their survival in the cold. J Clin Invest *120*, 3179-3190.

Neelakanta, G., Sultana, H., Sonenshine, D.E., and Andersen, J.F. (2018). Identification and characterization of a histamine-binding lipocalin-like molecule from the relapsing fever tick *Ornithodoros turicata*. Insect Mol Biol *27*, 177-187.

Nelson, C.M., Herron, M.J., Felsheim, R.F., Schloeder, B.R., Grindle, S.M., Chavez, A.O., Kurtti, T.J., and Munderloh, U.G. (2008). Whole genome transcription profiling of *Anaplasma phagocytophilum* in human and tick host cells by tiling array analysis. BMC Genomics *9*, 364.

Nigam, S.K., Bush, K.T., Martovetsky, G., Ahn, S.Y., Liu, H.C., Richard, E., Bhatnagar, V., and Wu, W. (2015). The organic anion transporter (OAT) family: a systems biology perspective. Physiol Rev *95*, 83-123.

Nogueira, S.V., Smith, A.A., Qin, J.H., and Pal, U. (2012). A surface enolase participates in *Borrelia burgdorferi*-plasminogen interaction and contributes to pathogen survival within feeding ticks. Infect Immun *80*, 82-90.

Odegaard, F. (2008). How many species of arthropods? Erwin's estimate revised. Biol Jour of the Linnean Soc *71*, 583-597.

Oxenkrug, G., Ratner, R., and Summergrad, P. (2013). Kynurenines and vitamin B6: link between diabetes and depression. J Bioinform Diabetes *1*.

Oxenkrug, G.F. (2015). Increased Plasma Levels of Xanthurenic and Kynurenic Acids in Type 2 Diabetes. Mol Neurobiol *52*, 805-810.

Parola, P., and Raoult, D. (2001). Tick-borne bacterial diseases emerging in Europe. Clin Microbiol Infect *7*, 80-83.

Pedra, J.H., Narasimhan, S., Rendic, D., DePonte, K., Bell-Sakyi, L., Wilson, I.B., and Fikrig, E. (2010). Fucosylation enhances colonization of ticks by *Anaplasma phagocytophilum*. Cell Microbiol *12*, 1222-1234.

Penza, P., Moniuszko-Malinowska, A., Czupryna, P., Pancewicz, S., and Zajkowska, J. (2016). *Borrelia burgdorferi* - morphological structure and motility as adaptation for transmission and survival in the habitat of a tick-vertebrate setup. Przegl Epidemiol *70*, 420-427.

Perez, G., Bastian, S., Chastagner, A., Agoulon, A., Plantard, O., Vourc'h, G., and Butet, A. (2017). Ecological factors influencing small mammal infection by *Anaplasma phagocytophilum* and *Borrelia burgdorferi* s.l. in agricultural and forest landscapes. Environ Microbiol *19*, 4205-4219.

Petrovec, M., Bidovec, A., Sumner, J.W., Nicholson, W.L., Childs, J.E., and Avsic-Zupanc, T. (2002). Infection with *Anaplasma phagocytophila* in cervids from Slovenia: evidence of two genotypic lineages. Wien Klin Wochenschr *114*, 641-647.

Popov, V.L., Han, V.C., Chen, S.M., Dumler, J.S., Feng, H.M., Andreadis, T.G., Tesh, R.B., and Walker, D.H. (1998). Ultrastructural differentiation of the genogroups in the genus *Ehrlichia*. J Med Microbiol *47*, 235-251.

Powell, J., Farasyn, T., Kock, K., Meng, X., Pahwa, S., Brouwer, K.L., and Yue, W. (2014). Novel mechanism of impaired function of organic anion-transporting polypeptide 1B3 in human hepatocytes: post-translational regulation of OATP1B3 by protein kinase C activation. Drug Metab Dispos *42*, 1964-1970.

Pritt, B.S., Sloan, L.M., Johnson, D.K., Munderloh, U.G., Paskewitz, S.M., McElroy, K.M., McFadden, J.D., Binnicker, M.J., Neitzel, D.F., Liu, G.*, et al.* (2011). Emergence of a new pathogenic Ehrlichia species, Wisconsin and Minnesota, 2009. N Engl J Med *365*, 422-429.

Radulovic, Z., Porter, L.M., Kim, T.K., and Mulenga, A. (2014). Comparative bioinformatics, temporal and spatial expression analyses of *Ixodes scapularis* organic anion transporting polypeptides. Ticks Tick Borne Dis *5*, 287-298.

Ribet, D., and Cossart, P. (2010). Pathogen-mediated posttranslational modifications: A re-emerging field. Cell *143*, 694-702.

Rikihisa, Y. (1991). The tribe Ehrlichieae and ehrlichial diseases. Clin Microbiol Rev *4*, 286-308.

Rikihisa, Y. (2010). *Anaplasma phagocytophilum* and *Ehrlichia chaffeensis*: subversive manipulators of host cells. Nat Rev Microbiol *8*, 328-339.

Rikihisa, Y. (2011). Mechanisms of obligatory intracellular infection with *Anaplasma phagocytophilum*. Clin Microbiol Rev *24*, 469-489.

Roth, M., Obaidat, A., and Hagenbuch, B. (2012). OATPs, OATs and OCTs: the organic anion and cation transporters of the SLCO and SLC22A gene superfamilies. Br J Pharmacol *165*, 1260-1287.

Roussel, G., Bessede, A., Klein, C., Maitre, M., and Mensah-Nyagan, A.G. (2016). Xanthurenic acid is localized in neurons in the central nervous system. Neuroscience *329*, 226-238.

Rover, S., Cesura, A.M., Huguenin, P., Kettler, R., and Szente, A. (1997). Synthesis and biochemical evaluation of N-(4-phenylthiazol-2-yl)benzenesulfonamides as high-affinity inhibitors of kynurenine 3-hydroxylase. J Med Chem *40*, 4378-4385.

Salkeld, D.J., Leonhard, S., Girard, Y.A., Hahn, N., Mun, J., Padgett, K.A., and Lane, R.S. (2008). Identifying the reservoir hosts of the Lyme disease spirochete *Borrelia burgdorferi* in California: the role of the western gray squirrel (*Sciurus griseus*). Am J Trop Med Hyg *79*, 535-540.

Scott, J.D., Clark, K.L., Foley, J.E., Anderson, J.F., Bierman, B.C., and Durden, L.A. (2018). Extensive Distribution of the Lyme Disease Bacterium, *Borrelia burgdorferi* Sensu Lato, in Multiple Tick Species Parasitizing Avian and Mammalian Hosts across Canada. Healthcare (Basel) *6*.

Seinost, G., Dykhuizen, D.E., Dattwyler, R.J., Golde, W.T., Dunn, J.J., Wang, I.N., Wormser, G.P., Schriefer, M.E., and Luft, B.J. (1999). Four clones of *Borrelia burgdorferi* sensu stricto cause invasive infection in humans. Infect Immun *67*, 3518-3524.

Severo, M.S., Choy, A., Stephens, K.D., Sakhon, O.S., Chen, G., Chung, D.W., Le Roch, K.G., Blaha, G., and Pedra, J.H. (2013). The E3 ubiquitin ligase XIAP restricts *Anaplasma phagocytophilum* colonization of *Ixodes scapularis* ticks. J Infect Dis *208*, 1830-1840.

Severo, M.S., Stephens, K.D., Kotsyfakis, M., and Pedra, J.H. (2012). *Anaplasma phagocytophilum*: deceptively simple or simply deceptive? Future Microbiol *7*, 719-731.

Smith, C.E. (1956). A virus resembling Russian spring-summer encephalitis virus from an *ixodid* tick in Malaya. Nature *178*, 581-582.

Song, P., Ramprasath, T., Wang, H., and Zou, M.H. (2017). Abnormal kynurenine pathway of tryptophan catabolism in cardiovascular diseases. Cell Mol Life Sci *74*, 2899-2916.

Spiro, R.G. (2002). Protein glycosylation: nature, distribution, enzymatic formation, and disease implications of glycopeptide bonds. Glycobiology *12*, 43R-56R.

Stanek, G., Wormser, G.P., Gray, J., and Strle, F. (2012). Lyme borreliosis. Lancet *379*, 461-473.

Steere, A.C., Malawista, S.E., Snydman, D.R., Shope, R.E., Andiman, W.A., Ross, M.R., and Steele, F.M. (1977). Lyme arthritis: an epidemic of oligoarticular arthritis in children and adults in three Connecticut communities. Arthritis Rheum *20*, 7-17.

Stieger, B., and Hagenbuch, B. (2014). Organic anion-transporting polypeptides. Curr Top Membr *73*, 205-232.

Stuen, S., Granquist, E.G., and Silaghi, C. (2013). *Anaplasma phagocytophilum* -a widespread multi-host pathogen with highly adaptive strategies. Front Cell Infect Microbiol *3*, 31.

Sukumaran, B., Narasimhan, S., Anderson, J.F., DePonte, K., Marcantonio, N., Krishnan, M.N., Fish, D., Telford, S.R., Kantor, F.S., and Fikrig, E. (2006). An *Ixodes scapularis* protein required for survival of *Anaplasma phagocytophilum* in tick salivary glands. J Exp Med *203*, 1507-1517.

Sultana, H., Neelakanta, G., Kantor, F.S., Malawista, S.E., Fish, D., Montgomery, R.R., and Fikrig, E. (2010). *Anaplasma phagocytophilum* induces actin phosphorylation to selectively regulate gene transcription in *Ixodes scapularis* ticks. J Exp Med *207*, 1727-1743.

Sultana, H., Patel, U., Toliver, M., Maggi, R.G., and Neelakanta, G. (2016). Molecular identification and bioinformatics analysis of a potential anti-vector vaccine candidate, 15-kDa salivary gland protein (Salp15), from Ixodes affinis ticks. Ticks Tick Borne Dis *7*, 46-53.

Taank, V., Dutta, S., Dasgupta, A., Steeves, T.K., Fish, D., Anderson, J.F., Sultana, H., and Neelakanta, G. (2017). Human rickettsial pathogen modulates arthropod organic anion transporting polypeptide and tryptophan pathway for its survival in ticks. Sci Rep *7*, 13256.

Taank, V., Zhou, W., Zhuang, X., Anderson, J.F., Pal, U., Sultana, H., and Neelakanta, G. (2018). Characterization of tick organic anion transporting polypeptides (OATPs) upon bacterial and viral infections. Parasit Vectors *11*, 593.

Tatum, R., ; Pearson-Shaver, A.L. (2018). *Borrelia Burgdorferi* (StatPearls [Internet]: Treasure Island (FL): StatPearls Publishing).

Thomas, V., and Fikrig, E. (2007). *Anaplasma phagocytophilum* specifically induces tyrosine phosphorylation of ROCK1 during infection. Cell Microbiol *9*, 1730-1737.

Turck, J.W., Taank, V., Neelakanta, G., and Sultana, H. (2019). *Ixodes scapularis* Src tyrosine kinase facilitates *Anaplasma phagocytophilum* survival in its arthropod vector. Ticks Tick Borne Dis (In Press).

Uchaipichat, V., Mackenzie, P.I., Elliot, D.J., and Miners, J.O. (2006). Selectivity of substrate (trifluoperazine) and inhibitor (amitriptyline, androsterone, canrenoic acid, hecogenin, phenylbutazone, quinidine, quinine, and sulfinpyrazone) "probes" for human udp-glucuronosyltransferases. Drug Metab Dispos *34*, 449-456.

Uwai, Y., and Honjo, E. (2013). Transport of xanthurenic acid by rat/human organic anion transporters OAT1 and OAT3. Biosci Biotechnol Biochem *77*, 1517-1521.

Vernick, K.D. (2004). Gamete interruptus; a novel calcium-dependent kinase is essential for malaria sexual reproduction. Cell *117*, 419-420.

Vora, A., Taank, V., Dutta, S.M., Anderson, J.F., Fish, D., Sonenshine, D.E., Catravas, J.D., Sultana, H., and Neelakanta, G. (2017). Ticks elicit variable fibrinogenolytic activities upon feeding on hosts with different immune backgrounds. Sci Rep *7*, 44593.

Wang, G., Liveris, D., Mukherjee, P., Jungnick, S., Margos, G., and Schwartz, I. (2014). Molecular Typing of *Borrelia burgdorferi*. Curr Protoc Microbiol *34*, 12C 15 11-31.

WHO (2014). A Global Brief on Vector-Borne Diseases (Geneva, Switzerland: World Health Organization).

WHO (2019). Vector-borne diseases (https://www.who.int/news-room/fact-sheets/detail/vector-borne-diseases: World Health Organization).

Williams, S.A., Monti, J.A., Boots, L.R., and Cornwell, P.E. (1984). Quantitation of xanthurenic acid in rabbit serum using high performance liquid chromatography. Am J Clin Nutr *40*, 159-167.

Work, T.H. (1963). Tick-Borne Viruses. A Review of an Arthropod-Borne Virus Problem of Growing Importance in the Tropics. Bull World Health Organ *29*, 59-74.

Yamamoto, D.S., Sumitani, M., Hatakeyama, M., and Matsuoka, H. (2018). Malaria infectivity of xanthurenic acid-deficient anopheline mosquitoes produced by TALEN-mediated targeted mutagenesis. Transgenic Res *27*, 51-60.

Yao, J., Hong, W., Huang, J., Zhan, K., Huang, H., and Hong, M. (2012). N-Glycosylation dictates proper processing of organic anion transporting polypeptide 1B1. PLoS One *7*, e52563.

Zeman, P., Januska, J., Orolinova, M., Stuen, S., Struhar, V., and Jebavy, L. (2004). High seroprevalence of granulocytic ehrlichiosis distinguishes sheep that were the source of an alimentary epidemic of tick-borne encephalitis. Wien Klin Wochenschr *116*, 614-616.

Zhang, B., and Lauschke, V.M. (2019). Genetic variability and population diversity of the human SLCO (OATP) transporter family. Pharmacol Res *139*, 550-559.

Zhou, F., Xu, W., Hong, M., Pan, Z., Sinko, P.J., Ma, J., and You, G. (2005). The role of N-linked glycosylation in protein folding, membrane targeting, and substrate binding of human organic anion transporter hOAT4. Mol Pharmacol *67*, 868-876.

Zhou, W., Woodson, M., Neupane, B., Bai, F., Sherman, M.B., Choi, K.H., Neelakanta, G., and Sultana, H. (2018). Exosomes serve as novel modes of tick-borne flavivirus transmission from arthropod to human cells and facilitates dissemination of viral RNA and proteins to the vertebrate neuronal cells. PLoS Pathog *14*, e1006764.

RIGHTS AND PERMISSIONS

Figure 1

Confirmation Number: 11793237 Citation Information Order Detail ID: 71820804 Journal of medical microbiology by PATHOLOGICAL SOCIETY OF GREAT BRITAIN AND IRELAND Reproduced with permission of Microbiology Society in the format Republish in a thesis/dissertation via Copyright Clearance Center.

Order Details

Journal of medical microbiology

Billing Status: **N/A**

Order detail ID:	71820804
ISSN:	0022-2615
Publication Type:	Journal
Volume:	
Issue:	
Start page:	
Publisher:	Microbiology Society
Author/Editor:	PATHOLOGICAL SOCIETY OF GREAT BRITAIN AND IRELAND

Permission Status: Granted

Permission type: Republish or display content
Type of use: Republish in a thesis/dissertation
Order License Id: 4534410404072

Requestor type	Academic institution
Format	Print, Electronic
Portion	image/photo
Number of images/photos requested	1
The requesting person/organization	Vikas Taank
Title or numeric reference of the portion(s)	Figure 3B
Title of the article or chapter the portion is from	Ultrastructural differentiation of the genogroups in the genus Ehrlichia
Editor of portion(s)	N/A
Author of portion(s)	N/A
Volume of serial or monograph	N/A
Issue, if republishing an article from a serial	N/A
Page range of portion	241
Publication date of portion	2/22/2019
Rights for	Main product
Duration of use	Current edition and up to 10 years
Creation of copies for the disabled	no
With minor editing privileges	no
For distribution to	Worldwide
In the following language(s)	Original language of publication
With incidental promotional use	no
Lifetime unit quantity of new product	Up to 499
Title	Arthropod Organic Anion Transporting Polypeptides (OATPs) in Tick-Borne Bacterial and Viral Infections
Institution name	Old Dominion University
Expected presentation date	Apr 2019

Figure 2

American Society for Microbiology authorizes an advanced degree candidate to republish the requested material in his/her doctoral thesis or dissertation. If your thesis, or dissertation, is to be published commercially, then you must reapply for permission. https://s100.copyright.com/help/rightslinkhelppages/Frequently_Asked_Questions_asm.htm#Dissertation_Thesis1

Chapter 2

The content used in chapter 2 is published in Scientific Reports (Nature press), Title: *Human rickettsial pathogen modulates arthropod organic anion transporting polypeptide and tryptophan pathway for its survival in ticks* (https://doi.org/10.1038/s41598-017-13559-x). Some figures were modified to fit according to the chapter format. This article is published with open access under the terms of the Creative Common Attribution 4.0 International License (https://creativecommons.org/licenses/by/4.0/) which permits unrestricted use, distribution, and reproduction in any medium.

Chapter 3

The content used in chapter 3 is published in Parasites and Vectors (BMC, part of Springer Nature), Title: *Characterization of tick organic anion transporting polypeptides (OATPs) upon bacterial and viral infections* (https://doi.org/10.1186/s13071-018-3160-6). Some content was modified to fit according to the chapter format.

VITA

VIKAS KUMAR TAANK

Department of Biological Sciences, 110 Mills Godwin Life Science Building,
Old Dominion University, Norfolk VA-23529.

EDUCATION

- **Master of Science, Cellular and Molecular Biology: December 2007,** University of New Haven, West Haven, CT 06516.
- **Master of Science, Microbiology: August 2001,** Chaudhary Charan Singh University, Dehradun, India-248001.
- **Bachelor of Science, Microbiology (Honors): August 1999,** SSN College, University of Delhi, Delhi, India-110007.

CERTIFICATE AND TRAINING

- Microbial Genome analysis using PATRIC, American Society for Microbiology (2018).
- Molecular Diagnostics Certificate Program (12 credits), (Old Dominion University, Norfolk VA): 2012
- Mushroom Production Technology (Directorate of Mushroom Research, Solan, India): 2010

PEER-REVIEWED PUBLICATIONS

- Turck, J.W., **Taank, V**., Neelakanta, G., Sultana, H. (2019*) Ixodes scapularis* Src tyrosine kinase facilitates *Anaplasma phagocytophilum* survival in its arthropod vector. (In press) Ticks and Tick-borne Diseases.
- Khanal, S., **Taank, V**., Anderson, J.F., Sultana, H., Neelakanta, G. (2018) Arthropod transcriptional activator protein1 (AP-1) aids tick- rickettsial pathogen survival in the cold. Sci Rep. 8(1): p. 11409.
- **Taank, V.,** Zhou, W., Zhuang, X., Anderson, J.F., Pal, U., Sultana, H., Neelakanta, G. (2018) Characterization of tick organic anion transporting polypeptides(OATPs) upon bacterial and viral infections. Parasite Vectors. 11(1): p. 593.
- **Taank, V**., Dutta, S., Dasgupta, A., Steeves, T.K., Fish, D., Anderson, J.F., Sultana, H., Neelakanta, G. (2017) Human rickettsial pathogen modulates arthropod organic anion transporting polypeptide and tryptophan pathway for its survival in ticks. Sci Rep, 2017. 7(1): p. 13256.
- Vora, A., **Taank, V**., Dutta, S., Anderson, J.F., Fish, D., Sonenshine, D.E., Catravas, J.D., Sultana, H., and Neelakanta, G. (2017). Ticks elicit variable fibrinogenolytic activities upon feeding on hosts with different immune backgrounds. Sci. Rep. 7, 44593.
- Prinz, A. C. B., **Taank, V**., Voegeli, V., Walters, E. L. (2016) A novel nest-monitoring camera system using a Raspberry Pi microcomputer. J. Field Ornithol. 87(4):427-435.
- Shirur, M., Vijay, B., Manikandan, K., Goraksha, W. C., **Taank, V**., Verma, S., and Bhatia, R. (2011) Impact assessment of national mushroom mela. Mushroom Research Published by DMR. Solan, India.
- Bajaj, B.K., **Taank, V**., and Thakur R.L. (2005) Potential industrial application of yeast capable of fermenting high-gravity cane molasses despite physiological stress. Indian Journal of Biotechnology, IBJT. 149-152.
- Bajaj, B.K., **Taank, V**., and Thakur R.L. (2003) Characterization of yeasts for ethanolic fermentation of molasses with high sugar concentration. Journal of Scientific and Industrial Research (JSIRAC). 62(11). 1078-1085.